ENVIRONMENTAL FATE AND PLANT UPTAKE OF CHEMICALS OF EMERGING CONCERN IN AGRICULTURAL SYSTEMS

By

Geoffrey Ryan Rhodes

A DISSERTATION

Submitted to
Michigan State University
in partial fulfillment of the requirements
for the degree of

Crop and Soil Sciences – Environmental Toxicology – Doctor of Philosophy

2021

ABSTRACT

ENVIRONMENTAL FATE AND PLANT UPTAKE OF CHEMICALS OF EMERGING CONCERN IN AGRICULTURAL SYSTEMS

By

Geoffrey Ryan Rhodes

Chemicals of emerging concern (CECs), such as pharmaceuticals and per- and polyfluoroalkyl substances (PFAS), have been frequently detected in agricultural systems, resulting from crop irrigation with contaminated water and land application of biosolids and animal manures. Crops can take up CECs from soil and water, leading to their accumulation in human and animal foodstuffs. The long-term consumption of contaminated foodstuffs and the resulting potential human and animal health impacts is of particular concern. Currently, the mechanism(s) controlling the uptake and accumulation of CECs in crops is not well understood. Additionally, agricultural lands contaminated by CECs can serve as a source that spread pollutants to the surrounding environment. The first study of this dissertation examined the accumulation and distribution of a commonly prescribed pharmaceutical (cephalexin) in lettuce, celery, and radish. Cephalexin did not accumulate in the shoots of all three vegetables but accumulated in the roots in the order of lettuce > celery > radish. Sorption of cephalexin to vegetable roots ranked in the order of lettuce > celery > radish, and the transformation of cephalexin by root enzyme extracts in the order of lettuce < radish < celery. Therefore, the sorption of cephalexin to plant roots and its transformation by plant enzymes could collectively determine the uptake and accumulation of cephalexin in vegetables.

The second study examined the mechanisms controlling the transport of PFAS, from roots to shoots, using *Arabidopsis thaliana* Columbia-0 (wild type) and a mutant of this ecotype with a compromised Casparian strip (a potential barrier root-to-shoot transport). *A. thaliana* wild

type and mutant plants were exposed to a mixture of PFAS and the pharmaceutical carbamazepine. Biomasses at harvest, amount of water transpired, carbamazepine concentration in shoots, and PFAS and carbamazepine concentration in roots were not significantly different between wild type and mutant plants. Significantly higher concentrations of PFAS were observed in the shoots of the mutant plants than in the wild type plant shoots suggesting that the Casparian strip plays a role in reducing the translocation of PFAS from roots to shoots.

Translocation factors for PFAS with a molecular weight <450 g/mol and PFAS with a molecular weight of >450 g/mol were 3.4 times and 1.5 times higher in mutant plants than in wild type plants, respectively. This suggests that the translocation of PFAS with molecular weight < 450 g/mol could be more impacted by the Casparian strip.

The final study investigated the concentrations and compositional profiles of PFAS in surface water and sediment samples collected near an agricultural field which received biosolids likely containing PFAS in the early 1980's. The total PFAS concentrations downstream of the biosolids-applied field ranged from 596 ng/L to 12,530 ng/L in surface water samples, with the highest concentration occurring immediately downstream of the biosolids-applied field. The total PFAS concentrations decreased with increasing distance away from the biosolids-applied field. The total PFAS concentrations in surface water samples upstream of the biosolids-applied field ranged from 40 to 173 ng/L. The highest concentration of total PFAS in the sediment samples (15,220 ng/kg) was found at an intermediate distance downstream of the biosolids-applied field, suggesting the transport of PFAS-contaminated sediments. These results indicate that the application of PFAS-containing biosolids to agricultural lands could have a long-term impact on the downstream environments.

ACKNOWLEDGEMENTS

I would like to thank my major advisor, Dr. Hui Li, for his advice, support, encouragement, and guidance throughout my graduate experience. I would also like to thank the members of my academic committee, Dr. Ray Hammerschmidt, Dr. Stephen Boyd, and Dr. Wei Zhang, for their excellent advice, mentoring, and contributions to my work. I am grateful to the members of our research group, both past and present, for the training and assistance: Dr. Yingjie Zhang, Dr. J. Brett Sallach, Dr. Zeyou Chen, Dr. Yuanbo Li, Dr. Ya-Hui Chuang, Dr. Cheng-Hua Liu, Dr. Feng Gao, Dr. Yike Shen, Dr. Jianzhou He, Dr. Qi Yuan, Dr. Wenfeng Wang, Jingyi Feng, Romilly Benedict, Zhiliang Xu, Chenxi Li, and all the visiting scholars I have worked with. Finally, I wish to thank my family for their support during my graduate studies.

This work was supported in part by Agriculture and Food Research Initiative Competitive Grant 2016-67017-24514 from USDA National Institute of Food and Agriculture, and Michigan State University AgBioResearch Project GREEEN.

TABLE OF CONTENTS

LIST OF TABLES	viii
LIST OF FIGURES	ix
CHAPTER I. LITERATURE REVIEW, RESEARCH OBJECTIVE	S AND
HYPOTHESES	
ABSTRACT	2
LITERATURE REVIEW	3
Background	3
Data sources	
Analysis of retrieved literatures	
Sources of PFAS in plants	
Plant uptake pathways	
Distribution of PFAS in plants	
Physiochemical properties of PFAS	
Plant physiological characteristics	
Surrounding environments	
Summary and prospective research	
RESEARCH OBJECTIVES AND HYPOTHESES	
REFERENCES	33
CHAPTER II. UPTAKE OF CEPHALEXIN BY LETTUCE, CELEIFROM WATER	
ABSTRACT	
INTRODUCTION	
MATERIALS AND METHODS	49
Chemicals and reagents	49
Vegetable uptake of cephalexin	
Cephalexin extraction	
Cephalexin analysis	
Sorption by vegetable roots	55
In vitro transformation of cephalexin	56
RESULTS AND DISCUSSION	57
Cephalexin uptake by vegetables	57
Cephalexin sorption by vegetable roots	61
In vitro transformation	
CONCLUSION	
REFERENCES	69
CHAPTER III. THE CASPARIAN STRIP REDUCES PER- AND	
POLYFLUOROALKYL SUBSTANCES TRANSPORT FROM PLA	NT ROOTS TO
SHOOTS	77
ARSTRACT	78

INTRODUCTION	80
MATERIALS AND METHODS	82
Chemicals and reagents	
Arabidopsis thaliana growth experiments	
PFAS and carbamazepine extraction	
PFAS and carbamazepine analysis	
RESULTS AND DISCUSSION	
Plant transpiration and biomass	
PFAS and carbamazepine accumulation in A. thaliana roots	
PFAS and carbamazepine accumulation in A. thaliana shoots	
CONCLUSION	
REFERENCES	
CHAPTER IV. PFAS CONTAMINATION IN SURFACE WATER AND SEDIMENT	
FROM HISTORICAL LAND APPLICATION OF BIOSOLIDS	103
ABSTRACT	104
INTRODUCTION	105
SITE HISTORY AND DESCRIPTION	107
MATERIAL AND METHODS	111
Soil samples	111
Surface water samples	111
Sediment samples	112
PFAS analysis	
RESULTS AND DISCUSSION	115
PFAS in biosolids-amended soil	115
PFAS in surface water	118
PFAS in sediment	127
Paired sediment and surface water	131
Temporal changes	133
CONCLUSION	137
REFERENCES	138
CHAPTER V. FUTURE RESEARCH	145
IN VITRO SCREENING OF CHEMICALS OF EMERGING CONCERN FOR	
ASSESSING PLANT UPTAKE AND ACCUMULATION	146
USE OF SALK_043282 ARABIDOPSIS THALIANA MUTANT TO FURTHER	
EXAMINE THE IMPACT OF THE CASPARIAN STRIP	147
GENETIC SCREENING OF CROP VARIETIES FOR VARIATIONS IN THE	
CASPARIAN STRIP	147
EXAMINATION OF ADDITIONAL IMPACTS FROM PFAS IN SURFACE WATER	
AND SEDIMENTS	1/17

LIST OF TABLES

Table 1.1 Summary of field studies on plant accumulation of PFAS
Table 1.2 Summary of pot experiment studies on plant uptake of PFAS
Table 1.3 Summary of hydroponic studies on plant uptake of PFAS
Table 2.1 Physiochemical properties of Cephalexin
Table 2.2 Extraction efficiency (%) of cephalexin from nutrient solution, and lettuce, celery, and radish roots and shoots using the QuEChERS method
Table 3.1 Extraction efficiency (%) of PFAS and carbamazepine from <i>A. thaliana</i> root and shoot tissues
Table 3.2 HPLC-MS/MS parameters for PFAS and carbamazepine analysis
Table 4.1 Sampling location information for surface water and/or sediment
Table 4.2 PFAS analyzed in soil, surface water, and sediment samples
Table 4.3 Statistics of PFAS (ng/kg) detected in soils collected from the biosolids-applied field (n = 5) in December 2019
Table 4.4 Statistics of PFAS (ng/L) detected in surface water (n = 12) in September 2019119
Table 4.5 Statistics of PFAS (ng/kg) detected in sediment (n = 7) in August 2020128

LIST OF FIGURES

Figure 2.1 Cephalexin concentration in plant tissues (left y-axis), and in nutrient solution and the vegetable-free controls (right y-axis) for (A) lettuce, (B) celery, and (C) radish as a function of time
Figure 2.2 Sorption isotherm for cephalexin by lettuce, celery, and radish roots from nutrient solution
Figure 2.3 The natural log of cephalexin concentration in (A) lettuce, (B) celery, and (C) radish enzyme extracts as a function of time
Figure 3.1 PFAS accumulation in Arabidopsis thaliana roots from 48 to 144 hours $(n = 5)$ 92
Figure 3.2 PFAS accumulation in Arabidopsis thaliana shoots from 48 to 144 hours ($n = 5$)93
Figure 3.3 (A) PFAS concentration in roots, (B) PFAS concentration in shoots, and (C) PFAS translocation factor in Arabidopsis thaliana at 120 hours (n = 20)94
Figure 4.1 Map of surface water and sediment sampling sites in the studied area of the Brandymore/Howe Drain
Figure 4.2 PFAS in surface water samples collected in September 2019 (n = 12)
Figure 4.3 Radar plots of select PFAS concentrations (ng/L) in surface water samples
Figure 4.4 Radar plots of select PFAS concentrations (ng/L) in surface water samples influenced by the biosolids-applied field
Figure 4.5 PFAS in sediment samples collected in August 2020 (n = 7)
Figure 4.4 Comparison of PFAS concentrations in surface water and sediment samples collected in November 2019 (n = 3)
Figure 4.5 Temporal changes of PFAS concentrations in surface water samples (n = 3)

CHAPTER I.

LITERATURE REVIEW, RESEARCH OBJECTIVES AND HYPOTHESES

ABSTRACT

Per- and polyfluoroalkyl substances (PFAS) are a class of persistent environmental contaminants that are ubiquitous in the environment and have been found to accumulate in agricultural products. Consumption of PFAS-contaminated agricultural products represents a feasible pathway for the trophic transfer of these toxic chemicals along food chains/webs, leading to human and animal health risks. Recently, studies on plant uptake and accumulation of PFAS have rapidly increased, thereby a review to summarize the current knowledge and highlight the future research is needed. Analysis of the publications indicates that a large variety of plant species can take up PFAS from the environment. Vegetables and grains are the most commonly investigated crops, with perfluorooctanoic acid (PFOA) and perfluorooctanesulfonic acid (PFOS) as the most studied target PFAS. The potential sources of PFAS for plant uptake include industrial emissions, irrigation with contaminated water, land application of biosolids, leachates from landfill sites, and pesticide application. Root uptake is the predominant pathway for the accumulation of PFAS in agricultural crops, and uptake by plant aboveground portions from ambient atmosphere could play a minor role in the overall PFAS accumulation. PFAS uptake by plants is mainly influenced by the physicochemical properties of compounds (e.g., perfluorocarbon chain length, head group functionality, water solubility, and volatility), plant physiology (e.g., transpiration rate, lipid, and protein content), and abiotic factors (e.g., soil organic matters, pH, salinity, and temperature). Based on literature analysis, the current knowledge gaps are identified, and prospective future research avenues are suggested.

LITERATURE REVIEW

Background

Per- and polyfluoroalkyl substances (PFAS) are a large group of synthetic organic chemicals containing a hydrophilic head functional group and a hydrophobic –CF2 tail chain. The binding between C-F forms an extremely strong covalent bond (~110 kcal/mol), which confers excellent chemical and thermal stability to PFAS (Buck et al., 2011). Since the late 1940s, more than 6000 PFAS have been synthesized and extensively used in a myriad of industrial and household products such as aqueous firefighting foams (AFFFs), surfactants, adhesives, coatings, lubricants, food packages, paints, and pesticides (Prevedouros et al., 2006; Paul et al., 2008; Buck et al., 2011). The widespread applications of these products have led to the ubiquitous distributions of PFAS in the environment and in biota as well (Benskin et al., 2012; Chen et al., 2018; Dalahmeh et al., 2018; Vuong et al., 2018). Many PFAS, e.g., perfluorooctanoic acid (PFOA) and perfluorooctanesulfonic acid (PFOS), have been determined to be persistent in the environment, bioaccumulative, and toxic to animals and humans (Buck et al., 2011; Itoh et al., 2016; ASTDR, 2018). Consequently, PFOS and PFOA, have been listed in the annex to the Stockholm Convention on Persistent Organic Pollutants. The environmental prevalence and potential toxicity of PFAS render them high-priority contaminants of increasing concern.

Agricultural lands are important environmental reservoirs for the retention of PFAS.

PFAS can enter soils via multiple pathways including land application of biosolids, irrigation with PFAS-contaminated water, leaching from landfilled wastes, release from industrial manufacturing and pesticide application (Taniyasu et al., 2013; Blaine et al., 2014; Gallen et al., 2016; Liu et al., 2016; Tian et al., 2018). In some highly contaminated sites, the concentration of

PFAS in soils reached the mg/kg levels (Jin et al., 2015; Braunig et al., 2019). Due to their relatively high water solubility, large proportions of PFAS can remain dissolved in soil water, rendering them highly mobile and bioavailable to plant root uptake (Zhao et al., 2012; Zhu and Kannan, 2019). Plants grown in contaminated areas are frequently detected with measurable concentrations of PFAS, confirming the capability of plants to absorb these contaminants from soils (Blaine et al., 2013; Wen et al., 2014; Jin et al., 2018; Yu et al., 2018; Kim et al., 2019). Considering that agricultural crops constitute a major portion of livestock and human diets, consumption of the PFAS-laden food represents an important exposure route responsible for the accumulation of PFAS in animals and humans (van Asselt et al., 2011; Blaine et al., 2014; Perez et al., 2014; Brambilla et al., 2015). Exposure to PFAS could lead to various health issues including hepatic damage, cardiovascular disease, dysfunction of the immune system, endocrine disorders, reproductive and developmental problems, and cancer (ASTDR, 2018). Therefore, to better assess the potential risks associated with human consumption of PFAS-laden crops, it is imperative to clearly elucidate the transfer behaviors of PFAS from environmental media to plants and their distributions in edible plant structures.

Although there have been an increasing number of studies conducted on PFAS uptake by plants in the fields or in controlled environments (Blaine et al., 2013; Stahl et al., 2013; Felizeter et al., 2014; Wen et al., 2014), review papers focusing on this topic are scarce (Ghisi et al., 2018). Therefore, there is a need to collate the current literatures on the bioaccumulation of PFAS in plants to guide future research directions. The objective of this review is to summarize the current research progress on plant uptake and accumulation of PFAS and assess the potential sources, uptake pathways, and factors that influence the accumulation and distribution of PFAS

in plants. Based on the reviewed literatures, we highlight the current knowledge gaps and recommend several perspectives for future research.

Data sources

A bibliographic search was conducted using ISI Web of Science (http://apps.webofknowledge.com) to retrieve papers published by December 2019. The keywords used in the search included "perfluoroalkyl substances" or "perfluorinated substances" in combination with "plant". In addition, a complementary search was also performed by examining the reference lists of the retrieved literatures. The candidate publications were carefully checked to determine whether they contained relevant contents. A total of fifty publications were eventually acquired and summarized in Tables 1.1-1.3.

Analysis of retrieved literatures

Among the fifty selected publications regarding plant uptake of PFAS, sixteen studies were conducted as field experiments (Table 1.1), and thirty-one studies under the controlled experimental settings including seventeen pot studies (Table 1.2) and fourteen hydroponic studies (Table 1.3). Two studies were conducted via integrating field and greenhouse pot experiments (Blaine et al., 2013; Lee et al., 2014), and one study employed both pot and hydroponic experimental approaches (Zhao et al., 2018b).

Most field studies focused on the accumulation of PFAS in plants grown near a specific point source such as industrial manufacturing sites, fire training fields, landfills, or wastewater treatment plants (WWTPs) (Table 1.1). The results from these studies indicate the impacts of human activities to PFAS emissions (Gobelius et al., 2017; Liu et al., 2017a; Dalahmeh et al., 2018; Tian et al., 2018). Five studies indicated PFAS can be released from biosolids to soils and migrate into plants (Yoo et al., 2011; Blaine et al., 2013; Lee et al., 2014; Wen et al., 2014;

Gottschall et al., 2017). Other studies reported the detection of PFAS in the samples randomly collected from the fields, and in the vegetables and/or fruits acquired from local markets (Herzke et al., 2013; Sznajder-Katarzynska et al., 2018; Liu et al., 2019a). Out of the publications utilizing the pot experiment, there are eleven studies in which PFAS were spiked directly into soils as the source for plant uptake (Table 1.2). Soil amendment with biosolids represents another approach for plant exposure to PFAS in pot studies. Other exposure scenarios include irrigation with PFAS-contaminated water and utilization of soils collected from PFAS-contaminated sites (Blaine et al., 2014; Braunig et al., 2019). Compared with soil-based pot experiments, hydroponic study provides a clear insight into the mechanism of chemical uptake by plants because of the minimal interferences from sorption/desorption, transport, and transformation of target chemicals in soils (Li et al., 2018). The primary exposure method in hydroponic experiment is to cultivate plants in nutrient solution spiked with a predesigned amount of PFAS (Table 1.3).

Perfluoroalkyl carboxylic acids (PFCAs), particularly those with chain length of 4 to 12 - CF2 units, are the most studied PFAS in the retrieved publications. For instance, PFOA, one of the most prevalent PFCAs in the environment, appears in forty-one studies out of the fifty retrieved publications. Long-chain PFCAs such as perfluorotridecanoic acid (PFTrDA), perfluorotetradecanoic acid (PFTeDA), perfluorohexadecanoic acid (PFHxDA), and perfluorooctadecanoic acid (PFODA), were also widely detected in plant tissues collected from the contaminated fields (Gobelius et al., 2017; Dalahmeh et al., 2018); however, they were rarely used in pot or hydroponic plant uptake experiments. Perfluoroalkyl sulfonic acids (PFSAs) with 4 to 10 carbon chain length were frequently selected as target compounds in field and laboratory studies, and PFOS is the most studied compound. PFAS precursors such as fluorotelomer

alcohols (FTOHs), perfluoroalkyl sulfonamides (FOSAs), perfluoroalkyl sulfonamido ethanols (FOSEs), and fluorotelomer sulfonic acids (FTSAs), have been found in plants grown at the contaminated sites (Dalahmeh et al., 2018; Tian et al., 2018); however, few studies have been conducted to evaluate the uptake of these precursor compounds by plants in laboratory settings. Other PFCA precursors including polyfluoroalkyl phosphate diesters (diPAPs), fluorotelomer saturated carboxylates (FTCAs), and fluorotelomer unsaturated carboxylates (FTUCAs) are also rarely investigated in either field or laboratory studies (Lee et al., 2014; Bizkarguenaga et al., 2016b; Tian et al., 2018).

A large variety of plant species have exhibited the capability to take up PFAS via their roots from soil and water, and/or by their aboveground portions from the atmosphere. Most studies have focused on uptake by vegetables, followed by grains and fruits, with wheat, maize, lettuce, and tomato being the most investigated crop species in both field and laboratory studies (Tables 1.1 to 1.3). The diversity of plant species used in pot or hydroponic studies is much less than those documented in field investigations. A total of twenty-five types of vegetables and grains were reported to accumulate PFAS in the field studies, whereas only thirteen species were used in pot experiments and six in hydroponic settings. Grasses, which constitute an important portion of livestock forage, were also reported to take up PFAS, but the resultant risks to animal and human health were rarely evaluated (Stahl et al., 2009; Garcia-Valcarcel et al., 2014; Wen et al., 2016). In addition to root uptake from soils, tree leaves and bark were found to sorb vaporphase and particle-bound PFAS, confirming the potential of plant aboveground portions to take up airborne PFAS (Jin et al., 2018; Tian et al., 2018). Although PFAS were frequently detected in fruits such as apple, banana, orange, strawberry, and lemon collected from local markets, few

attempts were made to track the contamination sources in these products (Sznajder-Katarzynska et al., 2018).

Sources of PFAS in plants

There are several sources contributing to the accumulation of PFAS in plants. Emissions from industrial manufacturing can contaminate the surrounding soil, water, and air and consequently the plants. It was reported that the total concentrations of PFAS in soil, precipitation, surface water, and groundwater close to a mega fluorochemical industrial park reached up to 641 μ g/kg, 4.86 μ g/L, 1860 μ g/L, and 273 μ g/L, respectively (Liu et al., 2016; Liu et al., 2017a). In China, approximately 80~90% of PFOS/PFOA contamination can be traced back to industrial manufacturing (Liu et al., 2017b). These PFAS in the environment can enter plants in the surrounding areas of manufacturing sites. For instance, agricultural crops grown around fluorochemical industrial parks were detected with the high levels of PFAS; the total concentrations were up to 87 µg/kg wet weight (ww) in vegetables, 480 µg/kg dry weight (dw) in wheat grains, and 59 µg/kg dw in maize grains, which were attributed primarily to the nearby industrial discharges (Liu et al., 2016; Liu et al., 2017a; Bao et al., 2019). In addition, tree bark and leaves collected near a fluorochemical manufacturing park were also found to be contaminated with PFAS, suggesting that the airborne PFAS released from industries could be sorbed by the aboveground portions of plants (Jin et al., 2018).

Field irrigation with PFAS-contaminated water represents an important pathway responsible for PFAS accumulation in plants. The massive production and long-term use of PFAS has led to their ubiquitous presence in freshwater bodies such as lakes, rivers, and groundwater (Guo et al., 2015; Lu et al., 2015; Pan et al., 2018). Approximately 70% of freshwater resources are used in agricultural production (Pimentel et al., 2004). In some highly

contaminated sites, e.g., the areas surrounding fluorochemical manufacturing facilities, the total concentrations of PFAS were measured at mg/L levels in nearby surface waters (Chen et al., 2018; Bao et al., 2019). Comparable levels of PFAS were also found in surface water and groundwater close to the sites where AFFFs had been frequently used such as at airports, firefighter training sites, and military bases (Backe et al., 2013; Gobelius et al., 2017; Dauchy et al., 2019). In China, the annual release of PFAS to nearby surface waters from the applications of AFFFs was estimated to be 3.5 tons of PFOS and 0.35 tons of PFOA (Liu et al., 2017b). In Tyndall Air Force Base, USA, PFOA was found in groundwater with a concentration up to 6570 μg/L (Moody and Field, 1999). Surface runoff and infiltration from these AFFF-impacted sites can lead to considerable PFAS contamination in soils and plants (Gobelius et al., 2017; Braunig et al., 2019). The amphiphilic nature of PFAS enables these chemicals to remain dissolved, in large quantities, in the effluent streams from WWTPs (Kim et al., 2016). It was reported that the average concentration of the total PFAS in the effluents from three WWTPs in Guangzhou, China was between 0.016~0.234 μg/L, and the daily mass loads of PFAS to rivers ranged between 1.55~25.1 g (Pan et al., 2016). In Australia, the annual emission of PFOA and PFOS from the effluents of WWTPs is up to 65 and 26 kg, respectively (Gallen et al., 2018). The increasing use of treated wastewater in field irrigation consequently introduces more PFAS to agricultural products (Blaine et al., 2014).

Land application of biosolids is a common practice to improve soil quality and is another major pathway to introduce PFAS into agricultural fields (Blaine et al., 2014; Wen et al., 2014). As described above, PFAS can survive most municipal or industrial wastewater treatments and remain in significant amounts in the sewage sludge i.e., biosolids (Alder and van der Voet, 2015). PFAS concentration in biosolids can reach µg/kg to low mg/kg levels (Schultz et al.,

2006; Loganathan et al., 2007). Widespread and continuous land application of biosolids can lead to the accumulation of PFAS in soils. For example, farmlands in Decatur, Alabama, USA have received applications of biosolids for more than a decade, and the soils contained the total PFAS concentrations of up to several micrograms per gram of dry soils (Washington et al., 2010). It was estimated that the total annual loading of PFAS from the land application of biosolids to agricultural soils in the USA is 1.4 to 2.1 tons (Venkatesan and Halden, 2013). PFAS in soils can be taken up by agricultural crops posing high health risks to animals and humans via food consumption (Lindstrom et al., 2011; Blaine et al., 2014; Lee et al., 2014; Bizkarguenaga et al., 2016a).

Leachates from landfill sites have been identified as a point source contributing to the dissemination of PFAS in the environment (Paul et al., 2008). In northern Spain, the maximum total concentration of 11 PFAS in leachates from four solid waste landfill sites was up to 3.2 μg/L (Fuertes et al., 2017). In China, the total amount of PFAS leakages from landfills to soils and the surrounding groundwater was estimated to be 3.1 tons per year (Yan et al., 2015). PFAS in landfill leachates may enter soil and water, and further migrate to plants (Liu et al., 2017b; Hepburn et al., 2019). Landfills can also release vapor-phase and particle-bound PFAS and their precursor compounds to the ambient air (Ahrens et al., 2011). For example, the total concentrations of PFAS were up to 9.5 ng/m3 in the air, and 4100 μg/kg in the dry deposition around two landfill sites in Tianjin, China (Tian et al., 2018). Atmospheric emissions of PFAS from solid waste landfills in Ontario, Canada were approximately one kilogram per year (Ahrens et al., 2011). PFAS present in the ambient atmosphere of landfills were diverse, usually with 8:2 fluorotelomer alcohol (8:2 FTOH) and perfluorobutanoic acid (PFBA) as the dominant PFAS (Ahrens et al., 2011; Weinberg et al., 2011; Tian et al., 2018). Plant leaves and bark can sorb

these airborne PFAS, leading to the accumulation of PFAS in aboveground portions of plants (Jin et al., 2018; Tian et al., 2018).

N-Ethyl perfluorooctane sulfonamide (EtFOSA) is the active ingredient of sulfluramid, a widely used pesticide for controlling leaf-cutting ants and cockroaches (Lofstedt Gilljam et al., 2016; Nascimento et al., 2018). As a precursor compound, EtFOSA can be decomposed into several derivatives including perfluorooctane sulfonamide (FOSA) and PFOS (Plumlee et al., 2009; Lofstedt Gilljam et al., 2016; Zhao et al., 2018c). The extensive application of sulfluramid in agricultural production has resulted in considerable emissions of PFAS into the environment (Lofstedt Gilljam et al., 2016; Liu et al., 2017b). From 2004 to 2015, Brazil released 147.3 tons of FOSA and 19.5 tons of PFOS into the environment due to the use of sulfluramid (Lofstedt Gilljam et al., 2016). In China, emissions of PFOA and PFOS from the application of sulfluramid were estimated to be 2.6 and 1.4 tons, respectively, per year (Zhang et al., 2012). Plants can take up EtFOSA and its metabolites through roots and/or foliage, leading to accumulation of PFAS in plants (Nascimento et al., 2018; Tian et al., 2018; Zhao et al., 2018c).

Table 1.1 Summary of field studies on plant accumulation of PFAS

Plant species	Contamination sources	Compounds	Concentrations in plants	Reference
Tomato, cucumber, eggplant, pepper, & Chinese cabbage	Fluorochemical industrial park	PFBA, PFPeA, PFHxA, PFHpA, PFOA, PFNA, PFDA, PFBS, PFHxS, PFOS	ΣPFAS: 1.7~87 μg/kg ww.	(Bao et al., 2019)
Camphor, cypress, & magnolia	Fluorochemical industrial park	PFBA, PFPeA, PFHxA, PFHpA, PFOA, PFNA, PFDA, PFUnDA, PFDoDA, PFTrDA, PFTeDA, PFBS, PFHxS, PFOS	∑PFAS: Tree leaves: 46~1115 μg/kg dw; Tree bark: 37~774 μg/kg dw.	(Jin et al., 2018)
Wheat & maize	Fluorochemical industrial park	PFBA, PFPeA, PFHxA, PFHpA, PFOA, PFNA, PFDA, PFUnDA, PFDoDA, PFBS, PFHxS, PFOS	ΣPFAS: Wheat grain: 1.13~480 μg/kg dw; Maize grain: 0.7~58.8 μg/kg dw.	(Liu et al., 2017a)
Radish, carrot, Chinese cabbage, Chinese chives, lettuce, Welsh onion, celery, cauliflower, pepper, pumpkin, wheat, maize, & soybean	Fluorochemical industrial park	PFBA, PFPeA, PFHxA, PFHpA, PFOA, PFNA, PFDA, PFUnDA, PFDoDA, PFBS, PFHxS, PFOS	ΣPFAS: 1.36~8085 μg/kg dw.	(Liu et al., 2019b)
Sedge, Canada wildrye, & sumac	Fluorochemical industrial park	PFHpA, PFOA, PFNA, PFDA, PFUnDA, PFDoDA	Average ΣPFAS: Grass roots: 61 μg/kg dw; Grass leaves: 68 μg/kg dw; Tree leaves: 430 μg/kg dw.	(Zhu and Kannan, 2019)
Rice	Industrial complexes and wastewater treatment plant	PFBA, PFPeA, PFHxA, PFHpA, PFOA, PFNA, PFDA, PFUnDA, PFDoDA, PFTrDA, PFTeDA, PFHxDA, PFODA, PFBS, PFHxS, PFOS, PFDS	Σ PFAS: $0\sim1.85~\mu g/kg$ dw.	(Kim et al., 2019)
Yam, sugarcane, & maize	Wastewater treatment plant	PFBA, PFPeA, PFHxA, PFHpA, PFOA, PFNA, PFDA, PFUnDA, PFDoDA, PFTrDA, PFTeDA, PFHxDA, PFOcA, PFBS, PFHxS, PFOS, PFDS, PFOSA, MeFOSA, EtFOSA, MeFOSE, EtFOSE, MeFOSAA, EtFOSAA, 6:2FTSA	ΣPFAS: Yam root: 0.36±0.17 μg/kg dw; Sugarcane stem: 0.35±0.064 μg/kg dw; Maize cob: 0.2±0.064 μg/kg dw.	(Dalahmeh et al., 2018)
Silver birch, Norway spruce, bird cherry, mountain ash, ground elder, long beechfern, & wild strawberry	Fire Training Facility	PFHxS, PFOS, PFDS, PFBA, PFPeA, PFHxA, PFHpA, PFOA, PFNA, PFDA, PFUnDA, PFDoDA, PFTrDA, PFTeDA, PFHxDA, PFODA, PFOSA, MeFOSA, EtFOSE, FOSAA, MeFOSAA, EtFOSAA, 6:2 FTSA	ΣPFAS: Silver birch: 6.6~337 μg/kg dw; Norway spruce: 1.4~222 μg/kg dw; Bird cherry: 2.0~58 μg/kg dw; Mountain ash: 0.3~8.2 μg/kg dw; Ground elder: 2.9~83 μg/kg dw; Long beechfern: 3.1~35 μg/kg dw; Wild strawberry: 5.8~8 μg/kg dw.	(Gobelius et al., 2017)
Lettuce & tomato	Biosolids	PFBA, PFPeA, PFHxA, PFHpA, PFOA, PFNA, PFDA, PFBS, PFHxS, PFHpS, PFOS, PFDS	Lettuce: up to 27.5 μg/kg dw (PFBA); Tomato: up to 17.0 μg/kg dw (PFBA).	(Blaine et al., 2013)

Table 1.1 (cont'd)

Table 1.1 (cont'd)				
Pumpkin	Biosolids	diPAPs and PFBA, PFPeA, PFHxA, PFHpA, PFOA, PFNA, PFDA, PFUnDA, PFDoDA	ΣdiPAPs: 33.98 μg/kg ww; ΣPFCAs: 50.75 μg/kg ww.	(Lee et al., 2014)
Maize, soybean, & wheat	Biosolids	PFHxS, PFOS, PFDS, PFOSA, PFHpA, PFOA, PFNA, PFDA, PFUnDA, PFDoDA	No PFAS was detected.	(Gottschall et al., 2017)
Wheat	Biosolids	PFBA, PFPeA, PFHxA, PFHpA, PFOA, PFNA, PFDA, PFUnDA, PFDoDA, PFTrDA, PFTeDA, PFBS, PFHxS, PFHpS, PFOS, PFDS	ΣPFAS: Root: 140~472 μg/kg dw; Straw: 36.2~178 μg/kg dw; Husk: 6.15~37.8 μg/kg dw; Grain: 7.32~35.6 μg/kg dw.	(Wen et al., 2014)
Tall fescue, barley, bermuda grass, & Kentucky bluegrass	Biosolids	PFHxA, PFHpA, PFOA, PFNA, PFDA, PFUnDA, PFDoDA, PFTrDA, PFTeDA, PFBS, PFHxS, PFOS	Average $\sum PFAS$: Up to 709.1 $\mu g/kg$ dw.	(Yoo et al., 2011)
Chinese pine, oriental plane, & abele	Landfill sites	TFA, PFPrA, PFBA, PFPeA, PFHxA, PFHpA, PFOA, PFNA, PFDA, PFUnDA, PFDoDA, PFBS, PFHxS, PFOS, 6:2 diPAP, 8:2 diPAP, 6:2 FTOH, 8:2 FTOH, 10:2FTOH, MeFOSE, EtFOSE, MeFOSA, EtFOSA	Average ΣPFAS: >6200 μg/kg dw in tree leaves.	(Tian et al., 2018)
Canadian poplar, Chinese scholartree, weeping willow, & Chinese red pine	/	PFHxA, PFHpA, PFOA, PFNA, PFDA, PFDoDA, PFTeDA, PFBS, PFPeS, PFHxS, PFHpS, PFOS, PFNS, PFDS, MeFOSAA, EtFOSAA, 4:2 FTSA, 6:2 FTSA, 8:2 FTSA, 6:2 Cl- PFAES, 8:2 Cl-PFAES, PFECHS	Tree bark: ΣPFCAs: 10 μg/kg dw; ΣPFSAs: 0.65 μg/kg dw; CI-PFAESs: <0.15 μg/kg dw; PFECHS: <0.11 μg/kg dw; FTSAs: <1.7 μg/kg dw; FOSAs: <0.51 μg/kg dw.	(Liu et al., 2019a)
Carrot, onion, tomato, zucchini, cucumber, eggplant, pepper, cauliflower, cabbage, lettuce, spinach, chicory, asparagus, celery, fennel, potato, pea, & bean	/	PFHxA, PFHpA, PFOA, PFNA, PFDA, PFDoDA, PFUnDA, PFODA, PFOS, PFTrDA, PFTeDA, PFHxS	Average ΣPFAS: 10.5~38.1 μg/kg ww.	(Herzke et al., 2013)
Eucalyptus	Pesticide application	PFBA, PFPeA, PFHxA, PFHpA, PFOA, PFNA, PFDA, PFUnDA, PFDoDA, PFTrDA, PFTeDA, PFBS, PFHxS, PFOS, PFDS, FOSA, FOSAA, EtFOSA, EtFOSAA	Σ PFAS: 0.979 μg/kg dw in leaves	(Nascimento et al., 2018)
Banana, apple, lemon, orange, cherry, strawberry, potato, beetroot, carrot, white cabbage, & tomato	/	PFBA, PFPeA, PFHxA, PFHpA, PFOA, PFNA, PFDA, PFBS, PFHxS, PFOS	∑PFAS: Up to 49.6 μg/kg ww.	(Sznajder- Katarzynska et al., 2018)

Table 1.2 Summary of pot experiment studies on plant uptake of PFAS

Plant species	Compounds	Soil treatment	Initial concentration	Cultivation time	Observations	Reference
Alfalfa, Italian ryegrass, lettuce, maize, mung bean, radish, & soybean	EtFOSAA	Soil + spiked biosolids	258±21 pmol/g dw.	> 60 days	EtFOSAA was only accumulated in plant roots with BCFs in the range of 0.52~1.37 pmol/g soil. EtFOSAA metabolites including EtFOSA, FOSAA, FOSA, and PFOS were detected in plant roots and aerial parts. Plant concentrations of EtFOSAA correlated closely with the protein and lipid contents.	(Wen et al., 2018)
Carrot, potato, & cucumber	PFOA & PFOS	Soil + spiked sewage sludge	PFOA: 276~805 μg/kg dw. PFOS: 10~556 μg/kg dw.	63~96 days	Vegetative compartments concentrated more PFAS than peelings and peeled edible parts for all the plants. PFOA exhibited a higher transfer potential than PFOS.	(Lechner and Knapp, 2011)
Carrot & lettuce	8:2 diPAP	Soil + spiked compost (95:5, w/w)	500 μg/kg dw.	30~90 days	8:2 diPAP (4.6~7.8 μg/kg) and its metabolites including PFNA (1.0~1.3 μg/kg), PFOA (12~157 μg/kg), PFHpA (3~44 μg/kg), PFHxA (2.9~144 μg/kg), PFPeA (3.7~115 μg/kg), PFBA (3.9~130 μg/kg) were detected in root peels, root core, and leaves of carrot. 8:2 diPAP and PFOA were detected in lettuce heart. The total BCFs of 8:2 diPAP and its metabolites were <0.004 and 0.64~32.60 respectively in carrot, and 0.04~0.18 and 0.28~1.57 respectively in lettuce heart.	(Bizkarguena ga et al., 2016b)
Lettuce & tomato	PFBA, PFPeA, PFHxA, PFHpA, PFOA, PFNA, PFDA, PFBS, PFHxS, PFHpS, PFOS, PFDS	Soil + biosolids (90:10, w/w)	ΣPFAS: 335~434 μg/kg dw.	56~112 days	PFBA and PFPeA were the most accumulated PFAS with concentrations of 266 and 236 μg/kg respectively in lettuce, and 56 and 211 μg/kg respectively in tomato. The BCFs of PFAS were up to 56.8 (PFBA) in lettuce and 17.1 (PFPeA) in tomato.	(Blaine et al., 2013)
Radish, celery, tomato, & sugar snap pea	PFBA, PFPeA, PFHxA, PFHpA, PFOA, PFNA, PFDA, PFBS, PFHxS, PFOS	Soil + biosolids	ΣPFAS: 329.13~427.36 μg/kg dw.	67~224 days	PFOA (67 $\mu g/kg$) was the highest congener in celery shoot, while PFBA was the most accumulated in radish roots (232 $\mu g/kg$) and pea fruit (150 $\mu g/kg$). PFBA exhibited the highest BCFs in shoots of all crops. Fruit crops accumulated fewer long-chain PFAS than shoot or root crops.	(Blaine et al., 2014)
Alfalfa	6:2 diPAP	Soil + biosolids	167 μg/kg dw.	5.5 months	ΣPFAS were up to 58000 μg/kg ww in plant. Short-chain PFCAs dominated the accumulated PFAS in plant. The BCFs of PFAS in plant inversely correlated their carbon chain lengths.	(Lee et al., 2014)

Table 1.2 (cont'd)

Twenty	PFOA	Soil spiked with	200~1000 μg/kg.	50 days	PFOA exhibited different effects on root and shoot biomass of	(Xiang e	t al.,
lettuce cultivars		PFOA solution			different lettuce cultivars. The accumulation and translocation of PFOA varied significantly with different cultivars.	2018)	
					PFOA was mainly distributed in the plant cell walls, followed by organelles.		
Twenty-six lettuce cultivars	PFOS	Soil spiked with PFOS solution	200~1000 μg/kg.	45 days	Significant variations in the biomass of shoots and roots were observed among different lettuce cultivars. Different cultivars exhibited large variations in accumulating and translocating PFOS.	(Yu et 2018)	al.,
					Protein contents and protein-mediated transpiration related closely with PFOS accumulation in the lettuce cultivars.		
Maize	PFBA, PFPeA, PFHxA, PFHpA,	Soil spiked with PFAS solution	250~1000 μg/kg dw for individual	128 days	PFBA and PFPeA were the highest in maize straw and kernel, respectively.	(Krippner al., 2015)	
	PFOA, PFNA, PFDA, PFBS, PFHxS, PFOS		PFAS.		Short-chain PFAS predominated in both maize straw and kernel. PFAS were preferentially accumulated in maize straw relative to the kernel.		
Wheat	PFBA, PFHxA, PFOA, PFBS, PFHxS, PFOS	Soil spiked with PFAS solution	200~2000 μg/kg dw.	4 weeks	Higher exposure dose led to reduced shoot biomass in wheat. Exposure to PFBA and PFBS reduced <i>Chlorophyll a</i> content in wheat while PFOA and PFOS exhibited promoting effect. RCFs and TFs for short-chain PFAS were much higher than those for long-chain PFAS.	(Lan et 2018)	al.,
Wheat & rapeseed	PFOA & PFOS	Soil spiked with PFAS solution	PFOA: 285~292 μg/kg dw. PFOS: 264~294 μg/kg dw.	70 days	Plant biomass was increased by 15.2~31.0%. The contents of chlorophyll and malondialdehyde and activities of superoxide dismutase and peroxidase were decreased in wheat but were increased in rapeseed. PFAS concentrations in plant roots and shoots were in the range of	(Zhao et 2017)	al.,
Wheat	PFPeA, PFHxA, PFHpA, PFOA, PFNA, PFDA, PFUnDA, PFDoDA, PFBS, PFHxS, PFOS	Soil spiked with PFAS solution	200~1000 μg/kg.	30 days	332~1411 and 39.6~821 µg/kg, respectively. The accumulated PFAS in wheat roots and shoots increased with exposure dose. Log BCFs of PFAS in wheat decreased linearly with increasing carbon chain lengths. PFHxA exhibited the highest transfer potential in plant.	(Zhao et 2014)	al.,
Wheat	PFOA	Soil spiked with PFOA solution	200~800000 μg/kg dw.	28 days	Wheat germination rate was decreased as exposure dose increased. Low exposure dose stimulated the seedling growth and root length of wheat, while high exposure exhibited inhibiting effects. Plant proline content and peroxidase activity increased as PFOA exposure concentration increased, but the catalase activity decreased.	(Zhou et 2016)	al.,
Wheat	FOSA	Soil spiked with FOSA solution	2.128 nmol/g dw.	30 days	FOSA and its metabolites including PFOS, PFHxS and PFBS were detected in wheat roots and shoots. BCFs of FOSA in wheat roots was much higher than PFOS.	(Zhao et 2018b)	al.,

Table 1.2 (cont'd)

Table 1.2							
Spring wheat, oat, potato, maize, & perennial ryegrass	PFOA & PFOS	Soil spiked with PFAS solution	250~50000 μg/kg dw.	Up several months	to	Higher exposure levels led to higher plant accumulation of PFAS. Vegetative compartments accumulated more PFAS than storage organs. PFOA was more preferentially accumulated in plants except the potato peels.	(Stahl et al., 2009)
Wheat, rye, rapeseed, &	PFOA & PFOS	Soil spiked with PFAS solution	$25000 \mu g/kg dw$.	/		PFAS concentrations in plant straws were much higher than those in grains.	(Stahl et al., 2013)
barley Lettuce & strawberry	PFBA, PFPeA, PFHxA, PFHpA, PFOA, PFNA,	Irrigation with spiked reclaimed water	0.2~40 μg/L for individual PFAS.	/		Uptake of PFAS generally exhibited a decreasing temporal trend. Plant uptake of PFAS increased linearly with the exposure dose of compounds but decreased with their carbon chain lengths. PFCAs were more preferentially absorbed by plants than PFSAs.	(Blaine et al., 2014)
	PFBS, PFHxS, PFOS					BCFs for lettuce decreased 0.4~0.6 log unit per additional —CF ₂ group.	
Alfalfa, Italian ryegrass, lettuce, maize,	PFOA & PFOS	Soils collected from biosolids- amended field	PFOA: 416.8 μg/kg dw. PFOS: 154.4 μg/kg dw.	45 days		Root concentrations of PFOA and PFOS were 703.4~4310.3 and 212.4~723.6 μg/kg dw, respectively, and their shoot concentrations were 85.8~3500.9 and 25.5~105.5 μg/kg dw, respectively. RCFs of PFOS and PFOA were 1.37~4.68 and 1.69~10.3, respectively.	(Wen et al., 2016)
mung bean, radish & soybean						TFs of PFOA (0.09~1.78) were much higher than PFOS (0.06~0.179). The accumulation of PFOS and PFOA in roots correlated positively with root protein contents but negatively with root lipid contents.	
Wheat grass	PFBA, PFPeA, PFHxA, PFHpA, PFOA, PFNA,	Soils collected from airport sites	∑PFAS: 2400~14000 μg/kg dw.	10 weeks		PFHxS and PFOS were the most accumulated compounds with plant concentrations up to 2800 and 1100 μg/kg ww, respectively. BCFs of PFAS in wheat grass ranged from 0.06 (PFNA)~70 (PFBA).	(Braunig et al., 2019)
	PFDA, PFUnDA, PFDoDA, PFBS, PFHxS, PFOS					BCFs in grass shoots decreased $0.4\sim0.7$ log units per additional $-\text{CF}_2$ for PFCAs and $0.4\sim1.9$ for PFSAs;	
Red chicory		Combined use of contaminated irrigation water and spiked soil	0~80000 μg/L in irrigation water and 0 ~200 μg/kg dw in spiked soil.	87 days		PFBA, PFPeA, PFHxA and PFBS were the most accumulated PFAS. PFBA had the highest BCFs in plant root (221), leaf (109.4) and head (38); PFAS concentrations and BCFs decreased with their increasing carbon chain lengths in all plant compartments.	(Gredelj et al., 2019)

Table 1.3 Summary of hydroponic studies on plant uptake of PFAS

Plant species		Initial concentration			Reference
Lettuce	PFBA, PFPeA, PFHxA, PFHpA, PFOA, PFNA, PFDA, PFUnDA, PFDoDA, PFTrDA, PFTeDA, PFBS, PFHxS, PFOS	0.01~10 μg/L	40 days	The uptake isotherms for long-chain PFAS in plant roots were not linear. Long-chain PFAS demonstrated higher RCFs. TFs for PFAS generally decreased with their carbon chain lengths. Long-chain PFCAs exhibited better transferability from plant root to foliage.	(Felizeter et al., 2012)
Tomato, cabbage, & zucchini	PFBA, PFPeA, PFHxA, PFHpA, PFOA, PFNA, PFDA, PFUnDA, PFDoDA, PFTrDA, PFTeDA, PFBS, PFHxS, PFOS	0.01~10 μg/L	/	PFAS were present in different plant compartments. RCFs for PFCAs and PFSAs generally increased with carbon chain lengths. Short-chain PFAS (< C10) were more transferable to aerial parts.	(Felizeter et al., 2014)
Pumpkin, soybean, & wheat	EtFOSA	1.155 mmol/L	12 h	EtFOSA and its metabolites including FOSAA, FOSA, PFOS, PFHxS, and PFBS were present in plant roots and shoots. Root uptake followed the order: EtFOSA> FOSA~PFOS~FOSAA> PFBS~PFHxS. RCFs of EtFOSA correlated positively with the root lipid contents.	(Zhao et al., 2018c)
Pumpkin	6:2 FTSA	1.100 mmol/L	12 days	6:2 FTSA and its metabolites including PFHpA, PFHxA, PFPeA, PFBA, PFPrA, and TFA were accumulated in plant roots and shoots. RCFs of 6:2 FTSA were 2.6~24.2 times higher than those of its metabolites. TFs of 6:2 FTSA and its metabolites were negatively correlated with their logK _{ow} .	(Zhao et al., 2019)
Arabidopsis thaliana	PFOA	0~50000 μg/L	21 days	Exposure to PFOA led to decreased biomass in plant roots and shoots. PFOA concentrations in plant shoots were 8.5~12.5 times of those in roots. PFOA exposure significantly increased H ₂ O ₂ and malondialdehyde contents in shoots.	(Yang et al., 2015)
Soybean	8:2FTOH	0.215 mmol/L	12~144 h	The distribution of 8:2 FTOH and its metabolites followed the order of roots> stem> leaves. Glutathione-conjugated metabolites were present in soybean tissues. Activities of some 8:2 FTOH degrading enzymes were increased.	(Zhang et al., 2016)
Great brome	PFBA, PFBS, PFHxS, PFOA, PFOS, PFDA	500~1000 μg/L	1~20 days	Plant concentrations of PFAS increased with exposure time. Plant uptake of PFCAs decreased with carbon chain lengths. Higher exposure dose led to higher BCFs in plants.	(Garcia- Valcarcel et al., 2014)
Wheat	PFBA, PFHpA, PFOA, PFDoDA	1000 μg/L	0~7 days	Concentrations of PFAS in wheat roots and shoots increased with exposure time. RCFs increased but TFs decreased with carbon chain length of PFAS. The highest uptake of PFAS by wheat was observed at pH=7.	(Zhao et al., 2018a)
Wheat	PFOS	1000 μg/L	0~7 days	Accumulation of PFOS in the wheat roots and shoots increased with increasing salinity (0.03~7.25 psu), temperature (20~30 °C) and exposure concentration (100~100000 μg/L). The maximum uptake of PFOS by wheat was observed at pH=6.	(Zhao et al., 2013)
Wheat	PFBA, PFHpA, PFOA, PFDoDA	1000 μg/L	5 days	Plant uptake of PFAS increased by 2.8~4.2 times as the solution salinity increased from 0 to 0.4%. The uptake of PFAS increased by 1.5~2.3 times as the culture temperature increased from 20 to 30 °C.	(Zhao et al., 2016a)

Table 1.3 (cont'd)

Wheat	PFOS	100~200000 μg/L	7 days	High PFOS exposure (> 100000 μg/L) significantly inhabited the synthesis of plant chlorophyll and soluble protein contents and the biomass of roots and leaves. Plant peroxidase and superoxide dismutase activities were elevated at low exposure dose (< 10000 μg/L) but were inhibited at high exposure levels (>	(Qu et al., 2010)
***	700	1 000 17	10.1	200000 μg/L).	(71)
Wheat	FOSA	1.900 mmol/L	12 days	FOSA and its metabolites including PFOS, PFHxS, and PFBS were accumulated in wheat roots and shoots.	(Zhao et al., 2018b)
				Plant concentrations of PFAS followed order of root> shoot and FOSA> PFOS> PFHxA> PFBS.	,
Wheat	TFA, PFPrA, PFBA, PFHxA, PFOA, PFOS	0~25000 μg/L	2~80 h	Plant root and shoot exhibited different concentration trends with carbon chain lengths of PFAS. Root uptake of PFAS was a carrier-mediated process.	(Zhang et al., 2019)
				Different PFAS followed different uptake pathways.	
Maize	PFBA, PFPeA, PFHxA, PFHpA, PFOA, PFNA, PFDA, PFBS, PFHxS,	100 μg/L	5 days	Plant uptake of PFDA decreased significantly with increasing solution pH (5~7). PFBA (2460 μg/kg dw) and PFOS (3630 μg/kg dw) were respectively the most accumulated PFCA and PFSA in maize roots.	(Krippner et al., 2014)
	PFOS			TFs for both PFCAs and PFSAs decreased with carbon chain lengths.	
Maize	PFOS & PFOA	$100\sim200000~\mu g/L$	2~100 h	High exposure level (> $10000~\mu g/L$) significantly inhabited the root and shoot biomass.	(Wen et al., 2013)
				The root uptake of PFOA and PFOS fitted well with Michaelis-Menten model. Plant uptake of PFOA and PFOS might follow different pathways.	

Plant uptake pathways

Root uptake from soil and water is considered the primary pathway for PFAS to enter plants (Stahl et al., 2009; Lee et al., 2014; Wen et al., 2014). PFAS are typically comprised of a hydrophilic head functional group and a hydrophobic tail -CF2 chain, conferring relatively highwater solubility. PFAS generally demonstrated a relatively low sorption potential by soils, especially for the short-chain homologues (Buck et al., 2011; Zhao et al., 2012). PFAS in soils can migrate towards plant roots, driven primarily by the water potential gradient created by plant transpiration and PFAS concentration gradient (Lechner and Knapp, 2011). The uptake mechanism of PFAS into plant roots remains largely unexplored, though some studies have initiated the mechanistic research. Wen et al. (2013) observed that when maize roots were treated with sodium azide (NaN3, 0.1 mmol/L) and sodium vanadate (Na3VO4, 0.6 mmol/L) as metabolic inhibitors, the uptake of PFOA decreased by 83% and 43%, respectively. The authors suggested that PFOA movement into maize roots might be an energy-dependent active process. Additionally, they found PFOS uptake was insensitive to the presence of these two metabolic inhibitors. In the presence of aquaporin inhibitors (e.g., silver nitrate and glycerol) and an anion channel blocker (e.g., 5-nitro 2-(3-phenylpropylamine) benzoic acid), Wen et al. (2013) observed the decreased uptake of PFOS by 25~31% and 30~33%, respectively, and suggested that the uptake of PFOS by maize roots could be a passive process. More recently, Zhang et al. (2019) investigated wheat uptake of trifluoroacetic acid (TFA), pentafluoropropionic acid (PFPrA), PFBA, perfluorohexanoic acid (PFHxA), PFOA, and PFOS. The authors found that the accumulation of PFAS in wheat was reduced by 26~95% in the presence of Na3VO4, and that uptake inhibition rates for all tested PFAS exhibited a dose-response relationship with Na3VO4 concentrations between 0.06 and 0.6 mmol/L. Zhang et al. (2019) proposed that wheat uptake of

PFAS including PFOS was an energy-dependent active process. These studies have provided the initial investigation into the uptake mechanism of PFAS by plants, but metabolic inhibitors could cause the changes in stomatal opening, hydraulic conductivity, photosynthetic rate, etc. (Zelitch, 1965; Brauer and Stitt, 1990; Zhang and Tyerman, 1991), which might influence PFAS uptake. The factors responsible for the differences in PFOS uptake between maize and wheat remain unclear. However, both studies demonstrated that PFAS uptake by plants was a concentration-dependent process, which could be well described by the Michaelis-Menten model, implying that the penetration of PFAS into plant roots was probably mediated by carriers in cell membranes such as aquaporins and anion channels (Wen et al., 2013; Zhang et al., 2019). After penetration through a series of root cellular structures including epidermis, cortex, and endodermis via apoplastic and symplastic pathways, PFAS can enter the root vascular cylinder and subsequently move upward to plant shoots (Blaine et al., 2013; Blaine et al., 2014). Although some progress has been made, large knowledge gaps still exist regarding the mechanisms involved in the uptake and transport of PFAS in plants.

Vapor-phase and particle-bound PFAS and their precursors can also be sorbed by the aboveground portions of plants such as leaves and bark (Jin et al., 2018; Tian et al., 2018; Liu et al., 2019a). Although most PFAS have a low vapor pressure, they can be bound to atmospheric particulates, and deposit on plant aboveground surfaces (Shan et al., 2014). Fluorochemical manufacturers, WWTPs, and landfills can disseminate a substantial amount of PFAS to the surrounding atmosphere with the concentrations reaching ng/m3 levels in the air and mg/kg of atmospheric particulates (Ahrens et al., 2011; Weinberg et al., 2011; Jin et al., 2018). Short-chain PFAS homologues such as TFA and PFBA, are typically detected at higher concentrations in both the vapor and particulate phase (Scott et al., 2006; Wu et al., 2014; Tian et al., 2018). In a

field study conducted at Tianjin, China, the maximum concentration of 23 PFAS in tree leaves collected near landfill sites was reported to be > 6200 µg/kg dw, with TFA as the dominant congener in a concentration range of 560~3000 µg/kg dw (Tian et al., 2018). The accumulation of PFAS in tree leaves was partially attributed to foliar uptake of airborne PFAS and/or metabolism of their precursors because the dominant species of PFAS in tree leaves were also predominated in the ambient atmosphere. Additionally, the total concentrations of long-chain PFCAs (C9~C12) in tree leaves were found to be 1.2 to 50 times greater than those of shortchain homologues (C5~C7), suggesting the preference of foliar uptake for long-chain PFAS (Tian et al., 2018). PFAS were also detected in tree bark collected near a fluorochemical manufacturing park, with the total concentrations ranging from 37 to 774 µg/kg dw (Jin et al., 2018). PFHxA was the predominant PFAS congener (17~559 μg/kg dw) in the bark samples, followed by PFOA (4~269 μg/kg dw), PFBA (0~22 μg/kg dw), and PFTeDA (0~64 μg/kg dw). Since tree bark is composed primarily of inactive plant tissues with minimal water flow, the accumulated PFAS in tree bark were speculated to originate mainly from the atmosphere (Jin et al., 2018). In most cases, the contribution from aerial uptake to the overall accumulation of PFAS in plants could be small to minimal, as evidenced by the fact that no PFAS were detected in the aboveground portions of wheat grown in the uncontaminated soils located 8 km away from the fields amended with PFAS-contaminated biosolids (Wen et al., 2014). The minor contribution of foliar uptake to plant accumulation of PFAS could be due to the short contact time between vapor-phase and particulate-bound PFAS and plant aboveground surfaces, the resistance of waxy cuticles in foliage, and the relatively low concentration of airborne PFAS (Buck et al., 2011; Collins et al., 2011; Jin et al., 2018).

Distribution of PFAS in plants

Beyond the Casparian strip in plant roots, PFAS enter root xylem and move upwards to different plant structures, with the extent of translocation related closely with the transpiration stream. The plant structures which receive larger amount of water flow to the sites could accumulate more PFAS if sufficient domains are available for sorption or incorporation of PFAS. Stahl et al. (2009) studied the uptake of PFOA and PFOS by several cultivated plants including spring wheat, oat, potato, maize, and perennial ryegrass, and found that the concentrations of PFOA and PFOS were much higher in the straw of spring wheat, oat, and maize compared to the grain of the same plant. After exposure to 1000 µg/kg of mixed PFAS in soil for 128 days, the total concentration of PFAS in maize straw (52 mg/kg dw) was approximately 60 times higher than that in maize kernels (0.86 mg/kg dw) (Krippner et al., 2015). In a pot study with soils amended with sewage sludge, Lechner and Knapp (2011) found the predominant accumulation of PFOA and PFOS in carrot foliage, cucumber leaves and stalks, and potato leaves and stalks, and less amount in the peeled edible parts. As for the distribution of PFAS in trees around Stockholm Arlanda Airport, Sweden, Gobelius et al. (2017) reported that the total concentration of PFAS in birch (*Betula pendula*) followed the order of leaves (12~97 μg/kg ww) > twigs $(5.3\sim40 \,\mu\text{g/kg ww}) > \text{trunk/core} \,(0.37\sim31 \,\mu\text{g/kg ww}) > \text{roots} \,(2.6\sim6.2 \,\mu\text{g/kg ww})$. A similar trend was also observed for spruce (*Picea abies*) in the order of leaves > twigs > roots > trunk/core for the total PFAS concentration. These studies suggest the preferential accumulation of PFAS in vegetative structures of plants, which could be partly due to enrichment from the transpiration stream. Although some experimental data have been collected, the factors and driving force controlling PFAS distribution in plant structures remains largely unknown.

The distribution of PFAS within plants can be evaluated with translocation factor (TF) which is calculated as the ratio of PFAS concentration in shoots to that in roots (Ghisi et al., 2018; Scher et al., 2018). The reported TF values of PFAS varied in 3 to 4 orders of magnitude. Perfluorocarbon chain lengths and head functional groups of PFAS can affect the distribution of PFAS within plants (Felizeter et al., 2012; Wen et al., 2016; Lan et al., 2018; Xiang et al., 2018). In a pot study with wheat, the TF values of PFBA, PFBS, PFHxA, and PFHxS were in the range of 1.0 to 12, much higher than those of PFOA (< 0.5) and PFOS (< 0.1) (Lan et al., 2018). For hydroponically grown lettuce, PFBA and perfluoropentanoic acid (PFPeA) exhibited greater transferability with their TF values > 1 when the exposure dose was 1~10 μg/L, while PFCAs with 5 to 13 units of –CF2 (C6~C14) chain and PFSAs with 4 to 8 units of –CF2 chain were less transferable in plants with their TF values < 1 (Felizeter et al., 2012). Uptake of PFAS with large TF values leads to the high accumulation in leaves, grains, or fruits. On the other hand, for PFAS with low TF values, the higher accumulation is expected to be in the edible portions of tuber and root crops, such as radish, carrot, and potato.

The accumulation of PFAS in the edible structures of plants may pose health risks to animals and humans. For crops grown in soils amended with industrially contaminated biosolids, the total concentrations of PFAS in celery shoots, pea fruits, and radish roots were up to 814.3, 236.4, and 278.8 μg/kg dw, respectively (Blaine et al., 2014). Fruits and vegetables collected from local markets in several European countries were frequently found with PFAS contamination (Herzke et al., 2013; Sznajder-Katarzynska et al., 2018). In perennial grasses grown near a fluoropolymer manufacturing facility, the total concentrations of six PFCAs in grass leaves were in the range of 9~540 μg/kg dw (Zhu and Kannan, 2019). As grasses are primarily used as livestock forage, PFAS accumulated in grasses may migrate to animals and

eventually to humans via trophic food chains. At a Swedish dairy cattle farm, the daily intake of PFAS by cows from consumption of silage was estimated to be 0.027 μg/kg, and the concentration of PFAS in cow tissues and milk was measured up to 0.228 μg/kg and 0.018 μg/L, respectively (Vestergren et al., 2013). Consumption of PFAS-contaminated edible crops and transfer through food chains represent important pathways for humans for exposure to these chemicals (Domingo and Nadal, 2017).

Physiochemical properties of PFAS

The perfluorocarbon chain lengths of PFAS can significantly influence the uptake and transport of these chemicals in plants. Short-chain PFAS typically have relatively higher water solubility and smaller molecular size, both of which may facilitate their penetration through plant root layers (e.g., the epidermis, cortex, endodermis, and pericycle) to the vascular cylinder. Therefore, short-chain PFAS generally demonstrate a higher accumulation potential in plants compared to long-chain homologues (Yoo et al., 2011; Blaine et al., 2013; Krippner et al., 2015; Liu et al., 2017a). Lan et al. (2018) reported that wheat growing in soils containing 200 μg/kg of PFBA accumulated 3711 µg/kg dw in roots and 44088 µg/kg dw in shoots, which were 20 and 44 times greater than the accumulation of PFOA in roots and shoots, respectively. For lettuce grown in industrially impacted soils, short-chain PFAS such as PFBA, PFPeA, and PFBS were found to accumulate in plants with concentrations $> 200 \mu g/kg$ dw, whereas their concentrations in soils were relatively low 4.68 µg/kg for PFBA, 11.6 µg/kg for PFPeA, and 48.6 µg/kg for PFBS (Blaine et al., 2013). Although relatively higher concentrations were observed for longchain PFAS in soils 93.5 μg/kg for perfluorodecanoic acid (PFDA) and 49.7 μg/kg for PFOS, their concentration in the lettuce was measured to be $< 100 \mu g/kg$ dw. For several types of crops tested, the bioconcentration factors (BCFs) of PFAS ranged from < 1 to several thousand

depending on PFAS properties, plant species and structures, as well as soil compositions (Blaine et al., 2014; Lee et al., 2014; Wen et al., 2014; Ghisi et al., 2018). A general trend was found that BCFs decrease by 0.2~0.7 log units with one incremental –CF2 unit in the alkyl chain (Yoo et al., 2011; Blaine et al., 2013; Blaine et al., 2014; Liu et al., 2017a). For long-chain PFAS, sorption by soils limits their movement to plant root rhizosphere (Milinovic et al., 2015; Zhao et al., 2016b). One incremental –CF2 unit can lead to the increase of sorption coefficients in soils by approximately 0.5~0.6 log units (Higgins and Luthy, 2006). The increased sorption of PFAS, particularly for long-chain homologues, in soils could diminish their bioavailability to plant for uptake.

Hydroponic experiments eliminate the inference from sorption by soils, and the obtained results are better to elucidate the relationship between bioaccumulation in plants and PFAS structures. Krippner et al. (2014) found that PFCA accumulation in the roots of hydroponically grown maize decreased with increasing carbon chain length from C4 (PFBA) to C7 (PFHpA), and then increased with increasing carbon chain length from C7 to C10 (PFDA). A similar U-shape trend was also observed in hydroponically grown wheat (Felizeter et al., 2012). However, for several vegetables such as tomato, cabbage and zucchini, root concentration factors (RCFs) generally increased with increasing carbon chain length for both PFCAs (C4~C14) and PFSAs (C4~C8) (Felizeter et al., 2014). This is largely attributed to the higher sorption of longer-chain PFAS to root surfaces (Felizeter et al., 2012, 2014; Krippner et al., 2014).

Compared with long-chain homologues, short-chain PFAS exhibit a higher transferability from plant roots to the aboveground portions. Garcia-Valcarcel et al. (2014) reported that for *Bromus diandrus* exposed to a dosage of 500 µg/L of various PFAS, the concentration of PFBA in the aboveground portions was 3027 µg/kg after exposure for 20 days, which was 2.6 times

higher than the measured concentration of PFDA. In hydroponically grown lettuce, grass, and wheat, the TF values of PFAS were found to decrease with increasing –CF2 chain length (Felizeter et al., 2012; Krippner et al., 2014; Zhao et al., 2018a). The transport of chemicals from plant roots to the aboveground portions occurs in the xylem and is thought to be driven primarily by the transpiration stream (Collins et al., 2006; Yu et al., 2018). Short-chain PFAS are generally more mobile and less sorptive to plant tissues, conferring higher transferability with transpiration stream when compared to long-chain homologues (Felizeter et al., 2012). This could lead to higher accumulation of short-chain PFAS in the aboveground portions of plants (Felizeter et al., 2012; Krippner et al., 2014). Long-chain PFAS are less efficient in penetrating root surfaces and readily sorbed or blocked by the Casparian strip, and thus preferentially accumulate in plant roots (Felizeter et al., 2012, 2014; Krippner et al., 2015).

The head functional groups of PFAS also influence their accumulation in plants. In the case of PFAS with equal carbon chain lengths, PFCAs demonstrated a higher uptake potential than PFSAs. For instance, the accumulation of PFOA in spring wheat, oat, maize, perennial ryegrass, and peeled potato from soils was up to hundreds of times higher than that of PFOS (Stahl et al., 2009). Sorption of PFOS by soil was about 1.7 times more than PFOA (Higgins and Luthy, 2006), which is not sufficient to cause such difference in plant uptake. In a hydroponic study with lettuce, exposed to the same concentration of a mixture of PFAS (1 μg/L), the average PFBA concentration was 4.83 μg/kg in the roots and 11.7 μg/kg in the leaves, which was 2.7 and 22 times higher than PFBS in the corresponding lettuce structures (Felizeter et al., 2012). It has been documented that BCFs for perfluorocarboxylates could be one order of magnitude higher than those of perfluorosulfonate analogs (Yoo et al., 2011; Blaine et al., 2013; Liu et al., 2017a; Dalahmeh et al., 2018; Scher et al., 2018). However, the specific mechanism responsible for the

higher accumulation of PFCAs in plants relative to PFSAs with equal carbon chain lengths is still unclear.

Plant physiological characteristics

Transpiration plays an important role in controlling the uptake and transport of xenobiotic chemicals in plants (Collins et al., 2011). Difference in transpiration rate could lead to significant variation in PFAS accumulation among plant species, cultivars, plant structures, and even at different growth stages. In a field study conducted near a fluorochemical industrial park, the total concentration of 12 PFAS in wheat grains was > 11-fold higher than those in maize grains, with short-chain PFCAs (C4~C8) as the predominant congeners in both crops (Liu et al., 2017a). Compared to maize with transpiration coefficient of 250~300 g water/g dw, wheat possesses a greater transpiration coefficient 450~600 g water/g dw, which is considered as the major contributor to the higher accumulation of PFAS in wheat. In a pot study with 26 lettuce cultivars grown in PFOS-spiked soils, Yu et al. (2018) observed a significant positive correlation between BCF of PFOS in plant shoots and transpiration rate, confirming the important role of transpiration in transporting of PFAS in lettuce cultivars. Compared with storage structures (e.g., grain), vegetative structures (e.g., leaf and stalk) tend to accumulate higher levels of PFAS, which is probably due to enrichment from the transpiration stream. In a field study, PFAS accumulation in wheat straw was approximately 5 times more than that of wheat grain (Wen et al., 2014). The BCFs of PFOA and PFOS in the leaves and stalks of potato, carrot, and cucumber ranged between 0.12 to 0.99, significantly higher than those in peelings and peeled edible portions (BCFs < 0.05) (Lechner and Knapp, 2011). Muller et al. (2016) found a positive correlation between the accumulation mass of many PFAS and plant biomass. The increasing biomass with plant growth could provide more retention domains for accumulating PFAS.

The bioaccumulation and distribution of PFAS in plants is also dependent on plant composition, especially protein content. Wen et al. (2016) selected maize, soybean, radish, mung bean, lettuce, alfalfa, and Italian ryegrass as test plants with root protein content of 3.35 to 10.4% and lipid content of 2.33 to 5.40% and found that RCFs of PFOA and PFOS were positively related to root protein contents, but negatively related to root lipid contents. The TFs of PFOA and PFOS also exhibited a positive relationship with the ratio of shoot to root protein content. Similar relationships between RCFs/TFs of PFOS and plant protein contents have also been observed in different cultivars of lettuce (Yu et al., 2018). As a major component of carriers or channels in cell membranes, proteins could mediate the transport of PFAS into root cells (Wen et al., 2013; Zhang et al., 2019). Additionally, protein kinases can regulate the formation and development of stomata in plant leaves, which indirectly influences plant transpiration rate (Lai et al., 2005; Yu et al., 2018). The strong association between proteins and PFAS could enhance the accumulation of PFAS in plants.

Surrounding environments

Sorption of PFAS by soils could reduce their bioavailability to plant roots for uptake. Soil organic matter is considered the major domains influencing the sorption of PFAS by soils (Higgins and Luthy, 2006). A positive relationship has also been observed between sorption coefficient of PFAS in soils and soil organic carbon content (Milinovic et al., 2015). Increasing soil organic matter content can enhance the partitioning of PFAS in soils, decreasing the concentration of PFAS dissolved in soil water for plant uptake. Blaine et al. (2014) found that the concentration of PFAS in lettuce grown in a soil with 0.4% organic carbon content was 6.5 times greater than that in the lettuce grown in a soil with 6.0% organic carbon content. Long-chain PFAS are more readily sorbed by soils and demonstrate a lower bioavailability for plant uptake

(Zhao et al., 2012; Zhao et al., 2016b). Short-chain PFAS have a higher water solubility, exhibit less sorption by soils, and are more mobile in soils. This makes them more bioavailable for plant uptake (Zhao et al., 2012; Milinovic et al., 2015). PFAS containing equal carbon chains, but different hydrophilic head functional groups demonstrate varying sorption by soils (Higgins and Luthy, 2006). The difference in sorption of PFAS by soils could be partially responsible for their varying bioaccumulation potentials in plants. Aging can increase the sequestration of PFAS in soils, and further reduce the bioavailability of PFAS to plant roots for uptake (Blaine et al., 2013; Zhao et al., 2016b).

Other factors such as salinity, pH, and temperature could also influence the accumulation of PFAS in plants. Increasing salinity reduces plant transpiration, due to the decreasing osmotic potential of soil water, which might consequently diminish plant uptake of water, nutrients, and xenobiotic contaminants (Stofberg et al., 2015). However, in the two reported hydroponic experiments, increasing solution salinity was found to enhance the accumulation of PFAS in wheat, which might be due to the possible changes in the physicochemical properties of PFAS and/or physiological characteristics of plants (Zhao et al., 2013; Zhao et al., 2016a). Krippner et al. (2014) measured PFDA uptake by maize at pH 5, 6 and 7, and found that the highest uptake occurred at pH 5.0. For short-chain PFAS such as PFBA and PFHxA, the uptake by maize increased with increasing pH, but the underlying mechanism is still unknown. Temperature can promote plant physiological activities and biochemical processes such as increasing transpiration and metabolism, which would in turn influence plant uptake of xenobiotic contaminants (Ekvall and Greger, 2003). Zhao et al. (2016a) demonstrated that the accumulation of many PFAS in wheat increased by 1.5 to 2.3 times when the exposure temperature increased from 20 to 30 °C. However, such temperature effect was not consistent for all the PFAS tested; the uptake of longchain PFAS was found to be more sensitive to the change in temperature, which may be due to increases in membrane fluidity as temperature increases.

Summary and prospective research

The long manufacturing history of PFAS and their widespread use in industrial and household applications, coupled with their highly mobile and persistent natures, have caused their ubiquitous dissemination in the environment. This review summarizes the current knowledge regarding the uptake and accumulation of PFAS in plants. The primary sources responsible for the accumulation of PFAS in plants include the emissions from industrial manufacturing, irrigation with contaminated water, land application of biosolids, and leachates from landfills. Several field and laboratory studies have demonstrated that plants are capable of taking up PFAS from soil and water, as well as from the atmosphere; however, the fundamental mechanism governing the uptake and transport of PFAS in plants remains largely unknown, particularly the mechanism of PFAS movement through plant cell membranes and the mechanism that controls PFAS distribution in plants. Although adsorption of PFAS-bound particulates on the aboveground portions of plants or gas exchange into foliage can occur, root uptake is considered the predominant pathway for PFAS to enter plants. PFOA and PFOS, along with other PFCA and PFSA homologues, are the most investigated compounds in the reported studies. Few studies were conducted to elucidate uptake, transport, and metabolism of PFAS precursors in plants, though some precursor compounds such as FTOHs, FOSAs, FOSEs and FTSAs have been detected in plant samples at contaminated sites. Most studies on plant uptake of PFAS are limited to some common grains and vegetables, and the comparisons are infeasible among different plant species with varying physiological characteristic. Future research efforts are suggested to involve a broader suite of plant species and investigate the impact of PFAS

accumulation on plant health. This review extends the current knowledge on the uptake and accumulation of PFAS in plants, particularly agricultural crops, which could facilitate more accurate evaluation of the risks to human health via dietary consumption of agricultural products and provide guidance for development of best management practice to mitigate the accumulation of PFAS in agricultural foods at the field stage of farm production.

RESEARCH OBJECTIVES AND HYPOTHESES

The uptake and accumulation of chemicals of emerging concern (CECs) into agricultural crops involves many complex processes. These processes are influenced by a host of characteristics such as the compositional profile of CECs in the agricultural system, abiotic and biotic changes to that compositional profile, the physicochemical properties of the CECs themselves, and physiological and biological differences among crops. To adequately understand the risk that CECs, in the agricultural system, pose to not only human health, but to plant health, it is important to gain a holistic understanding of the agricultural system. What CECs are available for uptake? How is availability and uptake influenced by the physiochemical properties of the CEC? What aspects of plant physiology and biology impact accumulation of CECs? These important questions must be answered before a thorough evaluation of the risks that CECs pose to agricultural systems can be made. To this end, this dissertation seeks to analyze how the compositional profile of CECs can vary after environmental contamination, how biological and physicochemical properties may impact the uptake accumulation of CECs across different crops, and how plant anatomy may be controlling the accumulation of CECs. We hypothesize that (1) plant physiological and biological processes can influence the uptake and accumulation of CECs, (2) Casparian strip in plant roots could serves as a barrier to the translocation of organic compounds that cannot easily cross biological membranes, and (3) agricultural systems

contaminated with CECs can serve as sources of pollution to further contaminate the surrounding landscape. To test these hypotheses: (1) In vitro experiments examining the transformation of cephalexin in plant enzyme extracts and the sorption and affinity of cephalexin to plant roots could be used to explain the differences seen in the uptake and accumulation of cephalexin during in vivo hydroponic uptake experiments in lettuce, celery, and radish. (2) The characteristics of the hydroponic uptake of select PFAS into an *Arabidopsis thaliana* mutant, that does not develop a fully formed Casparian strip, and wild type *Arabidopsis thaliana* could be used to determine the influence of the Casparian strip on the magnitude and rate of accumulation of PFAS in plant shoots. (3) Data collected by the Michigan Department of Environment, Great Lakes, and Energy near Ft. Gratiot, Michigan, was examined to evaluate changes to the compositional profile of PFAS in surface waters and sediments over time and at sampling locations with varying distance from the contaminated source.

REFERENCES

REFERENCES

- Ahrens, L., Shoeib, M., Harner, T., Lee, S.C., Guo, R., Reiner, E.J., 2011. Wastewater treatment plant and landfills as sources of polyfluoroalkyl compounds to the atmosphere. Environ. Sci. Technol. 45, 8098-8105.
- Alder, A.C., van der Voet, J., 2015. Occurrence and point source characterization of perfluoroalkyl acids in sewage sludge. Chemosphere 129, 62-73.
- ASTDR, 2018. Toxicological profile for perfluoroalkyls department of health and human services, Public Health Service. https://www.atsdr.cdc.gov/toxprofiles/tp.asp?id=1117&tid=237.
- Backe, W.J., Day, T.C., Field, J.A., 2013. Zwitterionic, cationic, and anionic fluorinated chemicals in aqueous film forming foam formulations and groundwater from U.S. military bases by nonaqueous large-volume injection HPLC-MS/MS. Environ. Sci. Technol. 47, 5226-5234.
- Bao, J., Yu, W.J., Liu, Y., Wang, X., Jin, Y.H., Dong, G.H., 2019. Perfluoroalkyl substances in groundwater and home-produced vegetables and eggs around a fluorochemical industrial park in China. Ecotoxicol. Environ. Saf. 171, 199-205.
- Benskin, J.P., Muir, D.C., Scott, B.F., Spencer, C., De Silva, A.O., Kylin, H., Martin, J.W., Morris, A., Lohmann, R., Tomy, G., Rosenberg, B., Taniyasu, S., Yamashita, N., 2012. Perfluoroalkyl acids in the Atlantic and Canadian Arctic Oceans. Environ. Sci. Technol. 46, 5815-5823.
- Bizkarguenaga, E., Zabaleta, I., Mijangos, L., Iparraguirre, A., Fernandez, L.A., Prieto, A., Zuloaga, O., 2016a. Uptake of perfluorooctanoic acid, perfluorooctane sulfonate and perfluorooctane sulfonamide by carrot and lettuce from compost amended soil. Sci. Total Environ. 571, 444-451.
- Bizkarguenaga, E., Zabaleta, I., Prieto, A., Fernández, L.A., Zuloaga, O., 2016b. Uptake of 8:2 perfluoroalkyl phosphate diester and its degradation products by carrot and lettuce from compost-amended soil. Chemosphere 152, 309-317.
- Blaine, A.C., Rich, C.D., Hundal, L.S., Lau, C., Mills, M.A., Harris, K.M., Higgins, C.P., 2013. Uptake of perfluoroalkyl acids into edible crops via land applied biosolids: field and greenhouse studies. Environ. Sci. Technol. 47, 14062-14069.
- Blaine, A.C., Rich, C.D., Sedlacko, E.M., Hundal, L.S., Kumar, K., Lau, C., Mills, M.A., Harris, K.M., Higgins, C.P., 2014. Perfluoroalkyl acid distribution in various plant compartments of edible crops grown in biosolids-amended soils. Environ. Sci. Technol. 48, 7858-7865.

- Brambilla, G., D'Hollander, W., Oliaei, F., Stahl, T., Weber, R., 2015. Pathways and factors for food safety and food security at PFOS contaminated sites within a problem based learning approach. Chemosphere 129, 192-202.
- Brauer, M., Stitt, M., 1990. Vanadate inhibits fructose-2, 6-bisphosphatase and leads to an inhibition of sucrose synthesis in barley leaves. Physiol. Plantarum 78, 568-573.
- Braunig, J., Baduel, C., Barnes, C.M., Mueller, J.F., 2019. Leaching and bioavailability of selected perfluoroalkyl acids (PFAAs) from soil contaminated by firefighting activities. Sci. Total Environ. 646, 471-479.
- Buck, R.C., Franklin, J., Berger, U., Conder, J.M., Cousins, I.T., de Voogt, P., Jensen, A.A., Kannan, K., Mabury, S.A., van Leeuwen, S.P., 2011. Perfluoroalkyl and polyfluoroalkyl substances in the environment: terminology, classification, and origins. Integr. Environ. Assess. Manag. 7, 513-541.
- Chen, H., Yao, Y., Zhao, Z., Wang, Y., Wang, Q., Ren, C., Wang, B., Sun, H., Alder, A.C., Kannan, K., 2018. Multimedia distribution and transfer of per- and polyfluoroalkyl substances (PFASs) surrounding two fluorochemical manufacturing facilities in Fuxin, China. Environ. Sci. Technol. 52, 8263-8271.
- Collins, C., Fryer, M., Grosso, A., 2006. Plant uptake of non-ionic organic chemicals. Environ. Sci. Technol. 40, 45-52.
- Collins, C.D., Martin, I., Doucette, W., 2011. Plant uptake of xenobiotics. Plant Ecophysiology, Springer, Dordrecht 8, 3-16.
- Dalahmeh, S., Tirgani, S., Komakech, A.J., Niwagaba, C.B., Ahrens, L., 2018. Per- and polyfluoroalkyl substances (PFASs) in water, soil and plants in wetlands and agricultural areas in Kampala, Uganda. Sci. Total Environ. 631-632, 660-667.
- Dauchy, X., Boiteux, V., Colin, A., Hemard, J., Bach, C., Rosin, C., Munoz, J.F., 2019. Deep seepage of per- and polyfluoroalkyl substances through the soil of a firefighter training site and subsequent groundwater contamination. Chemosphere 214, 729-737.
- Domingo, J.L., Nadal, M., 2017. Per- and polyfluoroalkyl substances (PFASs) in food and human dietary intake: a review of the recent scientific literature. J. Agric. Food Chem. 65, 533-543.
- Ekvall, L., Greger, M., 2003. Effects of environmental biomass-producing factors on Cd uptake in two Swedish ecotypes of Pinus sylvestris. Environ. Pollut. 121, 401-411.
- Felizeter, S., McLachlan, M.S., de Voogt, P., 2012. Uptake of perfluorinated alkyl acids by hydroponically grown lettuce (Lactuca sativa). Environ. Sci. Technol. 46, 11735-11743.

- Felizeter, S., McLachlan, M.S., De Voogt, P., 2014. Root uptake and translocation of perfluorinated alkyl acids by three hydroponically grown crops. J. Agric. Food Chem. 62, 3334-3342.
- Fuertes, I., Gomez-Lavin, S., Elizalde, M.P., Urtiaga, A., 2017. Perfluorinated alkyl substances (PFASs) in northern Spain municipal solid waste landfill leachates. Chemosphere 168, 399-407.
- Gallen, C., Drage, D., Kaserzon, S., Baduel, C., Gallen, M., Banks, A., Broomhall, S., Mueller, J.F., 2016. Occurrence and distribution of brominated flame retardants and perfluoroalkyl substances in Australian landfill leachate and biosolids. J. Hazard. Mater. 312, 55-64.
- Gallen, C., Eaglesham, G., Drage, D., Nguyen, T.H., Mueller, J.F., 2018. A mass estimate of perfluoroalkyl substance (PFAS) release from Australian wastewater treatment plants. Chemosphere 208, 975-983.
- Garcia-Valcarcel, A.I., Molero, E., Escorial, M.C., Chueca, M.C., Tadeo, J.L., 2014. Uptake of perfluorinated compounds by plants grown in nutrient solution. Sci. Total Environ. 472, 20-26.
- Ghisi, R., Vamerali, T., Manzetti, S., 2018. Accumulation of perfluorinated alkyl substances (PFAS) in agricultural plants: A review. Environ. Res. 169, 326-341.
- Gobelius, L., Lewis, J., Ahrens, L., 2017. Plant uptake of per- and polyfluoroalkyl substances at a contaminated fire training facility to evaluate the phytoremediation potential of various plant species. Environ. Sci. Technol. 51, 12602-12610.
- Gottschall, N., Topp, E., Edwards, M., Payne, M., Kleywegt, S., Lapen, D.R., 2017. Brominated flame retardants and perfluoroalkyl acids in groundwater, tile drainage, soil, and crop grain following a high application of municipal biosolids to a field. Sci. Total Environ. 574, 1345-1359.
- Gredelj, A., Nicoletto, C., Valsecchi, S., Ferrario, C., Polesello, S., Lava, R., Zanon, F., Barausse, A., Palmeri, L., Guidolin, L., Bonato, M., 2019. Uptake and translocation of perfluoroalkyl acids (PFAA) in red chicory (Cichorium intybus L.) under various treatments with pre-contaminated soil and irrigation water. Sci. Total Environ. 708, 134766.
- Guo, C., Zhang, Y., Zhao, X., Du, P., Liu, S., Lv, J., Xu, F., Meng, W., Xu, J., 2015. Distribution, source characterization and inventory of perfluoroalkyl substances in Taihu Lake, China. Chemosphere 127, 201-207.
- Hepburn, E., Madden, C., Szabo, D., Coggan, T.L., Clarke, B., Currell, M., 2019. Contamination of groundwater with per- and polyfluoroalkyl substances (PFAS) from legacy landfills in an urban re-development precinct. Environ. Pollut. 248, 101-113.

- Herzke, D., Huber, S., Bervoets, L., D'Hollander, W., Hajslova, J., Pulkrabova, J., Brambilla, G., De Filippis, S.P., Klenow, S., Heinemeyer, G., de Voogt, P., 2013. Perfluorinated alkylated substances in vegetables collected in four European countries; occurrence and human exposure estimations. Environ. Sci. Pollut. Res. 20, 7930-7939.
- Higgins, C.P., Luthy, R.G., 2006. Sorption of perfluorinated surfactants on sediments. Environ. Sci. Technol. 40, 7251-7256.
- Itoh, S., Araki, A., Mitsui, T., Miyashita, C., Goudarzi, H., Sasaki, S., Cho, K., Nakazawa, H., Iwasaki, Y., Shinohara, N., Nonomura, K., Kishi, R., 2016. Association of perfluoroalkyl substances exposure in utero with reproductive hormone levels in cord blood in the Hokkaido Study on Environment and Children's Health. Environ. Int. 94, 51-59.
- Jin, H., Shan, G., Zhu, L., Sun, H., Luo, Y., 2018. Perfluoroalkyl acids including isomers in tree barks from a Chinese fluorochemical manufacturing park: implication for airborne transportation. Environ. Sci. Technol. 52, 2016-2024.
- Jin, H., Zhang, Y., Zhu, L., Martin, J.W., 2015. Isomer profiles of perfluoroalkyl substances in water and soil surrounding a chinese fluorochemical manufacturing park. Environ. Sci. Technol. 49, 4946-4954.
- Kim, H., Ekpe, O.D., Lee, J.H., Kim, D.H., Oh, J.E., 2019. Field-scale evaluation of the uptake of Perfluoroalkyl substances from soil by rice in paddy fields in South Korea. Sci. Total Environ. 671, 714-721.
- Kim, H.Y., Seok, H.W., Kwon, H.O., Choi, S.D., Seok, K.S., Oh, J.E., 2016. A national discharge load of perfluoroalkyl acids derived from industrial wastewater treatment plants in Korea. Sci. Total Environ. 563-564, 530-537.
- Krippner, J., Brunn, H., Falk, S., Georgii, S., Schubert, S., Stahl, T., 2014. Effects of chain length and pH on the uptake and distribution of perfluoroalkyl substances in maize (Zea mays). Chemosphere 94, 85-90.
- Krippner, J., Falk, S., Brunn, H., Georgii, S., Schubert, S., Stahl, T., 2015. Accumulation potentials of perfluoroalkyl carboxylic acids (PFCAs) and perfluoroalkyl sulfonic acids (PFSAs) in maize (Zea mays). J. Agric. Food Chem. 63, 3646-3653.
- Lai, L.B., Nadeau, J.A., Lucas, J., Lee, E.K., Nakagawa, T., Zhao, L., Geisler, M., Sack, F.D., 2005. The Arabidopsis R2R3 MYB proteins FOUR LIPS and MYB88 restrict divisions late in the stomatal cell lineage. Plant Cell 17, 2754-2767.
- Lan, Z., Zhou, M., Yao, Y., Sun, H., 2018. Plant uptake and translocation of perfluoroalkyl acids in a wheat-soil system. Environ. Sci. Pollut. Res. Int. 25, 30907-30916.
- Lechner, M., Knapp, H., 2011. Carryover of perfluorooctanoic acid (PFOA) and perfluorooctane sulfonate (PFOS) from soil to plant and distribution to the different plant compartments

- studied in cultures of carrots (Daucus carota ssp. Sativus), potatoes (Solanum tuberosum), and cucumbers (Cucumis Sativus). J. Agric. Food Chem. 59, 11011-11018.
- Lee, H., Tevlin, A.G., Mabury, S.A., Mabury, S.A., 2014. Fate of polyfluoroalkyl phosphate diesters and their metabolites in biosolids-applied soil: biodegradation and plant uptake in greenhouse and field experiments. Environ. Sci. Technol. 48, 340-349.
- Li, Y., Sallach, J.B., Zhang, W., Boyd, S.A., Li, H., 2018. Insight into the distribution of pharmaceuticals in soil-water-plant systems. Water Res. 152, 38-46.
- Lindstrom, A.B., Strynar, M.J., Delinsky, A.D., Nakayama, S.F., McMillan, L., Libelo, E.L., Neill, M., Thomas, L., 2011. Application of WWTP biosolids and resulting perfluorinated compound contamination of surface and well water in Decatur, Alabama, USA. Environ. Sci. Technol. 45, 8015-8021.
- Liu, Y., Hou, X., Chen, W., Kong, W., Wang, D., Liu, J., Jiang, G., 2019a. Occurrences of perfluoroalkyl and polyfluoroalkyl substances in tree bark: Interspecies variability related to chain length. Sci. Total Environ. 689, 1388-1395.
- Liu, Z., Lu, Y., Shi, Y., Wang, P., Jones, K., Sweetman, A.J., Johnson, A.C., Zhang, M., Zhou, Y., Lu, X., Su, C., Sarvajayakesavaluc, S., Khan, K., 2017a. Crop bioaccumulation and human exposure of perfluoroalkyl acids through multi-media transport from a mega fluorochemical industrial park, China. Environ. Int. 106, 37-47.
- Liu, Z., Lu, Y., Song, X., Jones, K., Sweetman, A.J., Johnson, A.C., Zhang, M., Lu, X., Su, C., 2019b. Multiple crop bioaccumulation and human exposure of perfluoroalkyl substances around a mega fluorochemical industrial park, China: Implication for planting optimization and food safety. Environ. Int. 127, 671-684.
- Liu, Z., Lu, Y., Wang, P., Wang, T., Liu, S., Johnson, A.C., Sweetman, A.J., Baninla, Y., 2017b. Pollution pathways and release estimation of perfluorooctane sulfonate (PFOS) and perfluorooctanoic acid (PFOA) in central and eastern China. Sci. Total Environ. 580, 1247-1256.
- Liu, Z., Lu, Y., Wang, T., Wang, P., Li, Q., Johnson, A.C., Sarvajayakesavalu, S., Sweetman, A.J., 2016. Risk assessment and source identification of perfluoroalkyl acids in surface and ground water: Spatial distribution around a mega-fluorochemical industrial park, China. Environ. Int. 91, 69-77.
- Lofstedt Gilljam, J., Leonel, J., Cousins, I.T., Benskin, J.P., 2016. Is ongoing sulfluramid use in South America a significant source of perfluorooctanesulfonate (PFOS)? production inventories, environmental fate, and local occurrence. Environ. Sci. Technol. 50, 653-659.

- Loganathan, B.G., Sajwan, K.S., Sinclair, E., Kumar, K.S., Kannan, K., 2007. Perfluoroalkyl sulfonates and perfluorocarboxylates in two wastewater treatment facilities in Kentucky and Georgia. Water Res. 41, 4611-4620.
- Lu, Z., Song, L., Zhao, Z., Ma, Y., Wang, J., Yang, H., Ma, H., Cai, M., Codling, G., Ebinghaus, R., Xie, Z., Giesy, J.P., 2015. Occurrence and trends in concentrations of perfluoroalkyl substances (PFASs) in surface waters of eastern China. Chemosphere 119, 820-827.
- Milinovic, J., Lacorte, S., Vidal, M., Rigol, A., 2015. Sorption behaviour of perfluoroalkyl substances in soils. Sci. Total Environ. 511, 63-71.
- Moody, C.A., Field, J.A., 1999. Determination of perfluorocarboxylates in groundwater impacted by fire-fighting activity. Environ. Sci. Technol. 33, 2800-2806.
- Muller, C.E., LeFevre, G.H., Timofte, A.E., Hussain, F.A., Sattely, E.S., Luthy, R.G., 2016. Competing mechanisms for perfluoroalkyl acid accumulation in plants revealed using an Arabidopsis model system. Environ. Toxicol. Chem. 35, 1138-1147.
- Nascimento, R.A., Nunoo, D.B.O., Bizkarguenaga, E., Schultes, L., Zabaleta, I., Benskin, J.P., Spano, S., Leonel, J., 2018. Sulfluramid use in Brazilian agriculture: A source of per- and polyfluoroalkyl substances (PFASs) to the environment. Environ. Pollut. 242, 1436-1443.
- Pan, C.G., Liu, Y.S., Ying, G.G., 2016. Perfluoroalkyl substances (PFASs) in wastewater treatment plants and drinking water treatment plants: Removal efficiency and exposure risk. Water Res. 106, 562-570.
- Pan, Y., Zhang, H., Cui, Q., Sheng, N., Yeung, L.W.Y., Sun, Y., Guo, Y., Dai, J., 2018. Worldwide distribution of novel perfluoroether carboxylic and sulfonic acids in surface water. Environ. Sci. Technol. 52, 7621-7629.
- Paul, A.G., Jones, K.C., Sweetman, A.J., 2008. A first global production, emission, and environmental inventory for perfluorooctane sulfonate. Environ. Sci. Technol. 43, 386-392.
- Perez, F., Llorca, M., Kock-Schulmeyer, M., Skrbic, B., Oliveira, L.S., da Boit Martinello, K., Al-Dhabi, N.A., Antic, I., Farre, M., Barcelo, D., 2014. Assessment of perfluoroalkyl substances in food items at global scale. Environ. Res. 135, 181-189.
- Pimentel, D., Berger, B., Filiberto, D., Newton, M., Wolfe, B., Karabinakis, E., Clark, S., Poon, E., Abbett, E., Nandagopal, S., 2004. Water resources: agricultural and environmental issues. BioScience 54, 909-918.
- Plumlee, M.H., McNeill, K., Reinhard, M., 2009. Indirect photolysis of perfluorochemicals: hydroxyl radical-initiated oxidation of N-ethyl perfluoroctane sulfonamido acetate (N-EtFOSAA) and other perfluoroalkanesulfonamides. Environ. Sci. Technol. 43, 3662-3668.

- Prevedouros, K., Cousins, I.T., Buck, R.C., Korzeniowski, S.H., 2006. Sources, fate and transport of perfluorocarboxylates. Environ. Sci. Technol. 40, 32-44.
- Qu, B., Zhao, H., Zhou, J., 2010. Toxic effects of perfluorooctane sulfonate (PFOS) on wheat (Triticum aestivum L.) plant. Chemosphere 79, 555-560.
- Scher, D.P., Kelly, J.E., Huset, C.A., Barry, K.M., Hoffbeck, R.W., Yingling, V.L., Messing, R.B., 2018. Occurrence of perfluoroalkyl substances (PFAS) in garden produce at homes with a history of PFAS-contaminated drinking water. Chemosphere 196, 548-555.
- Schultz, M.M., Higgins, C.P., Huset, C.A., Luthy, R.G., Barofsky, D.F., Field, J.A., 2006. Fluorochemical mass flows in a municipal wastewater treatment facility. Environ. Sci. Technol. 40, 7350-7357.
- Scott, B.F., Spencer, C., Mabury, S.A., Muir, D.C.G., 2006. Poly and perfluorinated carboxylates in North American precipitation. Environ. Sci. Technol. 40, 7167-7174.
- Shan, G., Wei, M., Zhu, L., Liu, Z., Zhang, Y., 2014. Concentration profiles and spatial distribution of perfluoroalkyl substances in an industrial center with condensed fluorochemical facilities. Sci. Total Environ. 490, 351-359.
- Stahl, T., Heyn, J., Thiele, H., Huther, J., Failing, K., Georgii, S., Brunn, H., 2009. Carryover of perfluorooctanoic acid (PFOA) and perfluorooctane sulfonate (PFOS) from soil to plants. Arch. Environ. Contam. Toxicol. 57, 289-298.
- Stahl, T., Riebe, R.A., Falk, S., Failing, K., Brunn, H., 2013. Long-term lysimeter experiment to investigate the leaching of perfluoroalkyl substances (PFASs) and the carry-over from soil to plants: results of a pilot study. J. Agric. Food Chem. 61, 1784-1793.
- Stofberg, S.F., Klimkowska, A., Paulissen, M.P.C.P., Witte, J.-P.M., van der Zee, S.E.A.T.M., 2015. Effects of salinity on growth of plant species from terrestrializing fens. Aquatic Botany 121, 83-90.
- Sznajder-Katarzynska, K., Surma, M., Cieslik, E., Wiczkowski, W., 2018. The perfluoroalkyl substances (PFASs) contamination of fruits and vegetables. Food Addit. Contam. Part A Chem. Anal. Control Expo. Risk Assess. 35, 1776-1786.
- Taniyasu, S., Yamashita, N., Moon, H.B., Kwok, K.Y., Lam, P.K., Horii, Y., Petrick, G., Kannan, K., 2013. Does wet precipitation represent local and regional atmospheric transportation by perfluorinated alkyl substances? Environ. Int. 55, 25-32.
- Tian, Y., Yao, Y., Chang, S., Zhao, Z., Zhao, Y., Yuan, X., Wu, F., Sun, H., 2018. Occurrence and phase distribution of neutral and ionizable per- and polyfluoroalkyl substances (PFASs) in the atmosphere and plant leaves around landfills: A case study in Tianjin, China. Environ. Sci. Technol. 52, 1301-1310.

- van Asselt, E.D., Rietra, R.P., Romkens, P.F., van der Fels-Klerx, H.J., 2011. Perfluorooctane sulphonate (PFOS) throughout the food production chain. Food Chem. 128, 1-6.
- Venkatesan, A.K., Halden, R.U., 2013. National inventory of perfluoroalkyl substances in archived US biosolids from the 2001 EPA National Sewage Sludge Survey. J. Hazard. Mater. 252, 413-418.
- Vestergren, R., Orata, F., Berger, U., Cousins, I.T., 2013. Bioaccumulation of perfluoroalkyl acids in dairy cows in a naturally contaminated environment. Environ. Sci. Pollut. Res. 20, 7959-7969.
- Vuong, A.M., Yolton, K., Wang, Z., Xie, C., Webster, G.M., Ye, X., Calafat, A.M., Braun, J.M., Dietrich, K.N., Lanphear, B.P., Chen, A., 2018. Childhood perfluoroalkyl substance exposure and executive function in children at 8years. Environ. Int. 119, 212-219.
- Washington, J.W., Yoo, H., Ellington, J.J., Jenkins, T.M., Libelo, E.L., 2010. Concentrations, distribution, and persistence of perfluoroalkylates in sludge-applied soils near Decatur, Alabama, USA. Environ. Sci. Technol. 44, 8390-8396.
- Weinberg, I., Dreyer, A., Ebinghaus, R., 2011. Landfills as sources of polyfluorinated compounds, polybrominated diphenyl ethers and musk fragrances to ambient air. Atmos. Environ. 45, 935-941.
- Wen, B., Li, L., Liu, Y., Zhang, H., Hu, X., Shan, X.-q., Zhang, S., 2013. Mechanistic studies of perfluorooctane sulfonate, perfluorooctanoic acid uptake by maize (Zea mays L. cv. TY2). Plant Soil 370, 345-354.
- Wen, B., Li, L., Zhang, H., Ma, Y., Shan, X.Q., Zhang, S., 2014. Field study on the uptake and translocation of perfluoroalkyl acids (PFAAs) by wheat (Triticum aestivum L.) grown in biosolids-amended soils. Environ. Pollut. 184, 547-554.
- Wen, B., Pan, Y., Shi, X., Zhang, H., Hu, X., Huang, H., Lv, J., Zhang, S., 2018. Behavior of Nethyl perfluorooctane sulfonamido acetic acid (N-EtFOSAA) in biosolids amended soilplant microcosms of seven plant species: Accumulation and degradation. Sci. Total Environ. 642, 366-373.
- Wen, B., Wu, Y., Zhang, H., Liu, Y., Hu, X., Huang, H., Zhang, S., 2016. The roles of protein and lipid in the accumulation and distribution of perfluorooctane sulfonate (PFOS) and perfluorooctanoate (PFOA) in plants grown in biosolids-amended soils. Environ. Pollut. 216, 682-688.
- Wu, J., Martin, J.W., Zhai, Z., Lu, K., Li, L., Fang, X., Jin, H., Hu, J., Zhang, J., 2014. Airborne trifluoroacetic acid and its fraction from the degradation of HFC-134a in Beijing, China. Environ. Sci. Technol. 48, 3675-3681.

- Xiang, L., Chen, L., Yu, L.Y., Yu, P.F., Zhao, H.M., Mo, C.H., Li, Y.W., Li, H., Cai, Q.Y., Zhou, D.M., Wong, M.H., 2018. Genotypic variation and mechanism in uptake and translocation of perfluorooctanoic acid (PFOA) in lettuce (Lactuca sativa L.) cultivars grown in PFOA-polluted soils. Sci. Total Environ. 636, 999-1008.
- Yan, H., Cousins, I.T., Zhang, C., Zhou, Q., 2015. Perfluoroalkyl acids in municipal landfill leachates from China: Occurrence, fate during leachate treatment and potential impact on groundwater. Sci. Total Environ. 524-525, 23-31.
- Yang, X., Ye, C., Liu, Y., Zhao, F.J., 2015. Accumulation and phytotoxicity of perfluorooctanoic acid in the model plant species Arabidopsis thaliana. Environ. Pollut. 206, 560-566.
- Yoo, H., Washington, J.W., Jenkins, T.M., Ellington, J.J., 2011. Quantitative determination of perfluorochemicals and fluorotelomer alcohols in plants from biosolid-amended fields using LC/MS/MS and GC/MS. Environ. Sci. Technol. 45, 7985-7990.
- Yu, P.F., Xiang, L., Li, X.H., Ding, Z.R., Mo, C.H., Li, Y.W., Li, H., Cai, Q.Y., Zhou, D.M., Wong, M.H., 2018. Cultivar-dependent accumulation and translocation of perfluorooctane sulfonate (PFOS) among lettuce (Lactuca sativa L.) cultivars grown on PFOS-contaminated soil. J. Agric. Food Chem. 66, 13096-13106.
- Zelitch, I., 1965. Environmental and biochemical control of stomatal movement in leaves. Biol. Rev. 40, 463-481.
- Zhang, H., Wen, B., Hu, X., Wu, Y., Pan, Y., Huang, H., Liu, L., Zhang, S., 2016. Uptake, translocation, and metabolism of 8:2 fluorotelomer alcohol in soybean (Glycine max L. Merrill). Environ. Sci. Technol. 50, 13309-13317.
- Zhang, L., Liu, J., Hu, J., Liu, C., Guo, W., Wang, Q., Wang, H., 2012. The inventory of sources, environmental releases and risk assessment for perfluorooctane sulfonate in China. Environ. Pollut. 165, 193-198.
- Zhang, L., Sun, H., Wang, Q., Chen, H., Yao, Y., Zhao, Z., Alder, A.C., 2019. Uptake mechanisms of perfluoroalkyl acids with different carbon chain lengths (C2-C8) by wheat (Triticum acstivnm L.). Sci. Total Environ. 654, 19-27.
- Zhang, W., Tyerman, S., 1991. Effect of low O2 concentration and azide on hydraulic conductivity and osmotic volume of the cortical cells of wheat roots. Funct. Plant Biol. 18, 603-613.
- Zhao, H., Guan, Y., Qu, B., 2018a. PFCA uptake and translocation in dominant wheat species (Triticum aestivum L.). Int. J. Phytoremediation 20, 68-74.
- Zhao, H., Guan, Y., Zhang, G., Zhang, Z., Tan, F., Quan, X., Chen, J., 2013. Uptake of perfluorooctane sulfonate (PFOS) by wheat (Triticum aestivum L.) plant. Chemosphere 91, 139-144.

- Zhao, H., Qu, B., Guan, Y., Jiang, J., Chen, X., 2016a. Influence of salinity and temperature on uptake of perfluorinated carboxylic acids (PFCAs) by hydroponically grown wheat (Triticum aestivum L.). Springerplus 5, 541.
- Zhao, L., Zhu, L., Yang, L., Liu, Z., Zhang, Y., 2012. Distribution and desorption of perfluorinated compounds in fractionated sediments. Chemosphere 88, 1390-1397.
- Zhao, L., Zhu, L., Zhao, S., Ma, X., 2016b. Sequestration and bioavailability of perfluoroalkyl acids (PFAAs) in soils: Implications for their underestimated risk. Sci. Total Environ. 572, 169-176.
- Zhao, S., Fan, Z., Sun, L., Zhou, T., Xing, Y., Liu, L., 2017. Interaction effects on uptake and toxicity of perfluoroalkyl substances and cadmium in wheat (Triticum aestivum L.) and rapeseed (Brassica campestris L.) from co-contaminated soil. Ecotoxicol. Environ. Saf. 137, 194-201.
- Zhao, S., Fang, S., Zhu, L., Liu, L., Liu, Z., Zhang, Y., 2014. Mutual impacts of wheat (Triticum aestivum L.) and earthworms (Eisenia fetida) on the bioavailability of perfluoroalkyl substances (PFASs) in soil. Environ. Pollut. 184, 495-501.
- Zhao, S., Liang, T., Zhu, L., Yang, L., Liu, T., Fu, J., Wang, B., Zhan, J., Liu, L., 2019. Fate of 6:2 fluorotelomer sulfonic acid in pumpkin (Cucurbita maxima L.) based on hydroponic culture: Uptake, translocation and biotransformation. Environ. Pollut. 252, 804-812.
- Zhao, S., Zhou, T., Wang, B., Zhu, L., Chen, M., Li, D., Yang, L., 2018b. Different biotransformation behaviors of perfluorooctane sulfonamide in wheat (Triticum aestivum L.) from earthworms (Eisenia fetida). J. Hazard. Mater. 346, 191-198.
- Zhao, S., Zhou, T., Zhu, L., Wang, B., Li, Z., Yang, L., Liu, L., 2018c. Uptake, translocation and biotransformation of N-ethyl perfluorooctanesulfonamide (N-EtFOSA) by hydroponically grown plants. Environ. Pollut. 235, 404-410.
- Zhou, L., Xia, M., Wang, L., Mao, H., 2016. Toxic effect of perfluorooctanoic acid (PFOA) on germination and seedling growth of wheat (Triticum aestivum L.). Chemosphere 159, 420-425.
- Zhu, H., Kannan, K., 2019. Distribution and partitioning of perfluoroalkyl carboxylic acids in surface soil, plants, and earthworms at a contaminated site. Sci. Total Environ. 647, 954-961.

CHAPTER II.

UPTAKE OF CEPHALEXIN BY LETTUCE, CELERY, AND RADISH FROM WATER

ABSTRACT

The introduction of pharmaceuticals into agricultural lands from the application of biosolids and animal manure, and irrigation with treated wastewater has led to concern for animal and human health after the ingestion of pharmaceutical-tainted agricultural products. The uptake and accumulation of cephalexin, a commonly prescribed antibiotic, was compared in three common vegetables (lettuce, celery, and radish) grown in nutrient solution for 144 hrs. During the uptake experiments, cephalexin concentration in the nutrient solution decreased in the order of radish > celery > lettuce, while the accumulation of cephalexin in vegetable roots followed the rank of lettuce > celery > radish. The accumulation of cephalexin was below the limit of detection in radish roots. No accumulation of cephalexin was observed in the shoots of all three vegetables. The behaviors of cephalexin in vivo were further elucidated using in vitro measurements of cephalexin sorption by vegetable roots and transformation in plant enzyme extracts. The affinity of cephalexin to lettuce > celery > radish roots, and the respective sorption coefficients of 687, 303, and 161 mL/g, coupled to the transformation of cephalexin in root enzyme extracts with estimated reaction rate constants of 0.020, 0.027 and 0.024 hr⁻¹ for lettuce, celery, and radish, could help elucidate the accumulation observed in the in vivo experiments. Overall, sorption by plant roots (affinity) and reaction with plant enzymes could collectively influence the uptake and accumulation of cephalexin in vegetables.

INTRODUCTION

The scarcity of water resources for agricultural use is a tremendous challenge in many arid and semi-arid regions of the world. As changes in precipitation patterns and increasing populations exacerbate the water scarcity, water reuse is becoming a common practice, particularly in agricultural irrigation (U.S. EPA, 2020). In addition, livestock manures from concentrated animal feeding operations and biosolids from wastewater treatment plants (WWTPs) are increasingly applied to agricultural fields to provide nutrients for plant growth and improve soil quality (U.S. EPA, 1999). These practices have led to the widespread dissemination of veterinary and human pharmaceuticals in agricultural systems across the globe (Aga et al., 2005; Edwards et al., 2009; Fu et al., 2019).

Many pharmaceuticals in soils can enter vegetables and other crops with concentrations reaching ng g⁻¹ levels (Sabourin et al., 2012; Wu et al., 2015; Malchi et al., 2014). Although the concentrations found in crops are typically far below the effective dose, there is increasing evidence that the presence of antibiotics, even at non-inhibitory levels, could lead to an increase in antibiotic resistant bacteria or resistance genes (Andersson and Hughes, 2014; Sinel et al., 2017; Shen et al., 2019). A rise in antibiotic resistance is a critical issue, given that bacteria can be internalized into plant tissues (Itoh et al. 1998; Nthenge et al., 2007; Koseki et al., 2011) and numerous outbreaks of food poisoning are associated with the ingestion of fresh vegetables (EFSA Panel on Biological Hazards, 2013; Lynch et al., 2009; Taylor et al., 2013). This leads to concerns about human and livestock health after the consumption of pharmaceutical-tainted agricultural products (Wu et al., 2013; Prosser and Sibley, 2015; Rehman et al., 2015). In addition, pharmaceuticals accumulated in plants can induce changes in plant hormone levels, which can negatively affect plant health (Carter et al., 2015; An et al., 2009). These concerns

have spurred significant research efforts into the mechanism(s) and factors that govern plant uptake and accumulation of pharmaceuticals.

Recent studies have advanced our understanding on the uptake and accumulation of pharmaceuticals by plants. Miller et al. (2016) analyzed literature data and found no apparent relationship between the root concentration factor and the pH-adjusted octanol-water partitioning coefficient normalized to neutral pharmaceutical speciation, indicating that the uptake and distribution of pharmaceuticals is not singularly governed by their lipophilicity. Chuang et al. (2019) showed that pharmaceutical distribution and transport in lettuce could be related to their affinity to lettuce tissues. Pharmaceuticals with a high affinity for root tissues are localized more in the roots, thereby limiting their transport to shoots. Transpiration stream is likely the major carrier transporting pharmaceuticals from roots to shoots; the large amount of transpired water could carry more pharmaceuticals to plant shoots leading to higher accumulation (Dodgen et al., 2015; Winker et al., 2010; Sauvêtre et al., 2018). Transport from lettuce roots to shoots could also be influenced by the charged speciation and molecular size of pharmaceuticals. Large-sized pharmaceuticals, e.g., molecular weight > 400 g mol⁻¹, can be localized primarily in lettuce roots during a short period of uptake (e.g., < 144 h) due to the difficulty in crossing plant cell membranes (Chuang et al., 2019). Many pharmaceuticals are intensively metabolized in plants (Li et al., 2018; Fu et al., 2017; Wu et al., 2016); however, little knowledge is available on the clear mechanisms of metabolization.

Although an understanding of some fundamental processes that regulate plant uptake of many pharmaceuticals has been developed, few studies have been conducted to investigate the uptake and accumulation of cephalexin by plants. Cephalexin, one the first generation of cephalosporin antibiotics, has been extensively used in veterinary and human medicine.

According to the Medical Expenditure Panel Survey, cephalexin was among the top 20 % of the most commonly prescribed medications in the United States; approximately 7,229,000 purchases were performed in 2017 (Agency for Healthcare Research and Quality, 2010-2017). Cephalexin is excreted relatively unchanged in human urine, with 85% of the initial dosage being accounted for after 24 hrs (Hartstein et al., 1977). As a result, cephalexin was frequently detected in wastewater with concentration up to 64 ng mL⁻¹ (Watkinson et al., 2009). Cephalexin exhibits widely varying removal rates, between 9 and 96% at WWTPs (Watkinson et al., 2009; Gulkowska et al., 2008). Yang et al. (2014) investigated the prevalence of antibiotic resistant bacteria at farms that used animal manures as fertilizers (from livestock treated with cephalexin), and found that plant tissues of celery, bok choy, and cucumber contained culturable bacteria resistant to cephalexin.

The purpose of this study was to assess uptake, accumulation, and transformation of cephalexin in three common vegetables, lettuce, celery, and radish. These three vegetables were grown hydroponically and exposed to cephalexin in a nutrient solution at an environmentally relevant concentration (20 ng mL⁻¹). Plant tissues were sampled at several times over the exposure period of 144 hrs, extracted and analyzed for cephalexin concentration. In addition, sorption of cephalexin by vegetable roots and reaction with extracted vegetable crude enzymes were used to further evaluate its accumulation and dissemination in lettuce, celery, and radish. The results from this study improve the understanding of the uptake, accumulation, and transformation of cephalexin in vegetables.

MATERIALS AND METHODS

Chemicals and reagents

Cephalexin (99.7%), HPLC-grade methanol and acetonitrile were purchased from Sigma-Aldrich (St. Louis, MO, USA). The physiochemical properties of cephalexin are given in Table 2.1. Ultrapure water was obtained from a Milli-Q water purification system (Millipore, Billerica, MA, USA). Disodium ethylenediaminetetraacetate (Na₂EDTA), sodium chloride (NaCl), glacial acetic acid, and formic acid were purchased from J.T. Baker (Phillipsburg, NJ, USA). Anhydrous sodium sulfate (Na₂SO₄) was obtained from EMD Chemicals (Gibbstown, NJ, USA). Ceramic homogenizers, primary secondary amine (PSA) and C18 powders were purchased from Agilent Technologies (Santa Clara, CA, USA). Oasis hydrophilic–lipophilic balance (HLB) cartridges were acquired from Waters Corporation (Milford, MA, USA). Bradford reagent and bovine serum albumin (BSA) were purchased from Bio-Rad Laboratories, Inc. (Hercules, CA, USA). Monobasic potassium phosphate (KH₂PO₄) and dibasic potassium phosphate (K₂HPO₄) were purchased from Fisher Scientific (Fair Lawn, NJ, USA).

 Table 2.1 Physiochemical properties of Cephalexin.

Molecular weight	Water Solubility ^a	$p{K_a}^a$	Predominant species (%)	$log K_{ow}{}^a$
(g mol ⁻¹)	$(mg mL^{-1})$		(pH at 5.8)	
347.39	10	5.2, 7.3	Zwitterion: 80	0.65

ahttps://pubchem.ncbi.nlm.nih.gov/

Vegetable uptake of cephalexin

The hydroponic method used in this study is similar to that used by Chuang et al. (2019). Black Seeded Simpson lettuce and Crimson Giant radish seeds were purchased from W. Atlee Burpee & Co. (Warminster, PA, USA), and Utah 52-70 celery seeds were purchased from Generic Seeds (Springville, UT, USA). The lettuce, celery, and radish seeds were sprouted on moistened paper towel for three, eight, and four days, respectively, in a sterile and clear-topped plastic container at 18°C. During sprouting, the seeds were exposed to 150 µmol photons/m²/s of photosynthetically available radiation for 2 hrs per day. After sprouting, the plant seedlings were transferred to polystyrene foam flats floating in 15 L of DI water (pH 5.6 to 5.8), and continuously aerated using a Fusion 600 air pump (JW Pet Company Inc., Teterboro, NJ, USA) with an air flow rate of ~10 L hr⁻¹. The photoperiod increased to 16 hrs per day since then. The temperature of the growth room was kept constant at 18°C. After four days, MaxiGro plant food (10-5-14) (General Hydroponics, Sevastopol, CA, USA) was added to the hydroponic solution so that electrical conductivity (EC) gradually increased to 0.8 mS/cm over the course of 24 days. The lettuce, celery, and radish seedlings grew for approximately 28, 34, and 26 days, respectively, before a single plant was transferred to an Erlenmeyer flask. The flasks each contained ~210 mL of nutrient solution, which was prepared by dissolving MaxiGro plant food (10-5-4) in DI water. The solution EC was adjusted at 0.8 mS/cm, pH at 5.6 to 5.8, and was continuously aerated at ~0.2 L hr⁻¹. The flasks were completely wrapped in aluminum foil to prevent algal growth and the potential photodegradation of cephalexin. After acclimating the plants to individual cultures for two days, the solution was replaced with nutrient solution containing 20 ng mL⁻¹ cephalexin. During the course of the experiment, at 12 hr intervals, water loss (mostly due to transpiration) and plant biomass was measured gravimetrically, and solution

volume, pH, and EC were checked and maintained at their original levels. At 10, 24, 48, 72, 106, and 144 hrs of sampling time, triplicate samples were collected for each type of plant, and the collected plant tissues were subject to extraction and analysis of cephalexin. The experimental controls included each type of plant that had not been exposed to cephalexin in the nutrient solution, and cephalexin in the nutrient solution (~20 ng mL⁻¹) but without plants. No apparent physiological differences were observed between the control plants and the plants exposed to cephalexin. The sampled plants were gently rinsed with deionized water and blotted dry with paper tissue. The plants were then separated into roots and shoots by a direct cut below the cotyledon, immediately frozen in liquid nitrogen and lyophilized, and ground to powder. The samples were stored at -20°C prior to extraction.

Cephalexin extraction

Cephalexin in the nutrient solution was extracted using Oasis HLB solid-phase extraction (SPE) cartridges. Twenty milliliters of nutrient solution were passed through the preconditioned cartridge and eluted with 5.0 mL of methanol. The elutes were diluted with an equal volume of Milli-Q water and stored in vials in a refrigerator prior to analysis. Plant root and shoot tissues were extracted using a modified QuEChERS method (Chuang et al., 2015). Plant tissue samples (250 mg shoots or 100 mg roots) were vortexed with 1.0 mL of 300 mg L⁻¹ Na₂EDTA for 1 minute, then two ceramic homogenizers were added, along with 1.75 mL of methanol, and the resulting mixture was vortexed for 2 min. Afterward, 2.0 g of Na₂SO₄ and 0.5 g of NaCl were added, and the mixture was vortexed for additional 2 min. The extracts were then centrifuged at 5050 g for 10 min at 4°C, and the supernatant was collected. The residues were extracted with 3.25 mL of acetonitrile by vortexing for 2 min and centrifuged at 5050 g for 10 min at 4°C. The two supernatants were combined, and 1.2 mL of the combined extract was cleaned up using

dispersed SPE (d-SPE) sorbents. The d-SPE consisted of 12.5 mg of PSA, 12.5 mg of C18, and 225 mg of Na₂SO₄. The d-SPE was added to the combined extracts, vortexed for 1 minute, and centrifuged at 9240 *g* for 10 min. The supernatant was transferred to a clean amber glass vial and stored at -20 °C until analysis. The analytical samples were prepared by mixing with the same volume of Milli-Q water prior to analysis. The extraction efficiencies were measured and are listed in Table 2.2.

Table 2.2 Extraction efficiency (%) of cephalexin from nutrient solution, and lettuce, celery, and radish roots and shoots using the QuEChERS method. *The extraction efficiency is presented as mean values and standard deviations* (n = 3).

Vegetable		Extraction Efficiency
Lettuce	Root	$70.5\% \pm 0.4$
	Shoot	$86.0\% \pm 2.0$
Celery	Root	$50.2\% \pm 2.6$
	Shoot	$83.1\% \pm 16.3$
Dadiah	Root	$62.0\% \pm 0.9$
Radish	Shoot	$37.9\% \pm 7.1$
Nutrient Solution		$93.6\% \pm 1.7$

Cephalexin analysis

Cephalexin concentration was determined using a Shimadzu prominence highperformance liquid chromatography system (LC, Shimadzu, Columbia, MD) coupled to an AB Sciex 4500 QTrap triple quadrupole mass spectrometer (MS/MS, SCIEX, Foster City, CA). An Agilent Eclipse Plus C18 column (50mm×2.1mm, 5μm) (Agilent, Santa Clara, CA) was used in the LC-MS/MS, and the ionization source was set to positive ionization mode. The sample injection volume was set at 10 μL, and the flow rate at 0.35 mL min⁻¹. The binary mobile phase consisted of water (mobile phase A) and acetonitrile (mobile phase B) both containing 0.1% (v/v) formic acid. The gradient program was as follows: after 1 min pre-equilibration with 100% mobile phase A, mobile phase B increased to 40% from 0.01 to 1.0 min, then to 70% from 1.0 to 2.0 min, remained at 70% from 2.0 to 3.2 min, then increased to 100% from 3.2 to 3.5 min, and remained at 100% until 4.5 min. The retention time of cephalexin was 2.56 min. The curtain gas pressure, ion spray voltage, temperature, and entrance potential were 20 psi, 5000 V, 700 °C, and 10 V, respectively. Multiple reaction monitoring (MRM) mode was used for identification and quantification with the parent ion and three daughter ions at m/z 348.0, m/z 190.5, m/z 174.0, and m/z 158.0, respectively. The ion transition 348.0/158.0 was used for quantification, and two pairs of ion transition 348.0/190.5 and 348.0/174.0 were used for qualification. All samples were quantified using matrix-matched standard curves.

Sorption by vegetable roots

Cephalexin sorption to dried lettuce, celery, and radish roots from the nutrient solution was determined using the batch equilibration method described by Card et al. (2012).

Lyophilized lettuce, celery, and radish root powders (25 mg) were mixed with 20 mL of nutrient solution containing cephalexin at 0, 10, 20, 30, 40, and 50 ng mL⁻¹. Experimental controls

consisted of nutrient solution containing cephalexin at the above concentrations but devoid of plant root powders. The tubes were rotated at 25 rpm on a RD4512 rotator (Glas-Col, Terra Haute, IN, USA) for 24 hrs in the dark. They were then centrifuged at 1460 g for 15 min. The supernatant was collected to measure cephalexin concentration using LC-MS/MS. The difference between the initial and final mass of cephalexin in the nutrient solution was assumed to be sorbed by lettuce, celery, or radish roots. To examine the strength of the interaction between cephalexin and root tissues, the recoverable cephalexin after sorption by vegetable root tissues was examined. The vegetable root residues mixed with the initial solution of 50 ng mL⁻¹ cephalexin were extracted using the modified QuEChERS method. The recoverable cephalexin was calculated on the basis of the amount of root-sorbed cephalexin.

In vitro transformation of cephalexin

In vitro cephalexin transformation was examined using crude plant enzyme extracts (Card et al., 2013). Fresh lettuce, celery, and radish tissues were separated into roots and shoots and immediately frozen in liquid nitrogen. The tissue was then ground in liquid nitrogen and extracted using 50 mM potassium phosphate buffer (pH 7.0) with a ratio of fresh plant tissue weight to solution volume of 1.0 : 4.5 (g : mL). The plant tissue and phosphate buffer mixture was rotated at 25 rpm and 4 °C for 30 minutes using the RD4512 rotator. The homogenate was centrifuged at 10,000 g for 25 min at 4 °C. The supernatant was collected and used immediately in the *in vitro* transformation experiments. Another set of the supernatant samples was used to measure the total protein content. The protein content in the crude enzyme extracts was measured using the Bradford Assay utilizing bovine serum albumin as the standard (Bradford, 1976). These measurements were used to adjust the amount of protein content to the same level in the reaction with cephalexin.

The *in vitro* transformation experiment was performed by gently mixing 950 μL of crude enzyme extracts with 50 μL of cephalexin solution in 50 mM potassium phosphate buffer (pH 7.0) to achieve the final concentration of 100 ng mL⁻¹. The reaction was incubated in a 25°C water bath and quenched via adding 50 μL glacial acetic acid. The experiments were conducted in triplicate, and were sampled at 1, 2, 6, 12, 24, 48, 72, and 96 hrs for LC-MS/MS analysis. The controls included cephalexin solution in the potassium phosphate buffer devoid of lettuce, celery, or radish enzyme extracts.

RESULTS AND DISCUSSION

Cephalexin uptake by vegetables

Cephalexin concentration in the nutrient solution and the roots and shoots of lettuce, celery, and radish was plotted against exposure time (Figure 2.1). Compared to the uptake by celery and radish, cephalexin in the nutrient solution of the lettuce uptake experiment disappeared at a comparatively slow rate, with an average cephalexin concentration of 10.2 ng mL⁻¹ remaining at 48 hrs, which was equivalent to 47.5% of the originally applied cephalexin (Figure 2.1A). This result is contrast to the uptake by celery, in which the cephalexin concentration in the nutrient solution was 0.6 ng mL⁻¹, approximately 3.9% of the original cephalexin, after exposure for 48 hrs (Figure 2.1B). As for uptake by radish, cephalexin was below the limit of detection (< 0.08 ng mL⁻¹) in the nutrient solution after 48 hrs of exposure (Figure 2.1C). In the nutrient solution with lettuce, cephalexin remained detectable throughout the 144-hr experimental period with the final concentration of ~ 0.9 ng mL⁻¹. However, in the nutrient solution for celery and radish, cephalexin was below the limit of detection after 72 and 48 hrs of exposure, respectively. In the vegetable-free controls, cephalexin remained relatively stable in the nutrient solution with 77.3% remaining at the end of the 144-hr uptake experiments

(Figure 2.1). The substantial decrease in cephalexin concentration in the nutrient solution over time could be due to the uptake by vegetables and metabolism in the plants, with the extent depending on plant species or cultivars (Calderón-Preciado et al., 2012; Wu et al., 2013). Pharmaceutical compounds could be extensively transformed within plants and/or in the nutrient solution in the presence of plant root exudates (Dodgen et al., 2013; Chuang et al., 2018). The disappearance of cephalexin from the nutrient solution indicates that cephalexin underwent substantial transformation in the vegetables, and lettuce uptake demonstrated the least degree of transformation among the three vegetables.

Cephalexin concentration in lettuce roots increased steadily to 1510 ng g $^{-1}$ dry weight (DW) at 48 hrs, and then slowly decreased to 957 ng g $^{-1}$ DW at 144 hrs (Figure 2.1A). The accumulation of cephalexin in celery roots was considerably less than that in lettuce, with the highest concentration of 171 ng g $^{-1}$ DW at 24 hrs. The concentration then decreased as time proceeded and declined to 11.5 ng g $^{-1}$ DW at 144 hrs (Figure 2.1B). A mass balance analysis revealed that 19.6 \pm 3.1% of the cephalexin initially present in the lettuce uptake experiment was accounted for at 144 hrs, whereas only 1.0 \pm 0.5% remained in the celery uptake experiment at 144 hrs. No cephalexin was measured above the limit of detection in radish roots during the entire 144 hrs of experimental period (Figure 2.1C). No accumulation of cephalexin in radish roots and the low concentration in celery roots, coupled with the comparatively rapid disappearance of cephalexin from the nutrient solutions of both vegetables, indicate that more extensive transformation of cephalexin occurred in celery and radish than that in lettuce. Riemenschneider et al. (2016) compared the uptake and transformation of carbamazepine by eggplant, cabbage, zucchini, pepper, tomato, parsley, rucola, lettuce, potato, and carrot, and

found that lettuce exhibited the least capability of transforming carbamazepine among the tested vegetables.

No apparent accumulation was measured for cephalexin in lettuce, celery, or radish shoots (Figure 2.1). The lack of transport to shoots may be caused by the physiochemical properties of cephalexin. Cephalexin molecular weight of 347.39 g mol⁻¹ is between the shoot transport boundary of ~300 g mol⁻¹ proposed by Kumar and Gupta (2016) and 400 g mol⁻¹ proposed by Chuang et al. (2019). Additionally, cephalexin exists predominately as a zwitterion in the nutrient solution (Table 2.1), which coupled with its relatively large molecular size, might inhibit and/or retard its diffusion through plant cell membranes (Goldstein et al., 2014; Wu et al., 2015). This could cause cephalexin to move in plants primarily by the apoplastic pathway (Chuang et al., 2019). The minimal transport from roots to shoots may be further exacerbated by the low initial cephalexin concentration, the relatively short duration of the uptake experiment and/or the rapid transformation in roots (to be described in Section 3.3). As for the transport from roots to shoots, Zhang, H. et al. (2017) found a detectable cephalexin concentration in the leaves of bok choy after 55 days of exposure to the high concentration of 500 ng mL⁻¹ in nutrient solution. Long-term exposure and high concentration can potentially allow charged and relatively large-sized pharmaceuticals to penetrate plant cell membranes and reach the upper portions of plants (Li et al., 2019). However, in this present study the relatively large molecular size, short experimental period and rapid transformation are believed to limit cephalexin transport from roots to shoots.

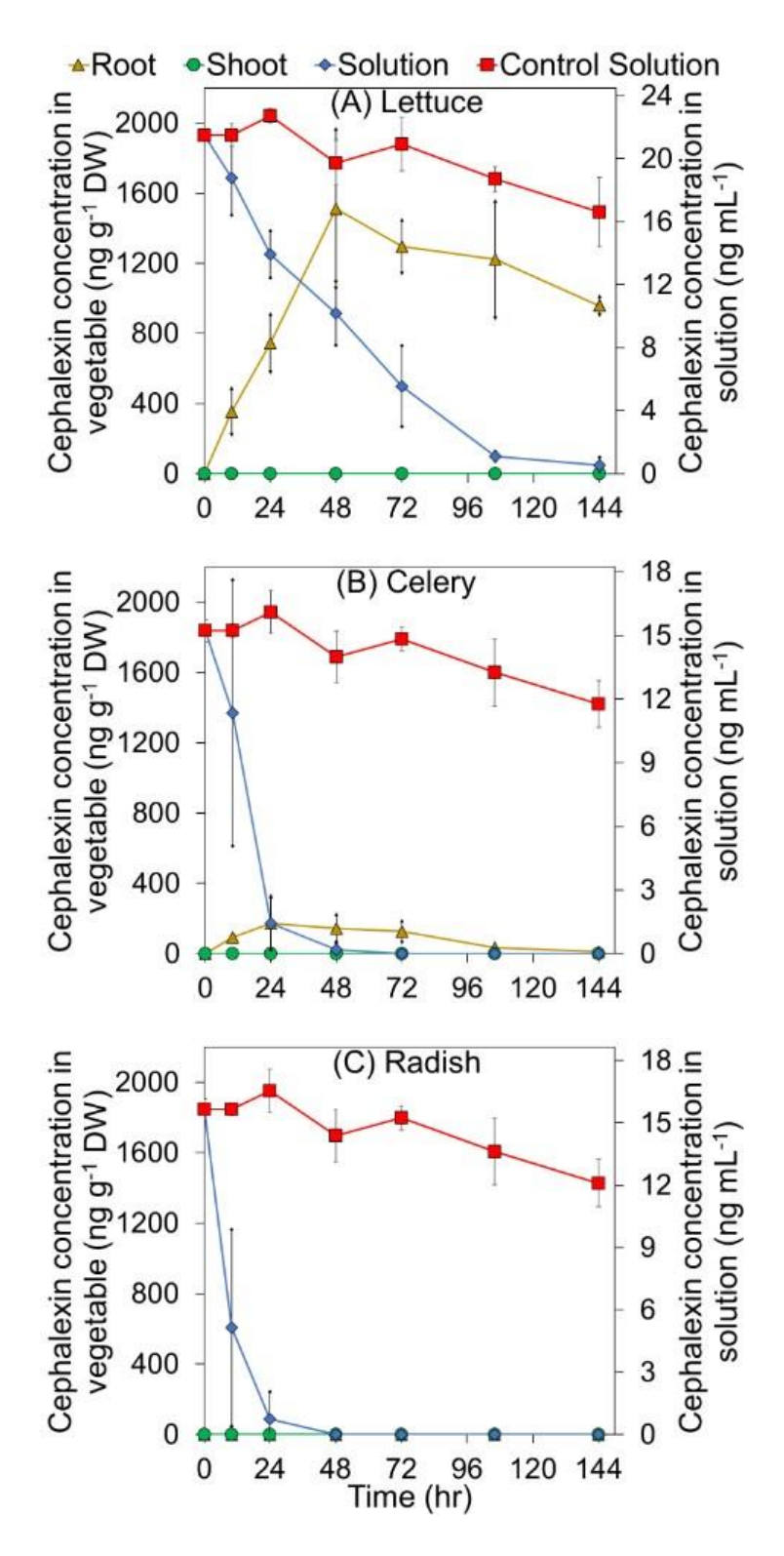


Figure 2.1 Cephalexin concentration in plant tissues (left y-axis), and in nutrient solution and the vegetable-free controls (right y-axis) for (A) lettuce, (B) celery, and (C) radish as a function of time.

Cephalexin sorption by vegetable roots

Sorption of cephalexin by dried lettuce, celery, and radish roots from nutrient solution was measured to establish sorption isotherms (Figure 2.2). The sorption isotherms are virtually linear within the range of cephalexin concentrations between 0 to 40 ng mL⁻¹. Therefore, the isotherm was fit to the linear sorption model $Q_s = K_d C_w$ where Q_s is vegetable root-sorbed concentration (ng g⁻¹), and Cw is cephalexin concentration in nutrient solution (ng mL⁻¹). The sorption coefficient (K_d) was estimated from the slope of the least square linear regression for the sorption isotherms. Lettuce roots displayed the strongest sorption with $K_d = 687$ mL g⁻¹, followed by celery roots with $K_d = 303$ mL g⁻¹, and radish roots with $K_d = 161$ mL g⁻¹. The decreasing trend of sorption coefficient is consistent with the order of accumulation of cephalexin (i.e., concentration in roots) in lettuce > celery > radish roots (Figure 2.1), implying that stronger sorption of cephalexin by vegetable roots could lead to a higher accumulation. A similar trend was also observed by Chuang et al. (2019) for the accumulation of many pharmaceuticals by lettuce roots. In general, the lyophilized root powders have the same chemical components as the living plant tissues, though they do not maintain some physiological characteristics of living plants, such as cell membrane potential or cell structure. These factors can also influence the uptake and accumulation of pharmaceuticals in plants (Goldstein et al., 2014).

The differences in cephalexin sorption by the roots of lettuce, celery, and radish could be partially due to plant root composition. The radish tissues designated as "roots", in fact, contain the enlarged hypocotyl, which may not be a strong sorbent for cephalexin. As a result, the lowest sorption was observed for radish roots (Figure 2.2). Vegetable roots contain many polyphenolic components (Llorach et al., 2008; Cieślik et al., 2006), which could be capable of interacting with the functional groups of cephalexin (Taiz et al., 2015), and plausibly lead to higher sorption

(Figure 2.2). If we assume that the accumulation of cephalexin reaches sorption equilibrium at 24 hrs in the hydroponic experiments, the estimated concentration in vegetable roots using sorption isotherm fittings is 9566 ng g⁻¹ DW in lettuce roots and 430 ng g⁻¹ DW in celery roots. These estimated concentrations are 12.8 and 2.5 times greater than the measured accumulation at 24 hrs. Such difference could be attributed to the occurrence of extensive transformation of cephalexin in vegetable roots.

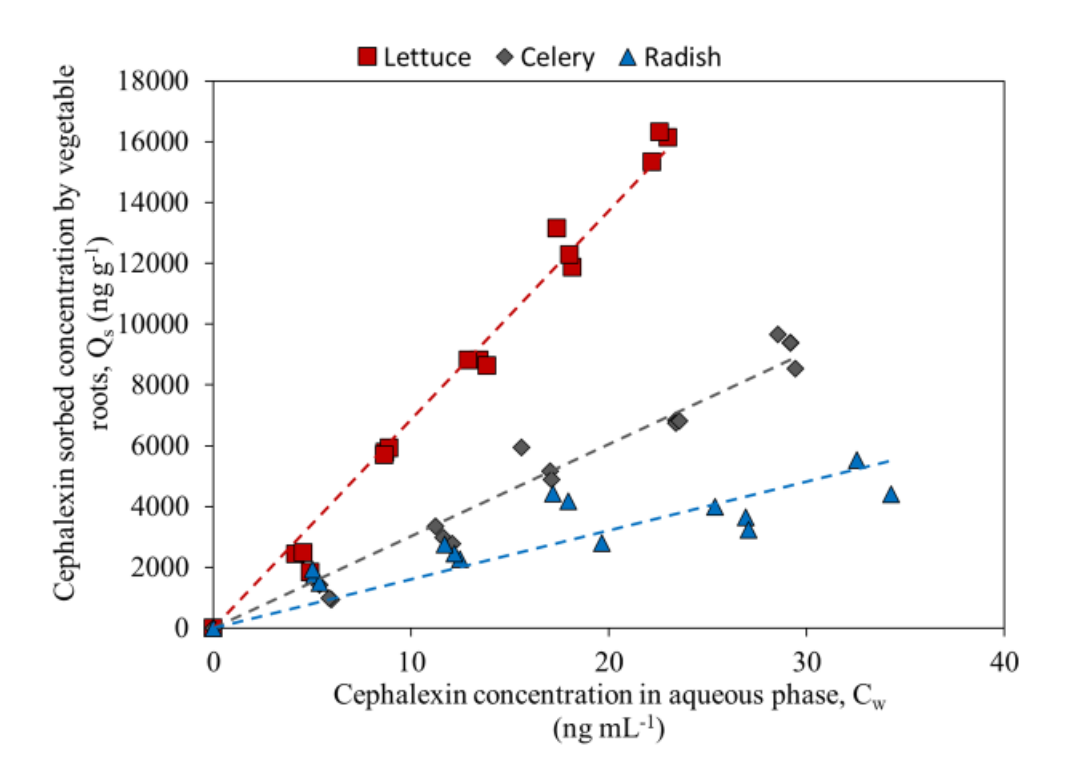


Figure 2.2 Sorption isotherm for cephalexin by lettuce, celery, and radish roots from nutrient solution. Sorption isotherms were fit to $Q_s = K_d C_w$, where K_d is sorption co-efficient ($mL \ g^{-1}$). The lines represent the least squares regression for each sorption isotherm.

To examine the strength of sorption to vegetable root tissues (affinity), cephalexin was extracted from the root tissue residues after sorption equilibrium was reached with the initial cephalexin concentration of 50 ng mL⁻¹ in nutrient solution. The recovery of cephalexin from lettuce, celery, and radish was 11.1 %, 19.9 %, and 52.3 %, respectively. These results suggest that cephalexin could develop relatively similar affinity to lettuce and celery root components, whereas it displayed a much weaker affinity to radish roots. The lower degree of transformation of cephalexin in lettuce (Figure 2.1A) could be due to the strong affinity of cephalexin to lettuce root tissues, thus limiting its interaction with reactive sites such as enzymes. The sorption by dry plant tissues could provide useful information for interpreting pharmaceutical accumulation and transport in plants; however, these results do not fully represent the potential interactions *in vivo*, as sample preparation steps of freezing, lyophilization, and grinding can destroy plant cell structures and many related plant functionalities (Zheng et al., 2011; Burke et al., 1976; Thaine and Bullas, 1966)

In vitro transformation

The potential transformation of cephalexin in vegetables was assessed by reactions with root and shoot enzyme extracts as an *in vitro* assay. The amount of enzyme present in each reaction system was adjusted to the same levels based on the measured protein content in the enzyme extracts. Natural log cephalexin concentration in vegetable root and shoot tissue enzyme extracts was plotted as a function of reaction time (Figure 2.3). Cephalexin concentration in the enzyme-free controls (n = 3) is also shown in Figure 2.3, with ~45 % of the initial concentration (100 ng mL⁻¹) lost after 96 hrs, which could be due to photolysis, oxidation and/or hydrolysis. (Wang and Lin, 2012; Yamana and Tsuji, 1976; Zhang, K. et al., 2017). Cephalexin demonstrated the greatest transformation in the enzyme extracts of celery. A cephalexin concentration of 9.6 ng

mL⁻¹ and 8.1 ng mL⁻¹ remained in the root and shoot enzyme extracts at 96 hrs, which corresponded to the transformation of 91 % and 93 % of the initially added cephalexin in the root and shoot enzyme extracts (Figure 2.3B). Lettuce and radish enzyme extracts displayed similar ability to transform cephalexin, with 85 % and 89 % of cephalexin transformed in the root enzyme extracts, and 85 % and 86 % transformed in the shoot enzyme extracts at 96 hrs, respectively (Figure 2.3A and 2.3C).

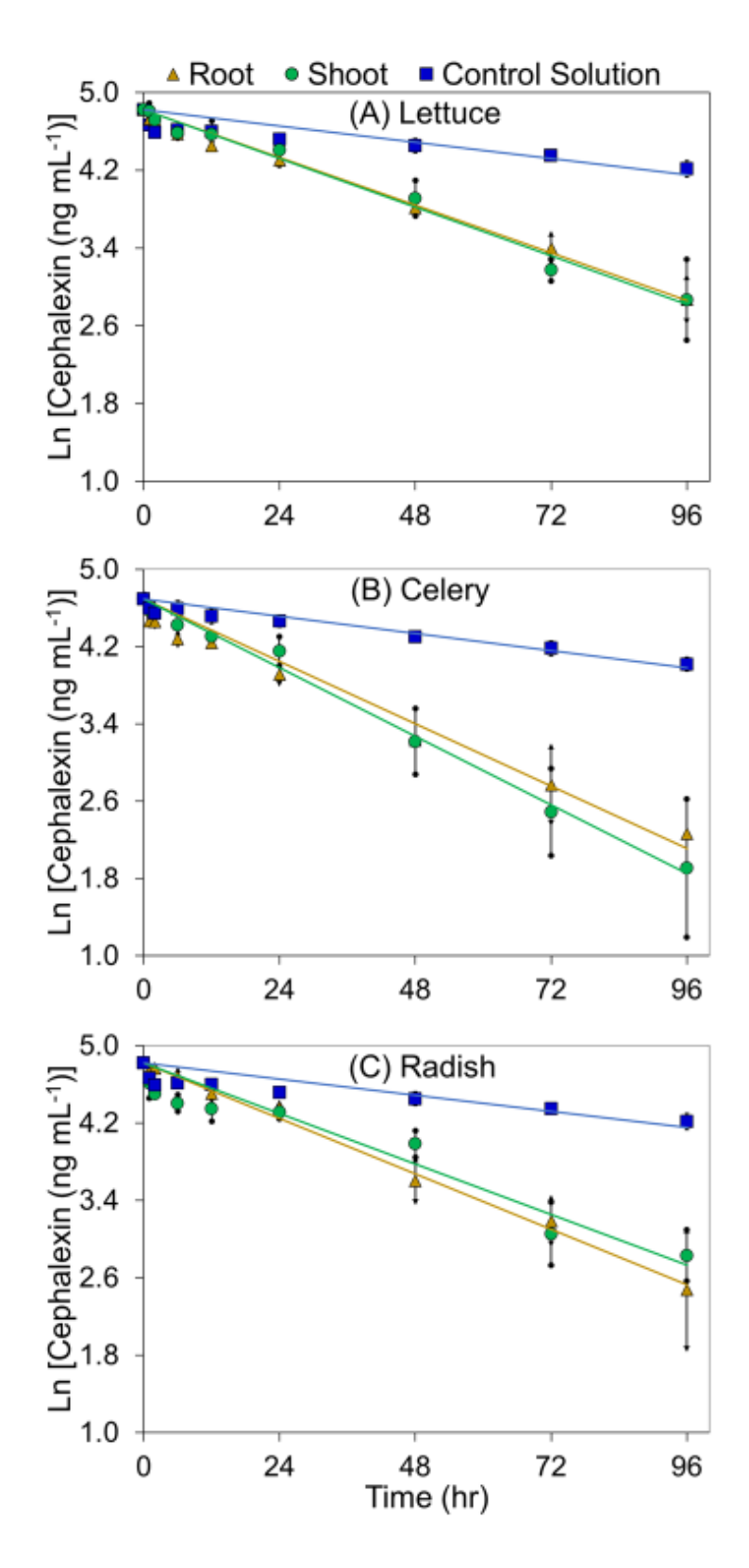


Figure 2.3 The natural log of cephalexin concentration in (A) lettuce, (B) celery, and (C) radish enzyme extracts as a function of time. *The lines represent the least squares regression for each degradation curve.*

Decreasing cephalexin concentration with reaction time in the *in vitro* transformation assays is well fit to the first order reaction model $\ln C_t = \ln C_0 - kt$ in which C_0 and C_t are cephalexin concentration at the initial time and reaction time t, and k is the reaction rate constant (hr⁻¹) (Figure 2.3). The estimated reaction rate constant was 0.007 hr⁻¹ for the enzyme-free control, 0.020, 0.027 and 0.024 hr⁻¹ for lettuce, celery, and radish root enzyme extracts, and 0.021, 0.030 and 0.022 hr⁻¹ for lettuce, celery and radish shoot enzyme extracts, respectively. The estimated reaction rate constants for the enzyme-free control, and the root and shoot enzyme extracts of the three vegetables (triplicate samples for each vegetable) were analyzed with a one-way analysis of variance (ANOVA). The ANOVA analysis revealed significant difference in the rate constants between all three vegetable extracts and enzyme-free controls (p < 0.05). No significant difference in the reaction rate constants was found between lettuce and radish root and shoot extracts (p > 0.05); however, the reaction rate constants of celery root and shoot extracts were significantly greater than those of lettuce and radish extracts (p < 0.05). The higher transformation rates in celery enzyme extracts are consistent with the *in vivo* experiments in which greater transformation of cephalexin occurred in hydroponically grown celery than that with lettuce (Figure 2.1). Radish and lettuce demonstrated similar enzyme reaction rate constants. However, compared to interaction with lettuce roots, cephalexin was weakly affiliated with radish root tissues as evidenced by a lower sorption coefficient and much higher extraction recovery (described in Section 3.2). This weak affinity of cephalexin for radish root tissues could allow more cephalexin to become available to react with enzymes, resulting in the greater transformation in radish observed in the *in vivo* hydroponic experiments (Figure 2.1C). We acknowledge that although the in vitro experimental results provide helpful information to elucidate the uptake and transformation of cephalexin in vegetables, more studies are needed to

evaluate how these processes and the characteristics of living plants collectively influence the accumulation of pharmaceuticals in vegetables.

CONCLUSION

Cephalexin demonstrated varying uptake and accumulation in different vegetables in the hydroponic experiments. The general trend of cephalexin uptake by vegetables showed a quickly increasing accumulation to the maximum followed by a decrease over time, implying the occurrence of transformation. The accumulation of cephalexin in roots followed the order of lettuce > celery > radish and is consistent with their sorption to dry root tissues. No apparent transport of cephalexin from roots to shoots was observed for the vegetables studied during the 144-hr period of exposure. The weak affinity of cephalexin to radish root tissues could increase the availability of cephalexin to reactive enzyme sites, leading to more transformation than that was observed in lettuce and celery during uptake. The results from this study provide valuable information on the uptake and accumulation of pharmaceuticals in plants, which is useful for environmental fate and risk assessment for human exposure. Further studies are needed to identify and quantify the metabolites derived from cephalexin in vegetables for a more comprehensive evaluation of potential risks to human health.

REFERENCES

REFERENCES

- Aga, D.S., O'Connor, S., Ensley, S., Payero, O., Snow, D., Tarkalson, D., 2005. Determination of the Persistence of Tetracycline Antibiotics and Their Degradates in Manure-Amended Soil Using Enzyme-Linked Immunosorbent Assay and Liquid Chromatography—Mass Spectrometry. J Agric. Food chem. 53, 7165-7171. https://doi.org/10.1021/jf050415
- Agency for Healthcare Research and Quality. Total purchases in thousands by prescribed drug, United States, 2010-2017. Medical Expenditure Panel Survey. Generated interactively: Tue May 12 2020.
- An, J., Zhou, Q., Sun, Y., Xu, Z., 2009. Ecotoxicological effects of typical personal care products on seed germination and seedling development of wheat (Triticum aestivum L.). Chemosphere 76, 1428–1434. https://doi.org/10.1016/j.chemosphere.2009.06.004
- Andersson, D.I., Hughes, D., 2014. Microbiological effects of sublethal levels of antibiotics. Nature Reviews Microbiology 12, 465–478. https://doi.org/10.1038/nrmicro3270
- Bradford, M.M., 1976. A Rapid and Sensitive Method for the Quantitation of Microgram Quantities of Protein Utilizing the Principle of Protein-Dye Binding. Anal. Biochem. 72, 248-254. https://doi.org/10.1016/0003-2697(76)90527-3
- Burke, M.J., Gusta, L.V., Quamme, H.A., Weiser, C.J., Li, P.H., 1976. Freezing and Injury in Plants. Annual Review of Plant Physiology 27, 507–528. https://doi.org/10.1146/annurev.pp.27.060176.002451
- Calderón-Preciado, D., Renault, Q., Matamoros, V., Cañameras, N., Bayona, J.M., 2012. Uptake of Organic Emergent Contaminants in Spath and Lettuce: An In Vitro Experiment. Journal of Agricultural and Food Chemistry 60, 2000–2007. https://doi.org/10.1021/jf2046224
- Card, M.L., Schnoor, J.L., Chin, Y.-P., 2012. Uptake of Natural and Synthetic Estrogens by Maize Seedlings. Journal of Agricultural and Food Chemistry 60, 8264–8271. https://doi.org/10.1021/jf3014074
- Card, M.L., Schnoor, J.L., Chin, Y.-P., 2013. Transformation of Natural and Synthetic Estrogens by Maize Seedlings. Environmental Science & Technology 47, 5101–5108. https://doi.org/10.1021/es3040335
- Carter, L.J., Williams, M., Böttcher, C., Kookana, R.S., 2015. Uptake of Pharmaceuticals Influences Plant Development and Affects Nutrient and Hormone Homeostases. Environmental Science & Technology 49, 12509–12518. https://doi.org/10.1021/acs.est.5b03468

- Christou, A., Karaolia, P., Hapeshi, E., Michael, C., Fatta-Kassinos, D., 2017. Long-term wastewater irrigation of vegetables in real agricultural systems: Concentration of pharmaceuticals in soil, uptake and bioaccumulation in tomato fruits and human health risk assessment. Water Research 109, 24–34. https://doi.org/10.1016/j.watres.2016.11.033
- Chuang, Y.-H., Liu, C.-H., Hammerschmidt, R., Zhang, W., Boyd, S.A., Li, H., 2018. Metabolic Demethylation and Oxidation of Caffeine during Uptake by Lettuce. Journal of Agricultural and Food Chemistry 66, 7907–7915. https://doi.org/10.1021/acs.jafc.8b02235
- Chuang, Y.-H., Liu, C.-H., Sallach, J.B., Hammerschmidt, R., Zhang, W., Boyd, S.A., Li, H., 2019. Mechanistic study on uptake and transport of pharmaceuticals in lettuce from water. Environment International 131, 104976. https://doi.org/10.1016/j.envint.2019.104976
- Chuang, Y.-H., Zhang, Y., Zhang, W., Boyd, S.A., Li, H., 2015. Comparison of accelerated solvent extraction and quick, easy, cheap, effective, rugged and safe method for extraction and determination of pharmaceuticals in vegetables. Journal of Chromatography A 1404, 1–9. https://doi.org/10.1016/j.chroma.2015.05.022
- Cieślik, E., Gręda, A., Adamus, W., 2006. Contents of polyphenols in fruit and vegetables. Food Chemistry 94, 135–142. https://doi.org/10.1016/j.foodchem.2004.11.015
- Collins, C., Fryer, M., Grosso, A., 2006. Plant Uptake of Non-Ionic Organic Chemicals. Environmental Science & Technology 40, 45–52. https://doi.org/10.1021/es0508166
- Dodgen, L.K., Li, J., Parker, D., Gan, J.J., 2013. Uptake and accumulation of four PPCP/EDCs in two leafy vegetables. Environmental Pollution 182, 150–156. https://doi.org/10.1016/j.envpol.2013.06.038
- Dodgen, L.K., Ueda, A., Wu, X., Parker, D.R., Gan, J., 2015. Effect of transpiration on plant accumulation and translocation of PPCP/EDCs. Environmental Pollution 198, 144–153. https://doi.org/10.1016/j.envpol.2015.01.002
- Edwards, M., Topp, E., Metcalfe, C.D., Li, H., Gottschall, N., Bolton, P., Curnoe, W., Payne, M., Beck, A., Kleywegt, S., Lapen, D.R., 2009. Pharmaceutical and personal care products in tile drainage following surface spreading and injection of dewatered municipal biosolids to an agricultural field. Science of The Total Environment 407, 4220–4230. https://doi.org/10.1016/j.scitotenv.2009.02.028
- EFSA Panel on Biological Hazards 2013: Scientific opinion on the risk posed by pathogens in food of non-animal origin. Part 1 (outbreak data analysis and risk ranking of

- food/pathogen combinations). EFSA J., 11, 3025. https://doi.org/10.2903/j.efsa.2013.3025
- Fu, Q., Malchi, T., Carter, L.J., Li, H., Gan, J., Chefetz, B., 2019. Pharmaceutical and Personal Care Products: From Wastewater Treatment into Agro-Food Systems. Environmental Science & Technology 53, 14083–14090. https://doi.org/10.1021/acs.est.9b06206
- Fu, Q., Zhang, J., Borchardt, D., Schlenk, D., Gan, J., 2017. Direct Conjugation of Emerging Contaminants in *Arabidopsis*: Indication for an Overlooked Risk in Plants? Environmental Science & Technology 51, 6071–6081. https://doi.org/10.1021/acs.est.6b06266
- Gawande, V.T., Bothara, K.G., Marathe, A.M., 2017. Stress Studies and Identification of Degradation Products of Cephalexin Using LC–PDA and LC–MS/MS. Chromatographia 80, 1545–1552. https://doi.org/10.1007/s10337-017-3385-0
- Goldstein, M., Shenker, M., Chefetz, B., 2014. Insights into the Uptake Processes of Wastewater-Borne Pharmaceuticals by Vegetables. Environmental Science & Technology 48, 5593–5600. https://doi.org/10.1021/es5008615
- Gulkowska, A., Leung, H.W., So, M.K., Taniyasu, S., Yamashita, N., Yeung, L.W.Y., Richardson, B.J., Lei, A.P., Giesy, J.P., Lam, P.K.S., 2008. Removal of antibiotics from wastewater by sewage treatment facilities in Hong Kong and Shenzhen, China. Water Research 42, 395–403. https://doi.org/10.1016/j.watres.2007.07.031
- Hartstein, A.I., Patrick, K.E., Jones, S.R., Miller, M.J., Bryant, R.E., 1977. Comparison of Pharmacological and Antimicrobial Properties of Cefadroxil and Cephalexin. Antimicrob. Agents Chemother. 12, 93. https://doi.org/10.1128/AAC.12.1.93
- Itoh, Y., Sugita-Konishi, Y., Kasuga, F., Iwaki, M., Hara-Kudo, Y., Saito, N., Noguchi, Y., Konuma, H., Kumagai, S., 1998. Enterohemorrhagic Escherichia coli O157:H7 Present in Radish Sprouts. Applied and Environmental Microbiology 64, 1532–1535. https://doi.org/10.1128/AEM.64.4.1532-1535.1998
- Koseki, S., Mizuno, Y., Yamamoto, K., 2011. Comparison of Two Possible Routes of Pathogen Contamination of Spinach Leaves in a Hydroponic Cultivation System. Journal of Food Protection 74, 1536–1542. https://doi.org/10.4315/0362-028X.JFP-11-031
- Kumar, K., Gupta, S.C., 2016. A Framework to Predict Uptake of Trace Organic Compounds by Plants. Journal of Environment Quality 45, 555. https://doi.org/10.2134/jeq2015.06.0261

- Li, Y., Chuang, Y.-H., Sallach, J.B., Zhang, W., Boyd, S.A., Li, H., 2018. Potential metabolism of pharmaceuticals in radish: Comparison of in vivo and in vitro exposure. Environmental Pollution 242, 962–969. https://doi.org/10.1016/j.envpol.2018.07.060
- Li, Y., Sallach, J.B., Zhang, W., Boyd, S.A., Li, H., 2019. Insight into the distribution of pharmaceuticals in soil-water-plant systems. Water Research 152, 38–46. https://doi.org/10.1016/j.watres.2018.12.039
- Llorach, R., Martinez-Sanchez, A., Tomas-Barberan, F.A., Gil, M.I., Ferreres, F., 2008. Characterisation of polyphenols and antioxidant properties of five lettuce varieties and escarole. Food Chem. 108, 1028–1038. https://doi.org/10.1016/j.foodchem.2007.11.032
- Lynch, M.F., Tauxe, R.V., Hedberg, C.W., 2009. The growing burden of foodborne outbreaks due to contaminated fresh produce: risks and opportunities. Epidemiology and Infection 137, 307–315. https://doi.org/10.1017/S0950268808001969
- Malchi, T., Maor, Y., Tadmor, G., Shenker, M., Chefetz, B., 2014. Irrigation of Root Vegetables with Treated Wastewater: Evaluating Uptake of Pharmaceuticals and the Associated Human Health Risks. Environmental Science & Technology 48, 9325–9333. https://doi.org/10.1021/es5017894
- Miller, E.L., Nason, S.L., Karthikeyan, K.G., Pedersen, J.A., 2016. Root Uptake of Pharmaceuticals and Personal Care Product Ingredients. Environmental Science & Technology 50, 525–541. https://doi.org/10.1021/acs.est.5b01546
- Müller, C.E., LeFevre, G.H., Timofte, A.E., Hussain, F.A., Sattely, E.S., Luthy, R.G., 2016. Competing mechanisms for perfluoroalkyl acid accumulation in plants revealed using an *Arabidopsis* model system. Environmental Toxicology and Chemistry 35, 1138–1147. https://doi.org/10.1002/etc.3251
- Nthenge, A.K., Weese, J.S., Carter, M., Wei, C.-I., Huang, T.-S., 2007. Efficacy of Gamma Radiation and Aqueous Chlorine on Escherichia coli O157:H7 in Hydroponically Grown Lettuce Plants. Journal of Food Protection 70, 748–752. https://doi.org/10.4315/0362-028X-70.3.748
- Prosser, R.S., Sibley, P.K., 2015. Human health risk assessment of pharmaceuticals and personal care products in plant tissue due to biosolids and manure amendments, and wastewater irrigation. Environment International 75, 223–233. https://doi.org/10.1016/j.envint.2014.11.020
- Rehman, M.S.U., Rashid, N., Ashfaq, M., Saif, A., Ahmad, N., Han, J.-I., 2015. Global risk of pharmaceutical contamination from highly populated developing countries. Chemosphere 138, 1045–1055. https://doi.org/10.1016/j.chemosphere.2013.02.036

- Riemenschneider, C., Al-Raggad, M., Moeder, M., Seiwert, B., Salameh, E., Reemtsma, T., 2016. Pharmaceuticals, Their Metabolites, and Other Polar Pollutants in Field-Grown Vegetables Irrigated with Treated Municipal Wastewater. Journal of Agricultural and Food Chemistry 64, 5784–5792. https://doi.org/10.1021/acs.jafc.6b01696
- Sabourin, L., Duenk, P., Bonte-Gelok, S., Payne, M., Lapen, D.R., Topp, E., 2012. Uptake of pharmaceuticals, hormones and parabens into vegetables grown in soil fertilized with municipal biosolids. Science of The Total Environment 431, 233–236. https://doi.org/10.1016/j.scitotenv.2012.05.017
- Sauvêtre, A., May, R., Harpaintner, R., Poschenrieder, C., Schröder, P., 2018. Metabolism of carbamazepine in plant roots and endophytic rhizobacteria isolated from Phragmites australis. Journal of Hazardous Materials 342, 85–95. https://doi.org/10.1016/j.jhazmat.2017.08.006
- Shen, Y., Stedtfeld, R.D., Guo, X., Bhalsod, G.D., Jeon, S., Tiedje, J.M., Li, H., Zhang, W., 2019. Pharmaceutical exposure changed antibiotic resistance genes and bacterial communities in soil-surface- and overhead-irrigated greenhouse lettuce. Environment International 131, 105031. https://doi.org/10.1016/j.envint.2019.105031
- Sinel, C., Cacaci, M., Meignen, P., Guérin, F., Davies, B.W., Sanguinetti, M., Giard, J.-C., Cattoir, V., 2017. Subinhibitory Concentrations of Ciprofloxacin Enhance Antimicrobial Resistance and Pathogenicity of Enterococcus faecium. Antimicrobial Agents and Chemotherapy 61. https://doi.org/10.1128/AAC.02763-16
- Taiz, L., Zeiger, E., Møller, I.M., Murphy, A., 2015. Plant Physiology and Development, 6th edition. Ringgold Inc., Beaverton.
- Taylor, E.V., Nguyen, T.A., Machesky, K.D., Koch, E., Sotir, M.J., Bohm, S.R., Folster, J.P., Bokanyi, R., Kupper, A., Bidol, S.A., Emanuel, A., Arends, K.D., Johnson, S.A., Dunn, J., Stroika, S., Patel, M.K., Williams, I., 2013. Multistate Outbreak of Escherichia coli O145 Infections Associated with Romaine Lettuce Consumption, 2010‡§. Journal of Food Protection 76, 939–944. https://doi.org/10.4315/0362-028X.JFP-12-503
- Thaine, R., Bullas, D.O., 1965. The Preservation of Plant Cells, particularly Sieve Tubes, by Vacuum Freeze-drying. Journal of Experimental Botany 16, 192–196. https://doi.org/10.1093/jxb/16.1.192
- Trapp, S., Matthies, M., McFarlane, C., 1994. Model for uptake of xenobiotics into plants: Validation with bromacil experiments. Environmental Toxicology and Chemistry 13, 413–422. https://doi.org/10.1002/etc.5620130308

- U.S. EPA, 1999. Biosolids Generation, Use, and Disposal in The United States. EPA530-R-99-009. US Environmental Protection Agency, Office of Water, Washington, D.C.
- U.S. EPA, 2020. National Water Reuse Action Plan: improving the security, sustainability, and resilience of our nations water resources. EPA-820-R-20-001. US Environmental Protection Agency, Office of Water, Washington, D.C.
- Wang, X.-H., Lin, A.Y.-C., 2012. Phototransformation of Cephalosporin Antibiotics in an Aqueous Environment Results in Higher Toxicity. Environmental Science & Technology 46, 12417–12426. https://doi.org/10.1021/es301929e
- Watkinson, A.J., Murby, E.J., Kolpin, D.W., Costanzo, S.D., 2009. The occurrence of antibiotics in an urban watershed: From wastewater to drinking water. Science of The Total Environment 407, 2711–2723. https://doi.org/10.1016/j.scitotenv.2008.11.059
- Winker, M., Clemens, J., Reich, M., Gulyas, H., Otterpohl, R., 2010. Ryegrass uptake of carbamazepine and ibuprofen applied by urine fertilization. Science of The Total Environment 408, 1902–1908. https://doi.org/10.1016/j.scitotenv.2010.01.028
- Wu, X., Conkle, J.L., Ernst, F., Gan, J., 2014. Treated Wastewater Irrigation: Uptake of Pharmaceutical and Personal Care Products by Common Vegetables under Field Conditions. Environmental Science & Technology 48, 11286–11293. https://doi.org/10.1021/es502868k
- Wu, X., Dodgen, L.K., Conkle, J.L., Gan, J., 2015. Plant uptake of pharmaceutical and personal care products from recycled water and biosolids: a review. Science of The Total Environment 536, 655–666. https://doi.org/10.1016/j.scitotenv.2015.07.129
- Wu, X., Ernst, F., Conkle, J.L., Gan, J., 2013. Comparative uptake and translocation of pharmaceutical and personal care products (PPCPs) by common vegetables. Environment International 60, 15–22. https://doi.org/10.1016/j.envint.2013.07.015
- Wu, X., Fu, Q., Gan, J., 2016. Metabolism of pharmaceutical and personal care products by carrot cell cultures. Environmental Pollution 211, 141–147. https://doi.org/10.1016/j.envpol.2015.12.050
- Yamana, T., Tsuji, A., 1976. Comparative Stability of Cephalosporins in Aqueous Solution: Kinetics and Mechanisms of Degradation. Journal of Pharmaceutical Sciences 65, 1563–1574. https://doi.org/10.1002/jps.2600651104
- Yang, Q., Ren, S., Niu, T., Guo, Y., Qi, S., Han, X., Liu, D., Pan, F., 2014. Distribution of antibiotic-resistant bacteria in chicken manure and manure-fertilized vegetables.

- Environmental Science and Pollution Research 21, 1231–1241. https://doi.org/10.1007/s11356-013-1994-1
- Zhang, H., Li, X., Yang, Q., Sun, L., Yang, X., Zhou, M., Deng, R., Bi, L., 2017. Plant Growth, Antibiotic Uptake, and Prevalence of Antibiotic Resistance in an Endophytic System of Pakchoi under Antibiotic Exposure. International Journal of Environmental Research and Public Health 14, 1336. https://doi.org/10.3390/ijerph14111336
- Zhang, K., Zhou, X., Du, P., Zhang, T., Cai, M., Sun, P., Huang, C.-H., 2017. Oxidation of β-lactam antibiotics by peracetic acid: Reaction kinetics, product and pathway evaluation. Water Research 123, 153–161. https://doi.org/10.1016/j.watres.2017.06.057
- Zheng, H., Yin, J., Gao, Z., Huang, H., Ji, X., Dou, C., 2011. Disruption of Chlorella vulgaris Cells for the Release of Biodiesel-Producing Lipids: A Comparison of Grinding, Ultrasonication, Bead Milling, Enzymatic Lysis, and Microwaves. Applied Biochemistry and Biotechnology 164, 1215–1224. https://doi.org/10.1007/s12010-011-9207-1

CHAPTER III.

THE CASPARIAN STRIP REDUCES PER- AND POLYFLUOROALKYL SUBSTANCES TRANSPORT FROM PLANT ROOTS TO SHOOTS

ABSTRACT

Per- and polyfluoroalkyl substances (PFAS) are widely dispersed to agricultural systems from many common practices such as irrigation with contaminated water and land application of biosolids as a soil amendment. These contaminants, when present in soil and water, can be taken up by crops and distributed within plants, including the edible portions. Many factors controlling the accumulation and distribution of PFAS in plants remain largely unclear, which impedes the development of effective measures to mitigate the accumulation of PFAS in crops. The Casparian strip is commonly considered a barrier that limits contaminant transport from plant roots to shoots, though no direct experimental investigation has been conducted to evaluate its impact to contaminant transport and accumulation in the scientific literature. In this study, the accumulation of PFAS in Arabidopsis thaliana roots and shoots was measured in a mutant which does not form a complete Casparian strip, which was compared to PFAS accumulation in a wild type A. thaliana with fully developed Casparian strip. The mutant and wild type A. thaliana maintained comparable biomasses at harvest, similar transpiration rates, and the same levels of PFAS concentration in roots after 120 h of uptake time. However, significantly higher PFAS concentrations were found in the mutant plant shoots compared to wild type A. thaliana shoots. PFAS uptake increased with uptake time, and their accumulation in shoots at 48, 96, and 144 h yielded a similar pattern between mutant and wild type A. thaliana. The enhanced PFAS accumulation in mutant plant shoots, when compared to wild type, suggests that the Casparian strip can function as a biological barrier to reduce the transport of PFAS from roots to shoots. Compared to their translocation factors in wild type A. thaliana, PFAS with a molecular weight > 450 g/mol demonstrated a smaller increase in translocation factor than PFAS with a molecular weight <450 g/mol in the mutant A. thaliana. These results suggest that although the Casparian

strip could inhibit the transport of PFAS from roots to shoots, for those PFAS with a molecular weight >450 g/mol, sorption by plant roots could also play an important role in the reduction of PFAS root-to-shoot translocation factors.

INTRODUCTION

Recently, the presence of per and polyfluoroalkyl substances (PFAS) in agricultural systems has been a focus of scientific research, stemming from the increased likelihood of human exposure after consumption of PFAS-contaminated agricultural products. PFAS commonly enter agricultural systems through atmospheric deposition, the use of biosolids as a soil amendment, and agricultural irrigation with PFAS-contaminated water (Wang et al., 2020; Scher et al., 2018). It has been observed that PFAS, after entering agricultural systems, can be taken up by and distributed within plants (Zhao et al., 2018; Liu et al., 2019; Navarro et al., 2017). The uptake of PFAS commonly occurs through either the root uptake from soil or soil water, or shoots uptake of PFAS from atmospheric deposition, vapor phase, and irrigation water. Root uptake of PFAS from contaminated soil and water is considered the major pathway responsible for the accumulation of PFAS in plants (Lee et al., 2014; Houtz et al., 2013).

Although significant research efforts have been dedicated to plant uptake of PFAS and other classes of emerging organic contaminants, understanding of the uptake mechanisms related to plant biology and physiology is very limited. Generally, plants take up organic contaminants from roots via passive, facilitated, and/or active diffusion. Passive diffusion along the contaminant concentration gradient is considered to be the most common uptake pathway (Kumar and Gupta, 2016). Once inside the root, contaminant movement can occur via two pathways, the symplastic pathway and the apoplastic pathway (Sicbaldi et al., 1992). The symplastic pathway refers to the transport on inner side of the plasma membrane. Organic contaminants can enter the symplastic pathway by crossing the plasma membrane and moving through plasmodesmata (Sicbaldi et al., 1992). The apoplastic pathway refers to the transport occurring on the outer side of plasma membranes, primarily within the cell wall spaces.

Contaminants moving in the apoplastic pathway (i.e., moving on the outer side of the plasma membrane) space are eventually blocked at the endodermis, by the Casparisan strip, before entering the xylem. At this point, the contaminants must enter the symplastic pathway (i.e., cross the plasma membrane) to pass the endodermis and enter the xylem. Thereafter, contaminants can move upwards towards the leaves with the transpiration stream, that is, transpiration water serves as a carrier to move organic contaminants from roots to leaves via plant xylem vessels (Chuang et al., 2019; Kumar and Gupta, 2016; Schnoor et al., 1995).

The Casparian strip is a hydrophobic ring-like band composed of suberin and lignin that is formed during root development in vascular plants. It is located at the junction of neighboring endodermal cells and forms, in conjunction with the plasma membranes of neighboring cells, a barrier to the apoplastic transport of compounds to the xylem (Alassimone et al., 2012). A search of current literature shows little experimental evidence to evaluate the role of the Casparian strip in plant uptake and accumulation of PFAS. Most previous studies focused on relationships between contaminant uptake/accumulation and the physiochemical properties of the contaminant, such as octanol-water partitioning coefficient, molecular size, and chemical speciation (Chuang et al., 2019; Kumar and Gupta, 2016; Sicbaldi et al., 1992; Briggs et al., 1982). The Casparian strip and the plasma membranes of neighboring cells have been proposed as a biological barrier that retards the translocation of large-sized contaminants (>300 g/mol) and ionic contaminants from roots to shoots. Large-sized contaminants are unable to cross the plasma membrane and anionic or cationic contaminants are, respectively, repelled or attracted to the negatively charged plasma membrane surface thus limiting their transport (Chuang et al., 2019; Blaine et al., 2014a; Miller et al., 2016).

To date, few experiments have been conducted to directly examine the role of the Casparian strip in the translocation of organic contaminants, despite its potential impact being frequently described in the literature. This study seeks to evaluate the role of the Casparian strip as a barrier to limit PFAS transport from plant roots to shoots using the model organism Arabidopsis thaliana under controlled hydroponic conditions. We hypothesize that the Casparian strip could serve as a major biological barrier that limits the transport PFAS from plant roots to shoots. Although this hypothesis is straightforward, it is difficult to test without comparable plants with/without a Casparian strip. Fortunately, recent work has characterized an A. thaliana ecotype Columbia-0 mutant (SALK_043282) which is incapable of forming a fully functional Casparian strip, due to mutations in the SGN1 kinase responsible for its positioning and integrity (Pfister et al., 2014; Alassimone et al., 2016). The uptake/accumulation of PFAS in this mutant can be compared to wildtype A. thaliana ecotype Columbia-0, which forms a fully functional Casparian strip during root development, to determine the impact that the Casparian strip has on PFAS transport. The model organism A. thaliana provides an ideal system to help clearly elucidate the role of Casparian strip in the transport of a series of PFAS with varying molecular weight from plant roots to shoots. In addition, previous studies reported that carbamazepine (a small sized neutral compound) can be easily translocated from roots to shoots and is hyperaccumulated in shoots (Chuang et al., 2019; Wu et al., 2013). Thus, carbamazepine was included as a positive control for comparison to PFAS.

MATERIALS AND METHODS

Chemicals and reagents

In this study perfluorododecanoic acid (purity 95%), perfluorodecanoic acid (98%), perfluorooctanoic acid (96%), perfluoroheptanoic acid (99%), perfluoropentanoic acid (97%),

perfluorohexanesulfonic acid (98%), carbamazepine (98%), ammonium acetate (reagent grade), and methanol (chromatography grade) and acetonitrile (chromatography grade) were purchased from Sigma-Aldrich (St. Louis, MO, USA). Perfluorooctanesulfonic acid (98%) was purchased from Tokyo Kasei Kogyo Co., LTD. (Tokyo, Japan). Perfluorobutanesulfonic acid (99%) was purchased from Merck KGaA. (Darmstadt, Germany). 2,3,3,3-tetrafluoro-2- (heptafluoropropoxy) propionic acid (97%) was purchased from Matrix Scientific (Columbia, SC, USA). Perfluoro-3,6-dioxaheptanoic acid (95%) was purchased from Combi-Blocks (San Diego, CA, USA). Perfluorooctanesulfonamide (98%) was purchased from Ochem Incoporation (Des Plaines, IL, USA). Ultrapure water was obtained from a Milli-Q water purification system (Millipore, Billerica, MA, USA). Sodium chloride (NaCl), and formic acid were purchased from J.T. Baker (Phillipsburg, NJ, USA). Anhydrous sodium sulfate (Na₂SO₄) was obtained from EMD Chemicals (Gibbstown, NJ, USA). Primary secondary amine (PSA) and C18 powders were purchased from Agilent Technologies (Santa Clara, CA, USA).

Arabidopsis thaliana growth experiments

The seeds of *Arabidopsis thaliana* ecotype Columbia-0 (hereinafter referred to as "wild type") and the Columbia-0 mutant SALK_043282 (hereinafter referred to as "mutant") were purchased from the Arabidopsis Biological Resource Center at The Ohio State University (Columbus, OH, USA). *A. thaliana* were grown hydroponically using the method adopted from Conn et al. (2013). Specifically, germination medium and standard growth solution consisted of ¼ Hoagland's solution and ¼ Hoagland's solution, respectively (Hoagland and Arnon, 1938). Plants were germinated and grown at a 12 h:12 h photoperiod and a constant temperature of 20 °C. *A. thaliana* plants were grown for approximately 44 days before being transferred to 50-mL black polypropylene centrifuge tubes containing ~40 mL of standard growth solution. After

acclimating the plants in individual tubes for two days, the solution was replaced with ~40 mL of standard growth solution spiked with an eleven PFAS mixture at a concentration of 100 µg/L for each PFAS and carbamazepine at a concentration of 500 µg/L. Over the course of the growth experiments water loss and plant biomass were measured gravimetrically at 24 h intervals, and the solution volume was maintained at its original level. In the first experiment, both wild type and mutant A. thaliana (five individual plants) were collected at 48, 96, and 144 h of exposure time. This experiment showed that differences in PFAS shoot accumulation could be observed between wild type and mutant A. thaliana after 96 h of exposure. More biological replicates were needed to statistically distinguish the differences. Thus, in the second experiment twenty individual plants, for both wild type and mutant A. thaliana, were collected after 120 h of exposure to PFAS and carbamazepine. At collection, solution volume and plant biomass were measured gravimetrically. The experimental controls included both wild type and mutant A. thaliana that had not been exposed to PFAS or carbamazepine in the standard growth solution, and standard growth solution spiked with PFAS and carbamazepine but without plants. The collected plants were rinsed with ultrapure water and blotted dry with paper tissue. Plants were separated into roots and shoots by a cut below cotyledon, immediately frozen in liquid nitrogen, and ground to powder. The samples were stored in 15-mL polypropylene centrifuge tubes at -18°C prior to extraction.

PFAS and carbamazepine extraction

A. thaliana root and shoot tissue samples were extracted using a modified QuEChERS method similar to Chuang et al. (2015). Briefly, approximately 250 mg of each root sample or 800 mg of each shoot sample (on a wet weight basis) were placed in 15-mL polypropylene centrifuge tubes, followed by vortexing in 1.0 mL of ultrapure water for 1 min, subsequent

addition of 1.75 mL of methanol containing 1% formic acid, and vortexing for 2 min. Afterward, 2.0 g of Na₂SO₄ and 0.5 g of NaCl were added, and the mixture was vortexed for an additional 2 min. The extracts were then centrifuged at 5050 g for 10 min at 20 °C, and the supernatant was collected in a separate 15-mL polypropylene centrifuge tube. The residues were extracted with 3.25 mL of acetonitrile containing 1% formic acid by vortexing for 2 min and subsequently centrifuged at 5050 g for 10 min at 20 °C. The two supernatants were combined, vortexed for 30 seconds, and centrifuged at 5050 g for 10 min at 20 °C. A certain volume (1.2 mL) of the combined extracts was cleaned up by adding dispersed solid phase extraction (d-SPE) sorbents (12.5 mg of PSA, 12.5 mg of C18, and 225 mg of Na₂SO4), followed by vortexing for 1 min, and centrifugation at 9240 g for 10 min. The supernatant was immediately transferred to an autosampler vial and analyzed by high-performance liquid chromatography and tandem mass spectrometry (HPLC-MS/MS). The extraction efficiencies for the A. thaliana shoot and root tissue samples were between 80.7% to 148% and 54.1% to 138%, respectively (Table 3.1). The extraction efficiencies were determined by spiking 100 µg/kg PFAS and carbamazepine in methanol to ground A. thaliana shoots and roots. The samples were placed in a fume hood for 24 h until the solvent was fully evaporated prior to extraction.

Table 3.1 Extraction efficiency (%) of PFAS and carbamazepine from *A. thaliana* root and shoot tissues

Compound	Abbreviation —	Extraction Efficiency ^a			
Compound	Abbreviation –	Shoot	Root		
Perfluoropentanoic acid	PFPeA	99.1 ± 1.2	54.1 ± 14.0		
Perfluoroheptanoic acid	PFHpA	80.7 ± 27.9	128 ± 20.0		
Perfluorooctanoic acid	PFOA	122 ± 12.6	112 ± 13.7		
	PFDA	147 ± 17.1	62.1 ± 7.9		
Perfluorododecanoic acid	PFDoA	94.8 ± 14.5	92.0 ± 7.5		
Perfluorobutanesulfonic acid	PFBS	92.0 ± 3.1	137 ± 4.8		
Perfluorohexanesulfonic acid	PFHxS	100 ± 1.1	109 ± 11.7		
Perfluorooctanesulfonic acid	PFOS	89.8 ± 17.0	84.6 ± 6.6		
Perfluorooctanesulfonamide	PFOSA	112 ± 9.3	82.2 ± 4.5		
2,3,3,3-tetrafluoro-2- (heptafluoropropoxy) propionic acid	HFPO-Da	119 ± 36.5	57.8 ± 9.9		
Perfluoro-3,6-dioxaheptanoic acid	PFECA B	103 ± 6.59	136 ± 32.9		
Carbamazepine	Cbz	96.2 ± 9.8	103 ± 4.2		

^aMean \pm standard deviation (n = 3)

PFAS and carbamazepine analysis

PFAS and carbamazepine concentrations were determined using a Shimadzu prominence high-performance liquid chromatography system (Columbia, MD, USA) coupled to an AB Sciex 4500 QTrap triple quadrupole mass spectrometer (Foster City, CA, USA). A Phenomenex Gemini C18 column (50 mm × 2 mm, 5 µm) (Torrance, CA, USA) was used for liquid chromatography separation. The sample injection volume was set at 5 µL and the flow rate at 0.6 mL min⁻¹. The binary mobile phase consisted of water with 20 mM ammonium acetate (mobile phase A) and acetonitrile (mobile phase B). The gradient program was as follows: after 1 min pre-equilibration with 100% mobile phase A, mobile phase B increased to 55% from 0.01 to 0.10 min, then increased from 55% to 99% from 0.10 to 4.50 min, remained at 99% from 4.50 to 4.95 min, then decreased from 99% to 10% from 4.95 to 5.00 min, and remained at 10% until 6.51 min. The ionspray voltage, temperature, and curtain gas pressure were -4500 V, 600 °C, and 35 psi for the negative ionization mode, and 4500 V, 600 °C, and 35 psi for the positive ionization mode. Abbreviation, Chemical Abstract Service Registry Number (CASRN), ionization mode, precursor ion, product ion, declustering potential, entrance potential, collision energy, and collision cell exit potential for all the analytes are provided in Table 3.2. Multiple reaction monitoring mode was used for identification and quantification. PFAS and carbamazepine in the standard growth solution were analyzed directly. PFAS and carbamazepine in A. thaliana roots and shoot samples were analyzed in their respective extracts. All samples were quantified using matrix-matched standard calibration curves.

Table 3.2 HPLC-MS/MS parameters for PFAS and carbamazepine analysis

Compound	CASRN	Precursor Ion (m/z)	Product Ion ^a (m/z)	$DP^{b}(V)$	$EP^{c}(V)$	$CE^{d}(V)$	$CXP^{e}(V)$	
Negative ionization mode								
PFDoA 307-55-1	207 55 1	613.00	569.00	-25	-10	-18	-10	
	307-33-1		268.70	-25	-10	-18	-10	
PFDA 335-76	335_76_2	513.00	469.00	-25	-10	-16	-10	
	333-70-2		218.70	-25	-10	-16	-10	
PFOA 335-67-	335-67-1	413.00	369.00	-25	-8	-15	-11	
	333 07 1		169.00	-25	-8	-15	-11	
PFHpA 375-	375-85-9	363.00	319.00	-25	-10	-12	-10	
	313 03 7		169.00	-25	-10	-12	-10	
PFPeA	2706-90-3	262.90	219.00	-20	-10	-12	-10	
PFOS 176	1763-23-1	499.00	80.00	-160	-5	-110	-12	
	1/03-23-1		99.00	-160	-5	-110	-12	
PFHxS 355-46-4	255 16 1	399.00	80.00	-60	-10	-74	-10	
	333-40-4		99.00	-60	-10	-74	-10	
PFRS	PFBS 375-73-5	298.90	80.00	-55	-10	-58	-10	
TTDS			98.90	-55	-10	-58	-10	
HFPO-Da 13252-13-	329.00	169.00	-30	-10	-18	-10		
		185.00	-30	-10	-32	-10		
PFECA B 151772- 58-6		295.00	200.90	-25	-14	-8	-10	
	58-6		84.90	-25	-14	-8	-10	
	754-91-6	498.00	77.90	-60	-10	-85	-10	
			47.90	-60	-10	-85	-10	
Positive ionization mode								
Cbz	298-46-4	236.96	193.70	80	10	30	10	
			192.00	80	10	30	12	

^aThe product ion coupled with precursor ion used to quantify (in bold) and qualify pharmaceuticals. ^bDeclustering potential. ^cEntrance potential. ^dCollision energy. ^eCollision cell exit potential.

RESULTS AND DISCUSSION

Plant transpiration and biomass

During the experimental period, no apparent physiological differences were observed between the A. thaliana plants grown in the controls and the PFAS/carbamazepine exposure treatments. There was no significant difference in the amount of water transpired by wild type and mutant, monitored at 24 h intervals, at 48, 96, 144 or 120 h (P < 0.05, Mann-Whitney U test). No significant difference in root and shoot biomass at harvest between the two plant types (P < 0.05, Mann-Whitney U test). These results warrant a reliable comparison in plant accumulation of PFAS and carbamazepine between wild type and mutant A. thaliana.

PFAS and carbamazepine accumulation in A. thaliana roots

No significant difference of the amount of accumulated PFAS or carbamazepine in A. thaliana wild type and mutant roots was found at 48, 96, and 144 h of exposure (P < 0.05, Mann-Whitney U test) (Figures 3.1). PFAS concentrations in A. thaliana roots at 120 h of exposure are shown in Figure 3.3A. PFDoA accumulated to the highest amount in the roots, with average concentrations of 6,757 μ g/kg in wild type and 6,535 μ g/kg in mutant A. thaliana. The lowest concentration in roots was observed for PFPeA, with an average concentration of 212 μ g/kg in wild type roots and 211 μ g/kg in mutant roots. PFAS concentrations in roots tended to increase with increasing molecular weight and hydrophobicity, which might be due to higher sorption by roots for more hydrophobic PFAS and/or more efficient transport of smaller-sized PFAS. A similar trend was observed by Felizeter et al. (2014) in which the percent mass distribution in roots for PFDoA, PFDA, PFOA, PFHpA, and PFPeA was 90, 72, 29, 12, and 5% of the initially applied PFAS mass, respectively. When comparing the root accumulation of perfluorinated carboxylic acids (PFCA) and perfluorinated sulfonic acids (PFSA) with the same fluoroalkyl

chain length (PFPeA vs PFBS and PFHpA vs PFHxS) no consistent pattern in the accumulation were observed. Blaine et al. (2014b) and Stahl et al. (2009) reported the increased uptake of PFCA relative to PFSA; however, both studies were conducted using pot experiments with soils. PFSA generally demonstrate higher sorption to soils in comparison to PFCA at the same perfluoroalkyl chain length (Campos Pereira et a., 2018; Higgins and Leuthy, 2006). The strong sorption of PFAS by soils could reduce the bioavailability to plant uptake.

PFAS and carbamazepine accumulation in A. thaliana shoots

Accumulation of PFAS in the shoots of wild type and mutant A. thaliana at 48, 96, and 144 h is shown in Figure 3.2. It is clearly shown that a larger amount of PFAS accumulated in mutant plants vs. wild type plants, though the variation was relatively large for both wild type and mutant A. thaliana. Because of the large variability in PFAS concentrations, an increased number of biological replicates were sampled after 120 h of exposure. The results showed that significantly higher PFAS concentrations were found in the shoots of the mutant plants compared to the wild type plants at 120 h (P < 0.05, Mann-Whitney U test), except for PFDA which was significant at the P level of < 0.10. PFAS concentrations in the mutant A. thaliana shoots were, on average, 2.2 times greater than those in wild type plant shoots (Figure 3.3). This could be due to the incomplete formation of the Casparian strip in mutant A. thaliana roots, which allows a complete transport process via apoplastic pathway into the xylem. In wild type A. thaliana, the fully formed Casparian strip could serve as a biological barrier to inhibit or slow down the transport of PFAS to shoots, as it blocks apoplastic transport at the endodermis. The transpiration stream, the water movement from roots to leaves via plant xylem vessels, carries PFAS from A. thaliana roots to shoots. Recall that there is no significant difference in the amount of water transpired between wild type and mutant A. thaliana in the experiments.

Although the Casparian strip has long been assumed to be a barrier to inhibit the transport of PFAS to plant leaves (Blaine et al., 2014a), this is, as far as we are aware of, the first study to provide solid experimental evidence to demonstrate this function of the Casparian strip.

Carbamazepine concentrations in the shoots of wild type and mutant *A. thaliana* were $3,944 \pm 524$ and $3,835 \pm 521$ µg/kg, respectively. The similar carbamazepine concentrations in the shoots of wild type and mutant *A. thaliana* indicate that the Casparian strip has a minimal impact on carbamazepine transport. Carbamazepine is a relatively small-sized molecule with a molecular weight of 236 g/mol, an intermediate hydrophobicity (log $K_{ow} = 0.6$), and is neutrally charged at the experimental pH 5.6 - 5.8 (Miller et al, 2016). These properties render carbamazepine to have the capability to cross plasma membranes and transport via the symplastic pathway. In fact, carbamazepine demonstrated high transport from roots to shoots, which has been documented for multiple plant species. The calculated root-to-shoot translocation factors ranged from 2.2 to 7.5 (Chuang et al., 2019; Shenker et al., 2011; Wu et al., 2013).

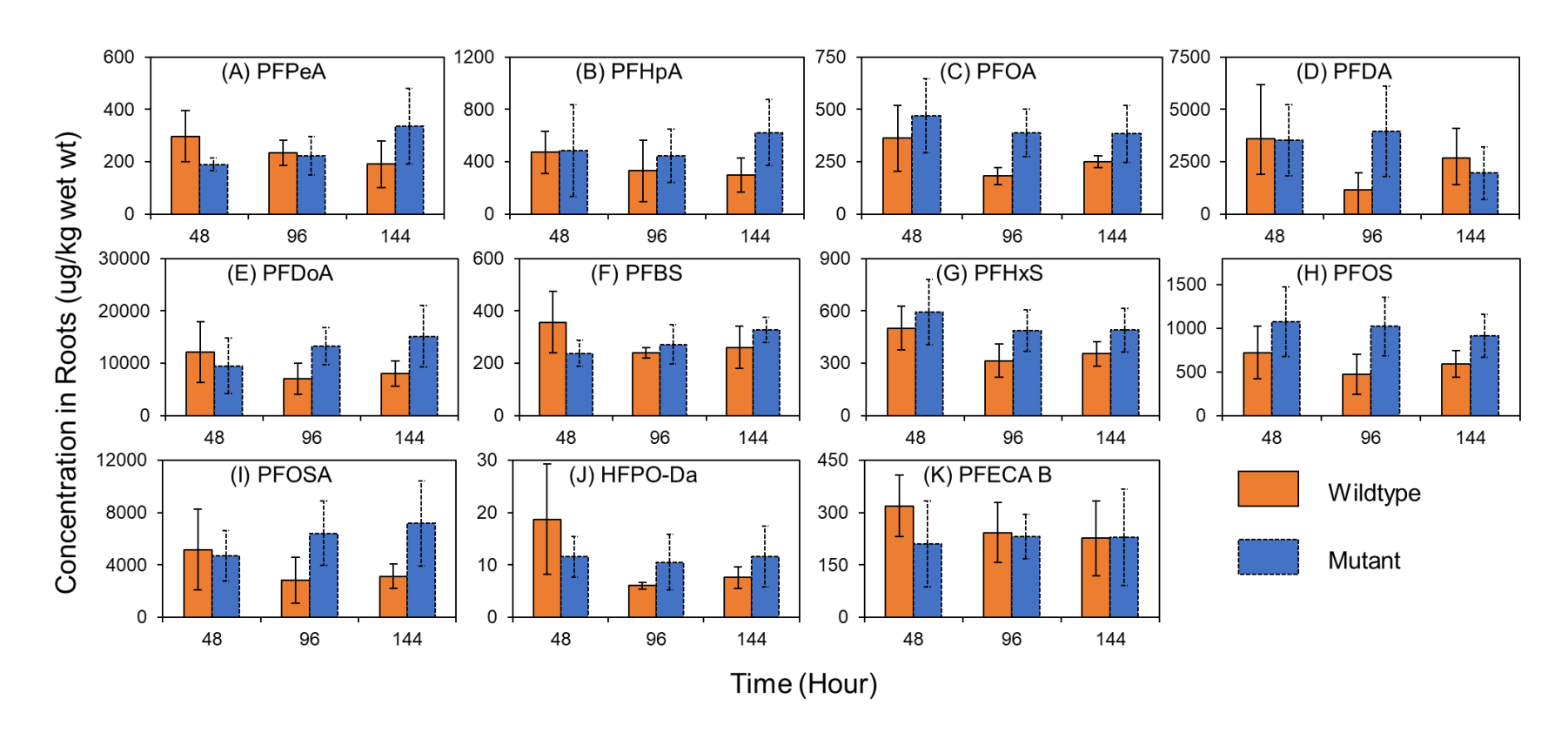


Figure 3.1 PFAS accumulation in *Arabidopsis thaliana* roots from 48 to 144 hours (n = 5)

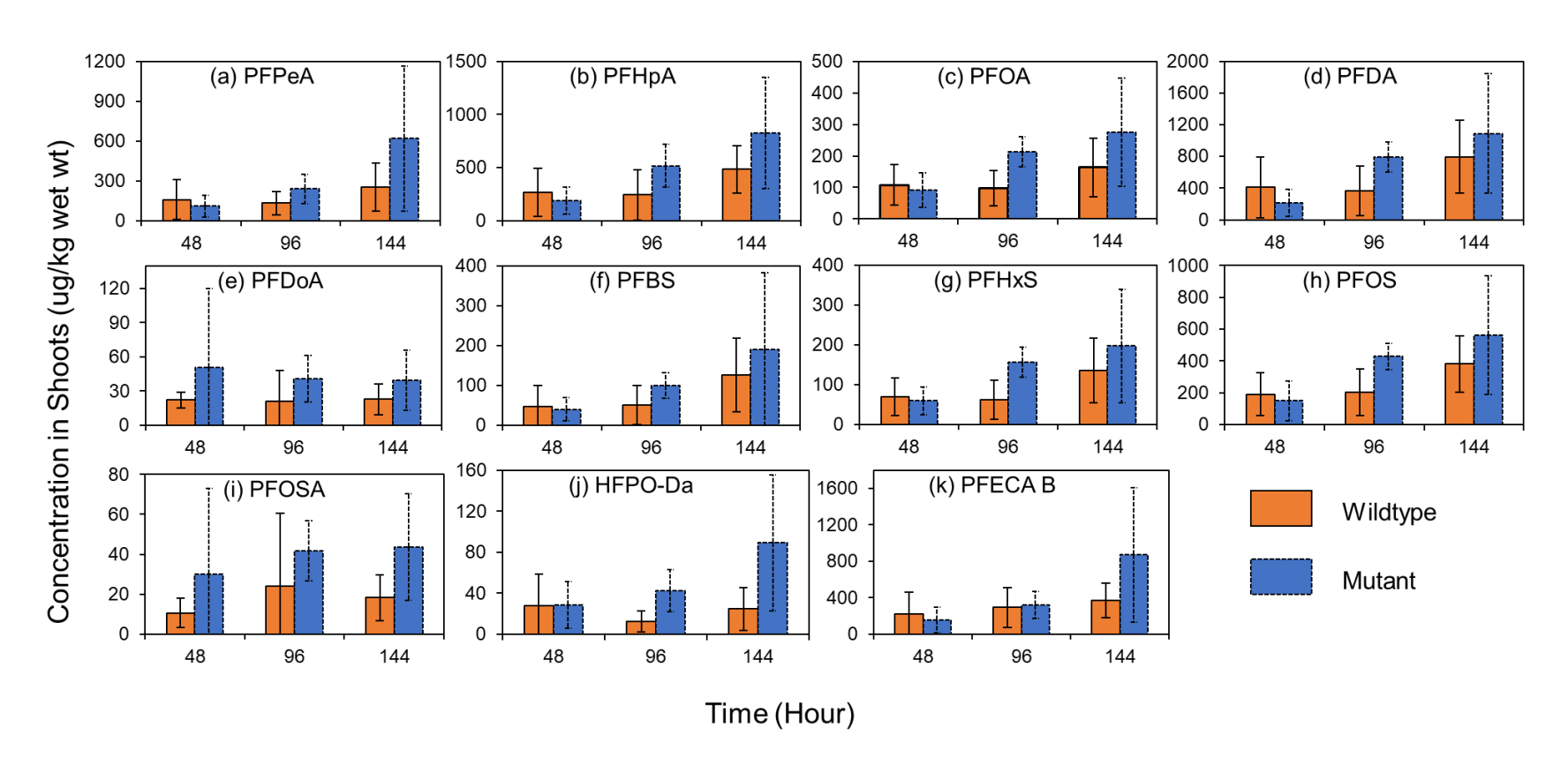


Figure 3.2 PFAS accumulation in *Arabidopsis thaliana* shoots from 48 to 144 hours (n = 5)

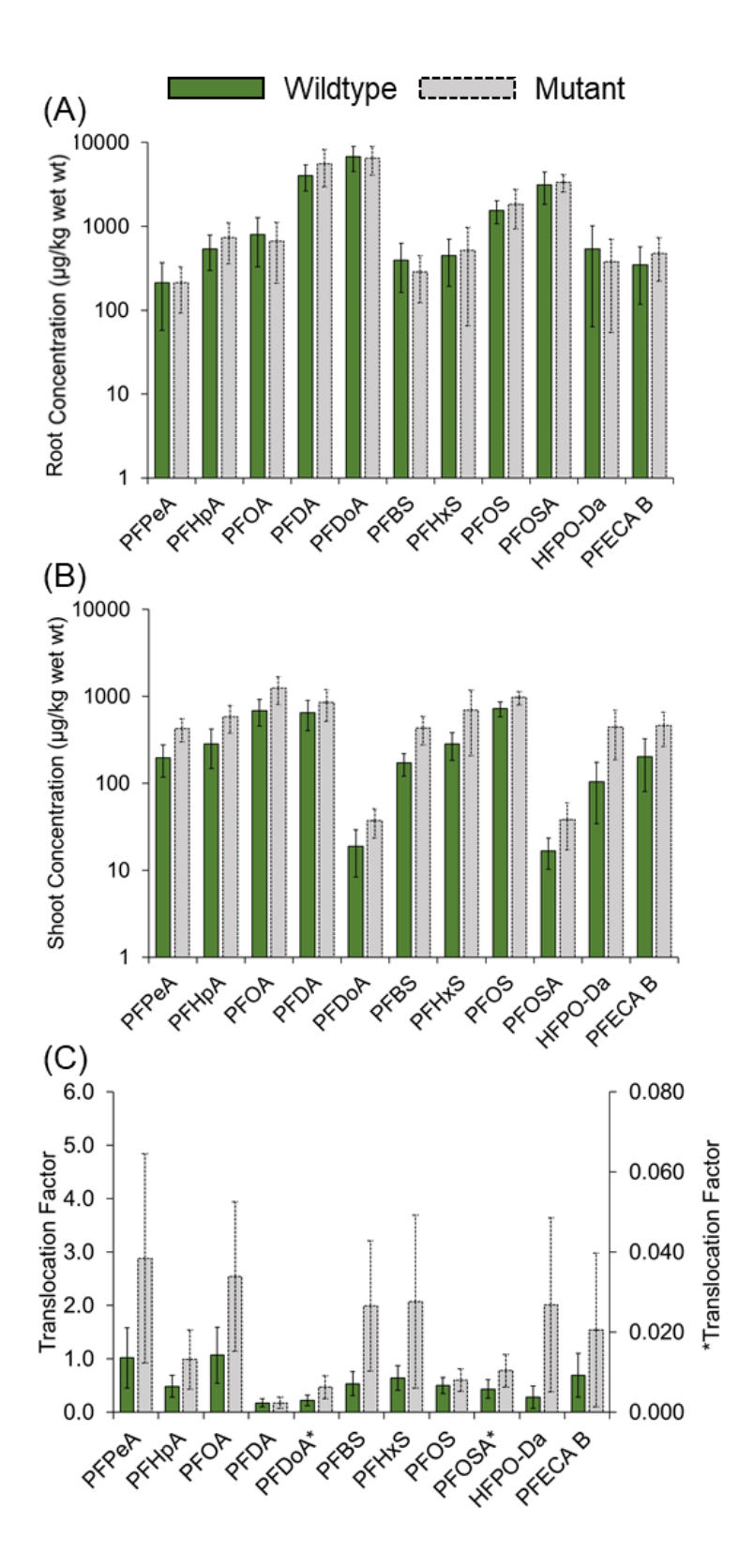


Figure 3.3 (A) PFAS concentration in roots, (B) PFAS concentration in shoots, and (C) PFAS translocation factor in *Arabidopsis thaliana* at 120 hours (n = 20). *Asterisk* * *indicates the concentration corresponds to the right Y-axis*.

that in roots. The comparison of PFAS translocation factors between wild type and mutant A. thaliana is shown in Figure 3.3C. The translocation factors of PFAS ranged from 0.003 ± 0.001 to 1.07 ± 0.52 in wild type plants, and 0.006 ± 0.003 to 2.88 ± 1.96 in mutant plants. Translocation factor values > 1 indicates high transport efficiency with chemical concentrations in shoots > those in roots. This was observed for PFAS with a molecular weight < 450 g/mol in mutant A. thaliana. That is, the translocation factors of PFPeA, PFHpA, PFOA, PFBS, PFHxS, HFPO-Da, and PFECA B in mutant A. thaliana were 2.88 ± 1.96 , 0.99 ± 0.55 , 2.54 ± 1.39 , 1.99 ± 1.21 , 2.07 ± 1.62 , 2.01 ± 1.63 , and 1.55 ± 1.44 , respectively. As expected, the translocation factors of PFPeA, PFHpA, PFOA, PFBS, PFHxS, HFPO-Da, and PFECA B were relatively low in wild type A. thaliana, and were 1.02 ± 0.57 , 0.49 ± 0.20 , 1.07 ± 0.52 , 0.54 ± 0.22 , 0.64 ± 0.23 , 0.28 ± 0.21 , and 0.69 ± 0.41 , respectively. Translocation factors for these PFAS in mutant A. thaliana were, on average, 3.4 times greater than the values in wild type A. thaliana.

The translocation factor is defined as the ratio of PFAS concentration in plant shoots to

For those PFAS with a molecular weight >450 g/mol, the translocation factors were relatively low, e.g., < 0.6. Specifically, the translocation factors of PFDA, PFDoA, PFOS, and PFOSA were 0.18 ± 0.11 , 0.006 ± 0.003 , 0.60 ± 0.21 , and 0.010 ± 0.004 , respectively, in mutant *A. thaliana*. In the wild type plants, the corresponding translocation factors were 0.17 ± 0.07 , 0.003 ± 0.001 , 0.50 ± 0.15 , and 0.006 ± 0.002 . For PFAS with a molecular weight > 450 g/mol, the translocation factors in the mutant plants were, on average, 1.5 times greater than the values in wild type plants.

Previous studies consider the Casparian strip to be a biological barrier that inhibits the diffusion of organic chemicals with a cutoff molecular weight between 400 to 500 g/mol. These studies suggest smaller-sized chemicals could readily enter the symplastic pathway without

hindrance. However, in the present study, we found that for PFAS with a molecular weight <450 g/mol, the translocation factors increased by approximately 3.4 times in mutant as compared to wild type A. thaliana, whereas the translocation factors increased only ~1.5 times for PFAS with a molecular weight > 450 g/mol. These results are in contrast to the previous assumption that the Casparian strip has a minimal impact on the transport of small molecules e.g., less than the molecular weight cutoff. Instead, the Casparian strip could effectively slow down the transport of PFAS with a molecular weight < 450 g/mol, leading to considerable differences in the translocation factors between mutant and wild type A. thaliana. Sorption of small-sized PFAS by plant roots might play a minor role in their transport from roots to shoots. For PFAS with a molecular weight >450 g/mol, their large molecular size limits their diffusion through plasma membranes and subsequent transport via the symplastic pathway, leading to lower translocation factors relative to small-sized PFAS. In addition, the large-sized PFAS could demonstrate strong sorption by plant roots, which could cause a further reduction in their translocation factor values. Felizeter et al. (2012) considered the sorption of long-chain PFCA species to lettuce roots as the dominant factor governing their accumulation in plant roots and reducing their transport to shoots. Overall, the Casparian strip could effectively retard the transport of PFAS from roots to shoots, but the extent of retardation varies in relation to molecular size, as well as sorption by plant roots.

CONCLUSION

This study evaluated the impact of the Casparian strip on PFAS transport from roots to shoots based on the comparison between a mutant without a fully formed Casparian strip vs. wild type *A. thaliana*. The mutant exhibited significantly increased PFAS accumulation in shoots compared to wild type (P < 0.1 and P < 0.05, Mann-Whitney U test). These results revealed that

the Casparian strip could effectively reduce PFAS translocation from roots to shoots. At the same time, transpiration rate, root, and shoot biomass, and PFAS accumulation in roots were not significantly different between mutant and wild type A. thaliana (P < 0.05, Mann-Whitney U test) under the same experimental conditions. The experimental results further implied that the Casparian strip plays an important role in limiting the transport of PFAS with a molecular weight < 450 g/mol. For PFAS with a molecular weight >450 g/mol, their transport was limited by the Casparian strip and sorption by plant root tissues; both factors contributed to the reduced PFAS accumulation in the plant shoots. Carbamazepine, a pharmaceutical known for its high accumulation in the shoots of multiple plant species, can accumulate to the same levels in the shoots and roots of both mutant and wild type A. thaliana. This result suggests that carbamazepine transport is not inhibited by the Casparian strip. Together, the findings reported herein provide an initial understanding of the role of the Casparian strip in PFAS transport in plants. Future research could focus on (1) quantitative evaluation of the impact of the Casparian strip to PFAS transport in plants, (2) further investigate the impacts of PFAS sorption by plant roots to root to shoot transport, (3) explore multiple plants for variations in the Casparian strip and their influence on contaminant transport, and (4) develop a genetically modified plant which alters the Casparian strip structures to achieve the goal of mitigating contaminant accumulation in the shoots of plants. This approach could be considered an innovative strategy to produce safer food from a contaminated environment.

REFERENCES

REFERENCES

- Alassimone J, Naseer S, Geldner N. 2010. A developmental framework for endodermal differentiation and polarity. Proceedings of the National Academy of Sciences of USA 107:5214–5219. https://doi.org/10.1073/pnas.0910772107
- Alassimone, J.; Roppolo, D.; Geldner, N.; Vermeer, J. E. M. The Endodermis—Development and Differentiation of the Plant's Inner Skin. Protoplasma 2012, 249 (3), 433–443. https://doi.org/10.1007/s00709-011-0302-5.
- Alassimone, J., Fujita, S., Doblas, V.G., van Dop, M., Barberon, M., Kalmbach, L., Vermeer, J.E.M., Rojas-Murcia, N., Santuari, L., Hardtke, C.S., Geldner, N., 2016. Polarly localized kinase SGN1 is required for Casparian strip integrity and positioning. Nature Plants 2. https://doi.org/10.1038/nplants.2016.113
- Blaine, A.C., Rich, C.D., Sedlacko, E.M., Hundal, L.S., Kumar, K., Lau, C., Mills, M.A., Harris, K.M., Higgins, C.P., 2014a. Perfluoroalkyl Acid Distribution in Various Plant Compartments of Edible Crops Grown in Biosolids-Amended soils. Environ. Sci. Technol. 48, 7858–7865. https://doi.org/10.1021/es500016s
- Blaine, A.C., Rich, C.D., Sedlacko, E.M., Hyland, K.C., Stushnoff, C., Dickenson, E.R.V., Higgins, C.P., 2014b. Perfluoroalkyl Acid Uptake in Lettuce (Lactuca sativa) and Strawberry (Fragaria ananassa) Irrigated with Reclaimed Water. Environ. Sci. Technol. 48, 14361–14368. https://doi.org/10.1021/es504150h
- Briggs, G.G., Bromilow, R.H., Evans, A.A., 1982. Relationships between lipophilicity and root uptake and translocation of non-ionised chemicals by barley. Pestic. Sci. 13, 495–504. https://doi.org/10.1002/ps.2780130506
- Campos Pereira, H., Ullberg, M., Kleja, D.B., Gustafsson, J.P., Ahrens, L., 2018. Sorption of perfluoroalkyl substances (PFASs) to an organic soil horizon Effect of cation composition and pH. Chemosphere 207, 183–191. https://doi.org/10.1016/j.chemosphere.2018.05.012
- Chuang, Y.-H., Liu, C.-H., Sallach, J.B., Hammerschmidt, R., Zhang, W., Boyd, S.A., Li, H., 2019. Mechanistic study on uptake and transport of pharmaceuticals in lettuce from water. Environment International 131, 104976. https://doi.org/10.1016/j.envint.2019.104976
- Chuang, Y.-H., Zhang, Y., Zhang, W., Boyd, S.A., Li, H., 2015. Comparison of accelerated solvent extraction and quick, easy, cheap, effective, rugged and safe method for extraction and determination of pharmaceuticals in vegetables. Journal of Chromatography A 1404, 1–9. https://doi.org/10.1016/j.chroma.2015.05.022

- Collins, C., Fryer, M., Grosso, A., 2006. Plant Uptake of Non-Ionic Organic Chemicals. Environ. Sci. Technol. 40, 45–52. https://doi.org/10.1021/es0508166
- Conn, S.J., Hocking, B., Dayod, M., Xu, B., Athman, A., Henderson, S., Aukett, L., Conn, V., Shearer, M.K., Fuentes, S., Tyerman, S.D., Gilliham, M., 2013. Protocol: optimising hydroponic growth systems for nutritional and physiological analysis of Arabidopsis thaliana and other plants. Plant Methods 9, 4. https://doi.org/10.1186/1746-4811-9-4
- Dong, W.Q.Y., Cui, Y., Liu, X., 2001. Instances of Soil and Crop Heavy Metal Contamination in China. Soil and Sediment Contamination: An International Journal 10, 497–510. https://doi.org/10.1080/20015891109392
- Fairbairn, D.J., Karpuzcu, M.E., Arnold, W.A., Barber, B.L., Kaufenberg, E.F., Koskinen, W.C., Novak, P.J., Rice, P.J., Swackhamer, D.L., 2016. Sources and transport of contaminants of emerging concern: A two-year study of occurrence and spatiotemporal variation in a mixed land use watershed. Science of The Total Environment 551–552, 605–613. https://doi.org/10.1016/j.scitotenv.2016.02.056
- Felizeter, S., McLachlan, M.S., de Voogt, P., 2012. Uptake of Perfluorinated Alkyl Acids by Hydroponically Grown Lettuce (Lactuca sativa). Environ. Sci. Technol. 46, 11735–11743. https://doi.org/10.1021/es302398u
- Felizeter, S., McLachlan, M.S., De Voogt, P., 2014. Root Uptake and Translocation of Perfluorinated Alkyl Acids by Three Hydroponically Grown Crops. J. Agric. Food Chem. 62, 3334–3342. https://doi.org/10.1021/jf500674j
- Higgins, C.P., Luthy, R.G., 2006. Sorption of Perfluorinated Surfactants on Sediments. Environ. Sci. Technol. 40, 7251–7256. https://doi.org/10.1021/es061000n
- Hoagland, D.R.; Arnon, D.I. The water-culture method for growing plants without soil. Calif. Agric. Ext. Publ. 1938, 347, 35–37.
- Holling, C.S., Bailey, J.L., Vanden Heuvel, B., Kinney, C.A., 2012. Uptake of human pharmaceuticals and personal care products by cabbage (Brassica campestris) from fortified and biosolids-amended soils. J. Environ. Monit. 14, 3029. https://doi.org/10.1039/c2em30456b
- Houtz, E.F., Higgins, C.P., Field, J.A., Sedlak, D.L., 2013. Persistence of Perfluoroalkyl Acid Precursors in AFFF-Impacted Groundwater and Soil. Environmental Science & Technology 47, 8187–8195. https://doi.org/10.1021/es4018877
- Keerthanan, S., Jayasinghe, C., Biswas, J.K., Vithanage, M., 2021. Pharmaceutical and Personal Care Products (PPCPs) in the environment: Plant uptake, translocation, bioaccumulation, and human health risks. Critical Reviews in Environmental Science and Technology 51, 1221–1258. https://doi.org/10.1080/10643389.2020.1753634

- Kumar, K., Gupta, S.C., 2016. A Framework to Predict Uptake of Trace Organic Compounds by Plants. J. Environ. Qual. 45, 555–564. https://doi.org/10.2134/jeq2015.06.0261
- Lee, H., Tevlin, A.G., Mabury, Scotia A., Mabury, Scott A., 2014. Fate of Polyfluoroalkyl Phosphate Diesters and Their Metabolites in Biosolids-Applied Soil: Biodegradation and Plant Uptake in Greenhouse and Field Experiments. Environ. Sci. Technol. 48, 340–349. https://doi.org/10.1021/es403949z
- Li, H., Sheng, G., Chiou, C.T., Xu, O., 2005. Relation of Organic Contaminant Equilibrium Sorption and Kinetic Uptake in Plants. Environ. Sci. Technol. 39, 4864–4870. https://doi.org/10.1021/es050424z
- Liu, Z., Lu, Y., Song, X., Jones, K., Sweetman, A.J., Johnson, A.C., Zhang, M., Lu, X., Su, C., 2019. Multiple crop bioaccumulation and human exposure of perfluoroalkyl substances around a mega fluorochemical industrial park, China: Implication for planting optimization and food safety. Environment International 127, 671–684. https://doi.org/10.1016/j.envint.2019.04.008
- Malamy, J.E., Benfey, P.N., 1997. Organization and cell differentiation in lateral roots of Arabidopsis thaliana. Development 124:33-44.
- Miller, E.L., Nason, S.L., Karthikeyan, K.G., Pedersen, J.A., 2016. Root Uptake of Pharmaceuticals and Personal Care Product Ingredients. Environ. Sci. Technol. 50, 525–541. https://doi.org/10.1021/acs.est.5b01546
- Navarro, I., de la Torre, A., Sanz, P., Porcel, M.Á., Pro, J., Carbonell, G., Martínez, M. de los Á., 2017. Uptake of perfluoroalkyl substances and halogenated flame retardants by crop plants grown in biosolids-amended soils. Environmental Research 152, 199–206. https://doi.org/10.1016/j.envres.2016.10.018
- Pfister, A., Barberon, M., Alassimone, J., Kalmbach, L., Lee, Y., Vermeer, J.E., Yamazaki, M., Li, G., Maurel, C., Takano, J., Kamiya, T., Salt, D.E., Roppolo, D., Geldner, N., 2014. A receptor-like kinase mutant with absent endodermal diffusion barrier displays selective nutrient homeostasis defects. eLife 3, e03115. https://doi.org/10.7554/eLife.03115
- Scher, D.P., Kelly, J.E., Huset, C.A., Barry, K.M., Hoffbeck, R.W., Yingling, V.L., Messing, R.B., 2018. Occurrence of perfluoroalkyl substances (PFAS) in garden produce at homes with a history of PFAS-contaminated drinking water. Chemosphere 196, 548–555. https://doi.org/10.1016/j.chemosphere.2017.12.179
- Shenker, M., Harush, D., Ben-Ari, J., Chefetz, B., 2011. Uptake of carbamazepine by cucumber plants A case study related to irrigation with reclaimed wastewater. Chemosphere 82, 905–910. https://doi.org/10.1016/j.chemosphere.2010.10.052

- Sicbaldi, F., Sacchi, G.A., Trevisan, M., Del Re, A.A.M., 1997. Root Uptake and Xylem Translocation of Pesticides from Different Chemical Classes. Pestic. Sci. 50, 111–119. https://doi.org/10.1002/(SICI)1096-9063(199706)50:2<111::AID-PS573>3.0.CO;2-3
- Schnoor, J.L., Light, L.A., McCutcheon, S.C., Wolfe, N.L. and Carreia, L.H., 1995. Phytoremediation of organic and nutrient contaminants. Environmental science & technology, 29(7), pp.318A-323A.
- Stahl, T., Heyn, J., Thiele, H., Hüther, J., Failing, K., Georgii, S., Brunn, H., 2009. Carryover of Perfluorooctanoic Acid (PFOA) and Perfluorooctane Sulfonate (PFOS) from Soil to Plants. Arch Environ Contam Toxicol 57, 289–298. https://doi.org/10.1007/s00244-008-9272-9
- Trapp, St., Pussemier, L., 1991. Model calculations and measurements of uptake and translocation of carbamates by bean plants. Chemosphere 22, 327–339. https://doi.org/10.1016/0045-6535(91)90321-4
- Wang, W., Rhodes, G., Ge, J., Yu, X., Li, H., 2020. Uptake and accumulation of per- and polyfluoroalkyl substances in plants. Chemosphere 261, 127584. https://doi.org/10.1016/j.chemosphere.2020.127584
- Wu, X., Ernst, F., Conkle, J.L., Gan, J., 2013. Comparative uptake and translocation of pharmaceutical and personal care products (PPCPs) by common vegetables. Environment International 60, 15–22. https://doi.org/10.1016/j.envint.2013.07.015
- Wu, X., Dodgen, L.K., Conkle, J.L., Gan, J., 2015. Plant uptake of pharmaceutical and personal care products from recycled water and biosolids: a review. Science of The Total Environment 536, 655–666. https://doi.org/10.1016/j.scitotenv.2015.07.129
- Zhao, H., Guan, Y., Qu, B., 2018. PFCA uptake and translocation in dominant wheat species (Triticum aestivum L.). International Journal of Phytoremediation 20, 68–74. https://doi.org/10.1080/15226514.2017.1337066

CHAPTER IV.

PFAS CONTAMINATION IN SURFACE WATER AND SEDIMENT FROM HISTORICAL LAND APPLICATION OF BIOSOLIDS

ABSTRACT

The impact of land applied per- and polyfluoroalkyl substances (PFAS)-contaminated biosolids to downstream surface water and sediment quality was examined using systematically collected samples from twenty locations in Fort Gratiot, Michigan. These locations included and bracketed an agricultural field that received a known application of biosolids in 1983, likely containing high concentrations of PFAS. Perfluorooctane sulfonic acid (PFOS) and Perfluorooctanoic acid (PFOA) were the dominant PFAS species present in the soil of the biosolids-applied field and in downstream surface water and sediment samples. Their concentrations ranged from 98,400 to 150,000 ng/kg PFOS and 831 to 3,000 ng/kg PFOA in the soil of the biosolids-applied field, from 0.9 to 11,000 ng/L PFOS and 5.4 to 1,200 ng/L PFOA in surface water samples, and from 550 to 13,000 ng/kg PFOS and non-detect to 530 ng/kg PFOA in sediment samples, respectively. The concentrations in the surface water and sediment samples decreased with increasing distance from the biosolids-applied field. The PFAS compositional profile among downstream surface water samples and sediment samples were remarkably consistent in general and displayed distinct differences from the upstream locations. The results indicate that historical applications of PFAS-containing biosolids to agricultural land could have a long-term impact on the surface water and sediment quality of the downstream area.

INTRODUCTION

Per- and polyfluoroalkyl substances (PFAS) are a large class of anthropogenic chemicals that have been used in numerous manufacturing processes and consumer products for over 50 years (Tuve and Jablonski, 1966). Their unique chemical structure manifests oil/water repellency and long-term stability against physical, biological, and chemical decomposition. These unique properties have made them ideal for use in surfactants, paper products, food packaging, textiles, aqueous film-forming foams (AFFF), and paints (Brendal et al., 2018; Buck et al., 2011). PFAS consist of a polar head group (e.g., carboxylic or sulfonic acid) and a perfluoroalkyl tail chain. Because the C-F bond is remarkably strong, PFAS are recalcitrant in the environment.

Globally, PFAS have been frequently detected in wastewater, surface water, groundwater, landfill effluents, soils, sediments, atmospheric deposition, and plant and animal tissues (Kwok et al., 2013; Dalahmeh et al., 2018; Hepburn et al., 2019; Sharp et al., 2021; Scher et al., 2018). Sources of PFAS to the environment are diverse, including AFFF used in firefighting/fire training sites, emissions from manufacturing sites and waste incineration, disposal of primary and secondary manufacturing wastes and wastewater, irrigation with treated wastewater, and the land application of biosolids (Aleksandrov et al., 2019; Hale et al., 2017; Gallen et al., 2018; Brusseau et al., 2020; Shigei et al., 2020; Washington et al., 2010). The frequent detection of PFAS in the environment is of particular concern considering the persistence, environmental prevalence, bioaccumulation, and toxicity of PFAS and that the likelihood of human exposure is increased when PFAS are found in drinking water, agricultural irrigation water, and fish and wildlife.

In response to these concerns, Michigan began monitoring surface water and fish tissue for PFAS in the early 2000s. PFOS and PFOA have since been found to be nearly ubiquitous in

surface waters across Michigan, with concentrations ranging from non-detect to 11,000 ng/L, and PFOS has been frequently detected in fish tissues collected from Michigan surface waterbodies (Armstrong et al., 2019). The State of Michigan currently regulates PFOA and PFOS in surface water through Rule 57 Human Noncancer Values, which were developed in 2011 and 2014 for PFOA and PFOS, respectively. PFOA and PFOS are regulated at 420 ng/L and 11 ng/L, respectively, in surface waters serving as a drinking water source. All other surface waterbodies are regulated at 12,000 ng/L and 12 ng/L, respectively, for PFOA and PFOS. Other regulatory values were developed by the State of Michigan in 2015, 2018, 2019, and 2020 (MPART, 2019).

A US national survey in 2007 revealed that about 7.2 million tons of biosolids (dry weight) were produced and approximately 55% of the biosolids were land-applied to soils (NEBRA, 2007). Substantial research on the occurrence of PFAS in biosolids has been documented in the published literature (Venkatesan and Halden, 2013; Gallen et al., 2018; Kim Lazcano et al., 2019; Navarro et al., 2016; Chen et al., 2012), and PFAS concentrations in biosolids have been observed at μg/kg or low mg/kg levels (Alder and van der Voet, 2105; Schultz et al., 2006; Loganathan et al., 2017). It has been estimated that the total annual loadings of PFAS to agricultural lands from biosolids application could range from 1.4 to 2.1 metric tons in the US (Venkatesan and Halden, 2013). Commonly, studies have focused on PFAS contamination in soil or groundwater resulting from the use of land-applied biosolids (Pepper et al., 2021; Gottschall et al., 2010). For example, agricultural land in Decatur, Alabama received biosolids for more than a decade, as a result, PFAS concentrations in the soils were observed at up to several mg/kg on a dry soil basis (Washington et al., 20210). However, studies evaluating the impact of the land application of biosolids to surface water and sediment quality are scarce.

The objective of this research was to examine an under-studied source of PFAS contamination to surface water and sediment, the land application of biosolids. Agricultural land where the land application of PFAS containing biosolids has taken place, could potentially serve as a source of PFAS contamination to surrounding waterbodies. The occurrence of 24 PFAS in samples collected from the Black River watershed in St. Clair County, Michigan, are used to identify and characterize a source of PFAS contamination and provide critical information on the occurrence and distribution of PFAS in surface water and sediments. The results provide a useful case study for researchers and regulatory agencies attempting to understand other instances of surface waters impacted by PFAS originating from the land application of PFAS contaminated biosolids.

SITE HISTORY AND DESCRIPTION

In 2018, routine monitoring of the Black River watershed, located in St. Clair County, Michigan, identified surface water samples in the Brandymore/Howe Drain with PFOS concentrations exceeding Michigan's Rule 57 Surface Water Quality Standard of 12 ng/L. These samples indicated that there was unknown but significant source of PFAS contamination in the area, as the elevated levels of PFOS were detected far outside of the area expected to be influenced by known sources. Extensive follow-up monitoring, consisting of surface water and sediment sampling was conducted in the Brandymore/Howe Drain area from 2019 to 2020. An agricultural field (29.3 acre), which had one known application of biosolids at 2.2 tons/acre in 1983, was identified in close proximity to this area. This agricultural field is highlighted in Figure 4.1. as the biosolids-applied field. The source of these biosolids was a municipal wastewater treatment plant likely receiving PFAS containing influent from a nearby secondary manufacturing facility at that time. Soil samples from the biosolids-applied field were collected

in 2019. Surface and subsurface flow from this field discharges into the Brandymore/Howe Drain, whose source waters are mainly agricultural in nature, with some suburban inputs. An overview of the studied area is shown in Figure 4.1. Sampling site information is shown in Table 4.1.

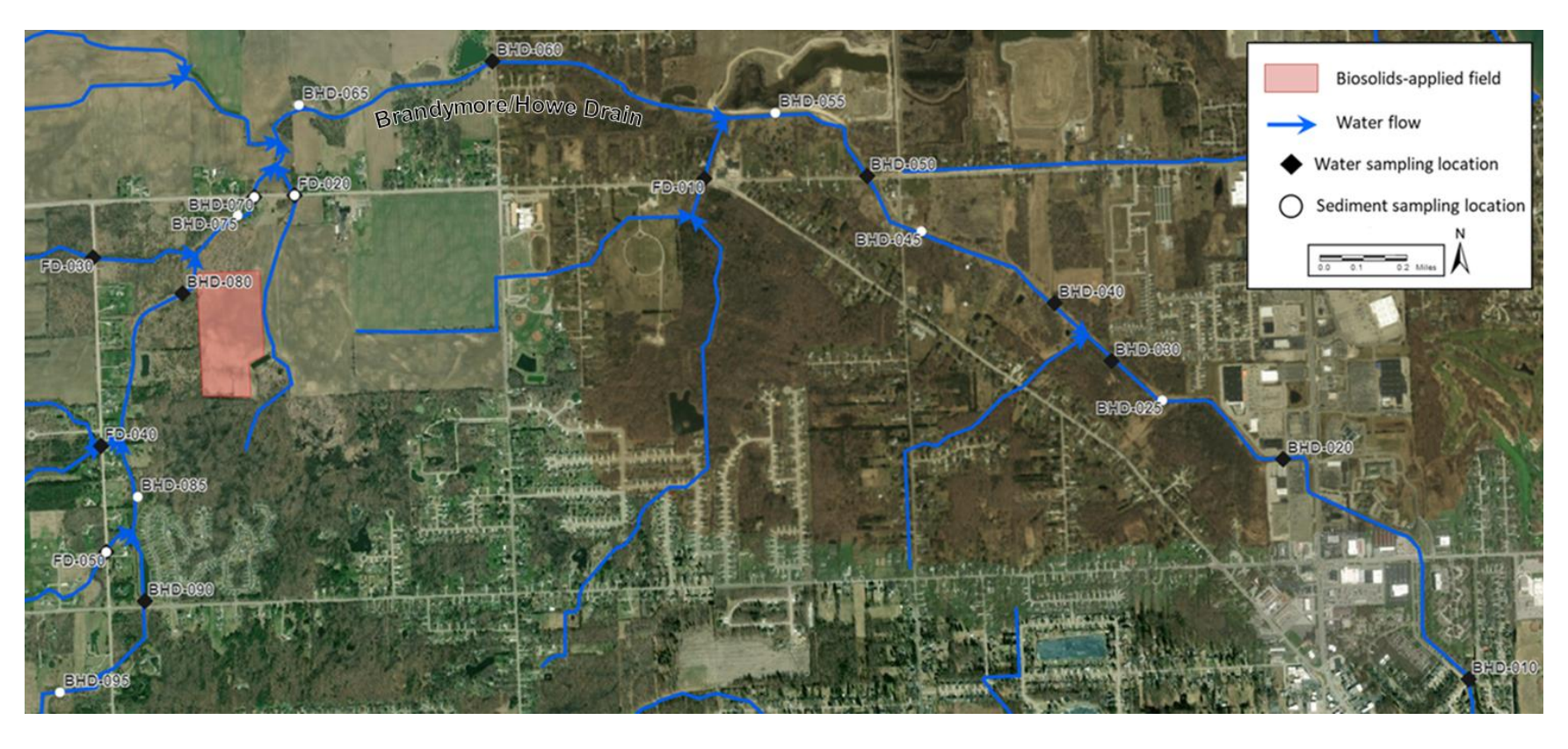


Figure 4.1 Map of surface water and sediment sampling sites in the studied area of the Brandymore/Howe Drain. *The field highlighted in red received one known historical application of contaminated biosolids. Water flow is shown with blue arrows. Black diamonds and white circles represent surface water and sediment sampling locations, respectively.*

 Table 4.1 Sampling location information for surface water and/or sediment

Site Name	Sample Type	Latitude	Longitude	Collection Date 1	Collection Date 2	Collection Date 3	Collection Date 4	Collection Date 5
BHD-090	W	43.02372	-82.51340	-	9/12/2019	-	-	-
FD-050	W, S	43.02548	-82.51529	-	9/12/2019	11/6/2019	-	-
FD-040	W	43.02928	-82.51553	-	9/12/2019	-	-	-
FD-030	W	43.03601	-82.51592	-	9/12/2019	-	-	-
BHD-070	W, S	43.03820	-82.50802	-	9/12/2019	11/6/2019	12/18/2019	-
FD-020	W, S	43.03825	-82.50605	-	9/12/2019	11/6/2019	12/18/2019	-
BHD-060	W	43.04305	-82.49634	-	9/12/2019	-	-	-
FD-010	W	43.03884	-82.48597	7/1/2019	9/12/2019	11/6/2019	-	-
BHD-050	W	43.03893	-82.47800	-	9/12/2019	-	-	-
BHD-040	W	43.03438	-82.46879	-	9/12/2019	-	-	-
BHD-020	W	43.02882	-82.45760	-	9/12/2019	-	-	-
BHD-010	W	43.02092	-82.44851	-	9/12/2019	-	-	-
BHD-095	S	43.02045	-82.51756	-	-	-	-	8/11/2020
BHD-085	S	43.02746	-82.51374	-	-	-	-	8/11/2020
BHD-075	S	43.03752	-82.50885	-	-	-	-	8/11/2020
BHD-065	S	43.04149	-82.50583	-	-	-	-	8/11/2020
BHD-055	S	43.04120	-82.48248	-	-	-	-	8/11/2020
BHD-045	S	43.03696	-82.47531	-	-	-	-	8/11/2020
BHD-025	S	43.03092	-82.46354	-	-	-	-	8/11/2020

W = Surface water sample, S = Sediment sample

MATERIALS AND METHODS

Soil samples

Soil samples were collected following the protocols described in the Michigan

Department of Environmental Quality Soil PFAS Sampling Guidance (11/2018). Five soil

samples were collected from the biosolids-applied field (Figure 4.1) in December 2019. Soil

samples were collected from approximately 0 to 20 cm depth with a shovel/pickaxe and stored in

certified PFAS-free containers provided by Vista Analytical Laboratory (El Dorado Hills, CA,

USA). The sampling equipment was cleaned prior to use with PFAS-free deionized water and

Alconox detergent (Alconox, Inc. White Plains, NY, USA). Sampling equipment was

decontaminated in the field between samples by triple rinsing with PFAS-free deionized water.

Nitrile gloves and PFAS-free field clothing were worn during sample collection and handling.

Duplicate soil samples, as well as an equipment rinsate blank, were collected to meet quality

assurance and quality control requirements. One trip blank was provided by Vista Analytical

Laboratory.

Surface water samples

Surface water samples were collected in accordance with the protocols described in the Michigan Department of Environmental Quality Surface Water PFAS Sampling Guidance (11/2018). Surface water samples were collected in July, September, November, and December 2019, with the specific sampling locations labeled in Figure 4.1. Surface water sampling locations were chosen to facilitate the identification of the unknown source of elevated PFOS concentrations detected in the Brandymore/Howe Drain. Surface water samples were collected using the direct hand-dipping method. Specifically, the sample collection bottles were inverted and immersed to a depth of 5 cm, upstream of the collector, then righted. All surface water

samples were collected in certified PFAS-free high density polyethylene bottles provided by Eurofins Environment Testing America (Sacramento, CA, USA). All personnel wore nitrile gloves and PFAS-free field clothing during sample collection and handling. Trip blanks, provided by Eurofins Environment Testing America, and field blanks, consisting of PFAS-free deionized water, were collected/prepared for each sampling event. For quality control, replicate and duplicate samples were collected.

Sediment samples

Sediment samples were collected in September, November, and December 2019, and August 2020 following protocols from the Michigan Department of Environmental Quality Sediment PFAS Sampling Guidance (06/2019). Specific sampling locations are shown in Figure 4.1. In general, the sediment sampling locations were selected from areas with known or suspected high concentrations of PFOS in surface water based on prior sampling and analysis. The sediment samples were collected from the top 20 cm of the sediment column using a stainless-steel spoon at the wadable locations or using a ponar 'grab' sampler in non-wadable locations. The collected sediment samples were placed into certified PFAS-free containers provided by Eurofins Environment Testing America. Nitrile gloves and PFAS-free field clothing were worn during sample collection and handling. Sampling equipment was cleaned prior to use with PFAS-free deionized water and Alconox detergent. Sampling equipment was decontaminated in the field between samples by triple rinsing with PFAS-free deionized water. For quality control, one replicate sample and one duplicate sample were collected, per 10 ambient samples, for each sampling event. An equipment rinsate blank was collected and a trip blank was provided, by Eurofins Environment Testing America, for each sampling event.

PFAS analysis

Surface water, soil, and sediment samples were analyzed for a suite of PFAS analytes by either Vista Analytical Laboratory or Eurofins Environment Testing America (Table 4.2). All samples were stored at 4°C and shipped to the laboratory within 14 days of collection for surface water samples and 60 days of collection for soil or sediment samples. Surface water and sediment samples were analyzed by Eurofins Environment Testing America and soil samples were analyzed by Vista Analytical Laboratory. Extraction and analyses occurred within 28 days after receipt of the samples. Both analytical laboratories utilized proprietary extraction procedures, solid phase extraction was used for aqueous samples and ultrasonic extraction for solid samples, and proprietary isotope dilution methods to quantify PFAS concentrations based on EPA Method 537.1 with modifications. Quality control procedures compliant with the Department of Defense, Quality Systems Manual v5.1 or higher, Table B-15, were employed by both laboratories. All Laboratory control samples had PFAS analytes which were within acceptable recovery limits. The standard deviation of the PFAS analytes of duplicate laboratory control samples were within the acceptable range. The recoveries of isotopically labeled standards were typically within the accepted range of 25%-150%. Quantification using isotopelabeled standards with recovery outside of the acceptable range, in fact, did not impact data quality, because the signal to noise ratios were greater than 10:1 in all cases. Equipment rinsate, trip blanks, and field blanks were all non-detect for all PFAS analytes, excluding the analytes found in the laboratory method blanks. No PFAS analytes were detected in the method blank above ½ of the limit of quantification. When PFAS analytes were detected in the method blank, the concentration detected was subtracted from the concentration detected in samples corresponding to that method blank samples

Table 4.2 PFAS analyzed in soil, surface water, and sediment samples

CASRN	Analyte	Structural Formula	MW (g/mol)
375-22-4	PFBA	$CF_3(CF_2)_2CO_2H$	214.04
2706-90-3	PFPeA	$CF_3(CF_2)_3CO_2H$	264.05
307-24-4	PFHxA	$CF_3(CF_2)_4CO_2H$	314.05
375-85-9	PFHpA	$CF_3(CF_2)_5CO_2H$	364.06
335-67-1	PFOA	$CF_3(CF_2)_6CO_2H$	414.07
375-95-1	PFNA	$CF_3(CF_2)_7CO_2H$	464.08
335-76-2	PFDA	$CF_3(CF_2)_8CO_2H$	514.08
2058-94-8	PFUnA	$CF_3(CF_2)_9CO_2H$	564.09
307-55-1	PFDoA	$CF_3(CF_2)_{10}CO_2H$	614.10
72629-94-8	PFTriA	$CF_3(CF_2)_{11}CO_2H$	664.10
376-06-7	PFTeA	$CF_3(CF_2)_{12}CO_2H$	714.11
375-73-5	PFBS	$CF_3(CF_2)_3SO_3H$	300.10
2706-91-4	PFPeS	$CF_3(CF_2)_4SO_3H$	350.11
355-46-4	PFHxS	$CF_3(CF_2)_5SO_3H$	400.12
375-92-8	PFHpS	$CF_3(CF_2)_6SO_3H$	450.12
1763-23-1	PFOS	$CF_3(CF_2)_7SO_3H$	500.13
68259-12-1	PFNS	$CF_3(CF_2)_8SO_3H$	550.14
335-77-3	PFDS	$CF_3(CF_2)_9SO_3H$	600.15
754-91-6	FOSA	$CF_3(CF_2)_7SO_2NH_2$	499.15
2355-31-9	NMeFOSAA	$CF_3(CF_2)_7SO_2NCH_3CH_2CO_2H$	571.21
2991-50-6	NEtFOSAA	$CF_3(CF_2)_7SO_2NCH_2CH_3CH_2CO_2H$	585.24
757124-72-4	4:2 FTS	$CF_3(CF_2)_3(CH_2)_2SO_3H$	328.15
27619-97-2	6:2 FTS	$CF_3(CF_2)_5(CH_2)_2SO_3H$	428.17
39108-34-4	8:2 FTS	$CF_3(CF_2)_7(CH_2)_2SO_3H$	528.18

RESULTS AND DISCUSSION

PFAS in biosolids-amended soil

PFAS concentrations in the soil samples collected from the biosolid-applied field (Figure 4.1) in December 2019 are summarized in Table 4.3. The analytes PFOS, N-ethylperfluorooctane sulfonamidoacetic acid (NEtFOSAA), perfluorooctanesulfonamide (FOSA), PFOA, and Nmethylperfluorooctane sulfonamidoacetic acid (NMeFOSAA) were detected in all soil samples. Other targeted PFAS analytes (see Table 4.2) were below the limit of detection. Among the analytes detected, PFOS occurred at the highest concentration, ranging from 98,400 to 150,000 ng/kg, with a mean concentration of 120,480 ng/kg. The mean concentrations of NEtFOSAA, FOSA, PFOA, and NMeFOSAA were 12,362 ng/kg, 7,446 ng/kg, 2,160 ng/kg, and 840 ng/kg, respectively. Previous comparable studies also observed PFOS detected at the highest concentration in soils amended with biosolids. However, the total PFAS concentrations were lower than those observed in this study, ranging from non-detect to 4,000 ng/kg (Pepper et al., 2021; Navarro et al., 2016). In the present study, the soils that received land-applied biosolids had a mean total PFAS concentration of 143,300 ng/kg. The known biosolids application at the site (29.3 acres, Figure 4.1) occurred at a rate of 2.2 tons/acre in 1983. The observed total PFAS concentration in soil was much higher than those reported by Pepper et al. (2021) for Arizona agricultural fields, where total PFAS concentrations ranged from 2,500 to 8,600 ng/kg, and biosolids were applied repetitively at rates of up to 30 tons/acre between 1984 and 2019. This suggests PFAS concentrations in biosolids from this study were significantly higher than what was observed in Pepper et al. (2021), where PFAS concentrations in biosolids ranged from 14 to $36 \mu g/kg$ for PFOS, <1.9 to 11 $\mu g/kg$ for NEtFOSAA, <0.44 to 1.2 $\mu g/kg$ for PFOA, and 18 to 23 μg/kg for NMeFOSAA.

A rough estimate of the PFAS concentrations in the original biosolids can be made if one assumes that the biosolids were fully incorporated into the field to plow depth and that an acre furrow slice (one acre to a plow depth of 6 inches) contains $\approx 9 \times 10^5$ kg soil. It follows that a total of 64.46 tons, or 58,477 kg, of biosolids were applied to the 29.3-acre field and incorporated into $\approx 2.64 \times 10^7$ kg soil. Using the mean concentrations of PFAS found in the biosolids-applied field, it follows that the original PFAS concentrations in the biosolids were 54.4 mg/kg, 5.58 mg/kg, 3.36 mg/kg, 0.98 mg/kg, and 0.38 mg/kg for PFOS, NEtFOSAA, FOSA, PFOA, and NMeFOSAA, respectively. This estimated PFOS concentration is roughly 20 to 3800 times higher than PFOS concentrations reported for biosolids within the US by Higgins et al. (2005). The estimated concentrations of NEtFOSAA, FOSA, PFOA, and NMeFOSAA are near what has been reported in the literature, where concentrations have ranged from ug/kg to low mg/kg levels (Alder and van der Voet, 2105; Schultz et al., 2006; Loganathan et al., 2017). For instance, PFOA concentrations in biosolids from wastewater treatment plants in New York state has been reported at up to 0.24 mg/kg (Sinclair and Kannan, 2006).

Table 4.3 Statistics of PFAS (ng/kg) detected in soils collected from the biosolids-applied field (n = 5) in December 2019

Analyte		PFAS Conc		Detection frequency	
	Min	Max	Mean	Median	
PFBA	ND	ND	ND	ND	0.0%
PFPeA	ND	ND	ND	ND	0.0%
PFHxA	ND	ND	ND	ND	0.0%
PFHpA	ND	ND	ND	ND	0.0%
PFOA	831	3000	2160	2330	100.0%
PFNA	ND	ND	ND	ND	0.0%
PFDA	ND	ND	ND	ND	0.0%
PFUnA	ND	ND	ND	ND	0.0%
PFDoA	ND	ND	ND	ND	0.0%
PFTriA	ND	ND	ND	ND	0.0%
PFTeA	ND	ND	ND	ND	0.0%
PFBS	ND	ND	ND	ND	0.0%
PFPeS	ND	ND	ND	ND	0.0%
PFHxS	ND	ND	ND	ND	0.0%
PFHpS	ND	ND	ND	ND	0.0%
PFOS	98400	150000	120480	112000	100.0%
PFNS	ND	ND	ND	ND	0.0%
PFDS	ND	ND	ND	ND	0.0%
FOSA	3360	13500	7446	7270	100.0%
NMeFOSAA	494	1630	840	732	100.0%
NEtFOSAA	7220	23600	12362	11000	100.0%
4:2 FTS	ND	ND	ND	ND	0.0%
6:2 FTS	ND	ND	ND	ND	0.0%
8:2 FTS	ND	ND	ND	ND	0.0%
Mean Total PFCA		Mean Total PFSA	<u> </u>	Mean Total PFA	1S
2,100 ng/kg		120,500 ng/kg		143,300 ng/kg	

ND: below the method detection limit, PFSA: perfluorosulfonic acids, PFCA: perfluorocarboxylic acids

PFAS in surface water

Statistics of PFAS concentrations in surface water samples collected in September 2019 are presented in Table 4.4. Out of the 24 individual PFAS analyzed, 14 were found in surface water samples from the studied area. In the present study, 11 analytes, perfluorobutanoic acid (PFBA), PFPeA, PFHxA, PFHpA, PFOA, perfluorononanoic acid (PFNA), perfluorodecanoic acid (PFDA), PFBS, PFHxS, perfluoroheptane sulfonic acid (PFHpS), and PFOS, were detected in 50% or more of the collected samples. The mean concentrations of these 11 analytes ranged from 2.5 to 1,149.7 ng/L (Table 4.4). In comparison, Bai and Son (2021) measured 17 PFAS species in surface water samples from the Las Vegas Wash, whose source waters include urban run-off and treated wastewater, and detected 11 PFAS species. Of the 11 PFAS species observed by Bai and Son (2021), seven PFAS perfluoropentanoic acid (PFPeA), perfluorohexanoic acid (PFHxA), perfluoroheptanoic acid (PFHpA), PFOA, PFBS, perfluorohexane sulfonic acid (PFHxS), and PFOS were detected in 50% or more of the samples. Goodrow et al. (2020) measured PFAS in surface waters of New Jersey that were suspected to be impacted by PFAS and were areas of recreational use and/or subsistence fishing, and found that concentrations of these same analytes, excluding PFHpS, ranged from non-detectable to 28.8 ng/L. The occurrence of multiple PFAS species in surface waters is commonly observed, likely due to their extensive use across multiple industries and in consumer products.

Table 4.4 Statistics of PFAS (ng/L) detected in surface water (n = 12) in September 2019

Analyte		PFAS Conce	Detection Frequency		
<u> </u>	Min	Max	Mean	Median	_ Detection Frequency
PFBA	1.9	20.0	11.0	11.0	100.0%
PFPeA	5.7	210	26.3	26.5	91.7%
PFHxA	7.9	93	27.8	26.5	91.7%
PFHpA	3.7	110	21.2	16.5	91.7%
PFOA	5.4	530	150.9	51.5	91.7%
PFNA	0.5	120	4.4	3.0	91.7%
PFDA	1.2	610	3.5	2.0	66.7%
PFUnA	ND	140	ND	ND	0.0%
PFDoA	ND	260	ND	ND	0.0%
PFTriA	ND	ND	ND	ND	0.0%
PFTeA	ND	ND	ND	ND	0.0%
PFBS	0.6	ND	4.0	3.0	100.0%
PFPeS	0.5	ND	0.5	ND	16.7%
PFHxS	1.1	76	2.5	1.5	91.7%
PFHpS	3.0	ND	30.3	1.5	50.0%
PFOS	0.9	13000	1149.7	243.0	100.0%
PFNS	1.1	ND	1.1	ND	8.3%
PFDS	ND	ND	ND	ND	0.0%
FOSA	ND	240	ND	ND	0.0%
NMeFOSAA	ND	ND	ND	ND	0.0%
NEtFOSAA	2.0	ND	4.6	ND	16.7%
4:2 FTS	ND	ND	ND	ND	0.0%
6:2 FTS	ND	ND	ND	ND	0.0%
8:2 FTS	ND	ND	ND	ND	0.0%
Mean Total PFCA		Mean Total PF	SA	Mean Total	PFAS
225 ng/L		1171 ng/L		1397 ng/L	

ND: below the method detection limit, PFSA: perfluorosulfonic acids, PFCA: perfluorocarboxylic acids.

Total PFAS concentration in surface water samples collected in September 2019, from the Brandymore/Howe Drain area are shown in Figure 4.2A. Notably, PFAS concentrations in the surface water samples collected upstream of the biosolid-applied field were lower than those measured in downstream surface water samples. The total PFAS concentration was 40.5 ng/L at BHD-090, 145.3 ng/L at FD-050, 173.3 ng/L at FD-040, and 3.4 ng/L at FD-030 (upstream of the biosolids-applied field), which were lower than 222.5 ng/L at BHD-070, 896.0 ng/L at BHD-060, 633.4 ng/L at BHD-050, 764.4 ng/L at BHD-040, 564.4 ng/L at BHD-020, and 596.1 ng/L at BHD-010 (downstream of the biosolids-applied field). The highest total PFAS concentration (12,530 ng/L) was found at the sampling location FD-020, located immediately downstream of the biosolids-applied field. The surface water sample at the sampling location FD-010, a tributary to the Brandymore/Howe Drain downstream of the biosolids-applied field, in comparison to the total PFAS concentrations upstream, indicate that the biosolids-applied field could be the source releasing PFAS into the Brandymore/Howe Drain.

Individual PFAS concentrations and the relative PFAS composition in surface water samples are shown in Figures 4.2B and 4.2C. Among the PFAS found downstream of the biosolids-applied field, PFOS and PFOA are the dominant species in surface water at the sampling locations FD-020, BHD-060, BHD-050, BHD-040, BHD-020, and BHD-010. Concentrations of PFAS at these sampling locations range from 410 to 11,000 ng/L for PFOS and 58 to 1,200 ng/L for PFOA, the sum of these two species is equivalent to 83 to 97 % of the total PFAS concentration. Similarly, PFOS and PFOA were the dominant PFAS species found in the soil samples taken from the biosolids applied field (Table 4.3). The ratio of PFOA to PFOS, at the sampling locations downstream of the biosolids-applied field ranged from 0.11 to 0.15,

with the ratio increasing with increasing distance downstream. The PFOA to PFOS ratio was 1.17 at the upstream sampling locations BHD-090 and 1.07 at the downstream location BHD-070. This suggests that the majority of the PFAS released from the biosolids-applied field traveled via the tributary passing through the sampling location FD-020. This is consistent with the analysis of total PFAS concentrations in surface water samples, where the highest total PFAS concentration was detected at sampling location FD-020.

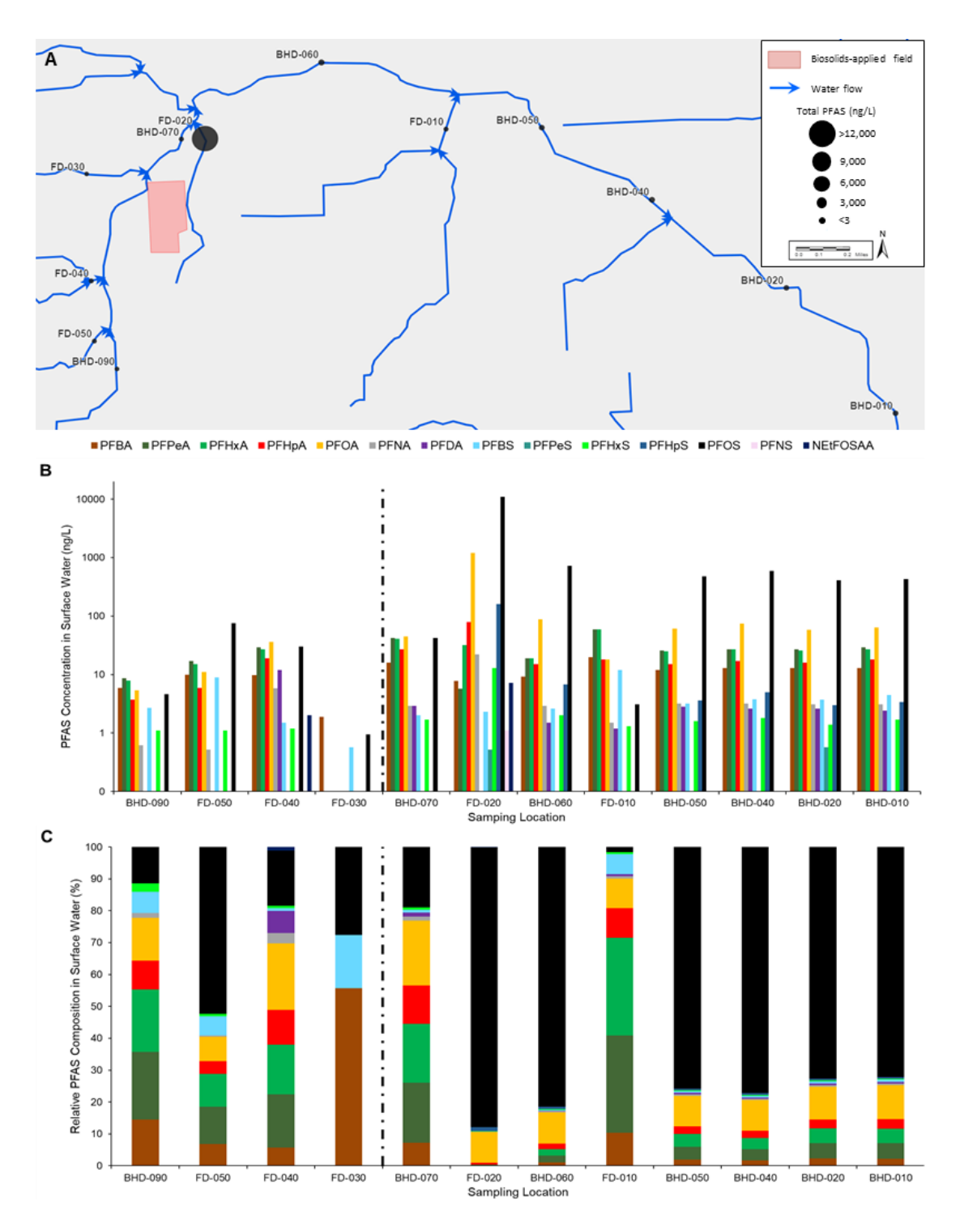


Figure 4.2 PFAS in surface water samples collected in September 2019 (n = 12). (A) Total PFAS concentrations. A field with known historical applications of contaminated biosolids is highlighted in red. Water flow is shown with blue arrows. Black circle size represents the total PFAS concentration (ng/L) in surface water. (B) Variation of PFAS concentrations and (C) relative composition of PFAS. The dashed line separates samples collected upstream and downstream of the field with known historical applications of contaminated biosolids, with samples upstream appearing to the left of the line.

Interestingly, PFHpS was observed only at the sampling locations downstream of the biosolids-applied field, i.e., FD-020, BHD-060, BHD-050, BHD-040, BHD-020, and BHD-010, with the concentration decreasing with increasing distance from the biosolids-applied field (Figure 4.2B). The concentration of PFHpS at these sampling locations ranged from 3.0 to 160 ng/L, whereas PFHpS was measured below the limit of detection in surface water samples at all upstream sampling locations, the sampling location FD-010 (a tributary to the Brandymore/Howe Drain located downstream of the biosolids-applied field), and the soil samples collected from the biosolids-applied field. The presence of PFHpS only in surface water samples collected downstream of the biosolids-applied field indicates it is possible that this PFAS formed from the transformation of PFAS precursors, such as NMeFOSAA and NetFOSAA, which have been observed to transform into PFSAs (Murakami et al., 2013; Ellis et al., 2004; Sima and Jaffé, 2021, Wang et al., 2011). The precursors FOSA and NMeFOSAA were not detected in surface water samples, while the precursor NEtFOSAA was detected in 16.7% of the surface water samples. These precursors were detected in all five soil samples (Table 4.3), with mean concentrations of 7,446 ng/kg for FOSA, 840 ng/kg for NMeFOSAA, and 12,362 ng/kg for NEtFOSAA. PFAS precursors in soils could transform into more stable PFAS and serve as a source for the release of PFAS contaminants.

The concentrations of individual PFAS in surface water that were detected at ≥50% of the sampling locations (Table 4.4) are shown as radar plots in Figures 4.3 and 4.4. Distinct differences in the PFAS compositional profile for sampling locations upstream of the biosolidsapplied field and tributaries to the Brandymore/Howe Drain downstream of the biosolidsapplied field are evident in the dissimilar patterns formed at each sampling location (Figure 4.3). This is consistent with the relative composition of PFAS observed at these same sampling locations in

Figure 4.2C. Sampling locations FD-020 and the Brandymore/Howe Drain sampling locations located downstream of the biosolids-applied field (i.e., BHD-060, BHD-050, BHD-040, BHD-020, BHD-010) were remarkably consistent in PFAS compositional profile, as evidenced by the similar patterns formed in the radar plots of these sampling locations (Figure 4.4). The similar PFAS compositional profiles downstream of the biosolids-applied field, in comparison to the distinct PFAS compositional profiles upstream, indicate that the biosolids-applied field could be the source releasing PFAS into the Brandymore/Howe Drain. This is consistent with the analyses of total PFAS in surface water samples and relative composition of PFAS in surface water samples (Figures 4.2A and 4.2C).

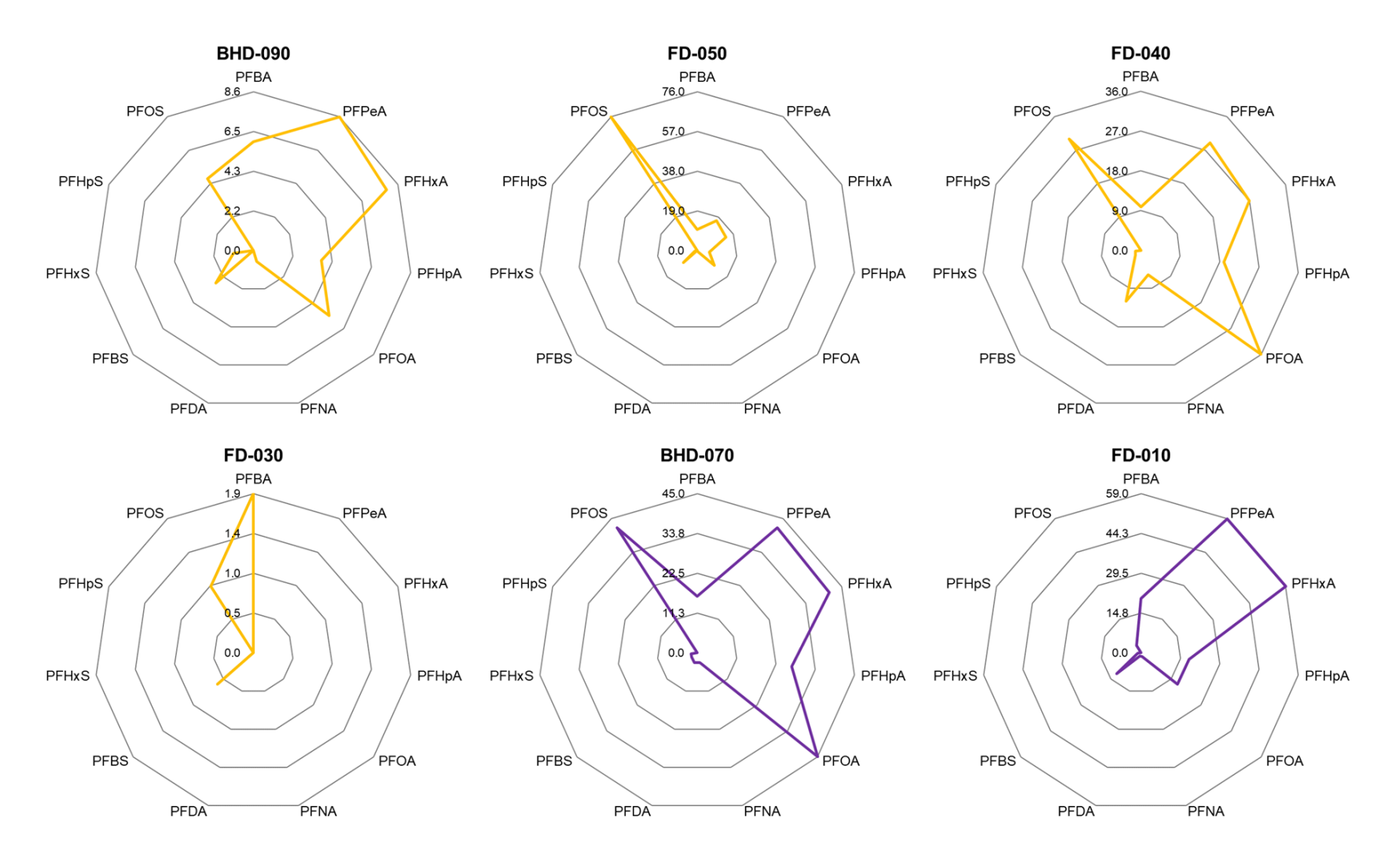


Figure 4.3 Radar plots of select PFAS concentrations (ng/L) in surface water samples. Sampling locations upstream of the biosolids-applied field are shown in orange. Sampling locations downstream of the biosolids-applied field are shown in purple. The maximum axis value is the maximum concentration of the most concentrated individual analyte at that sampling location.

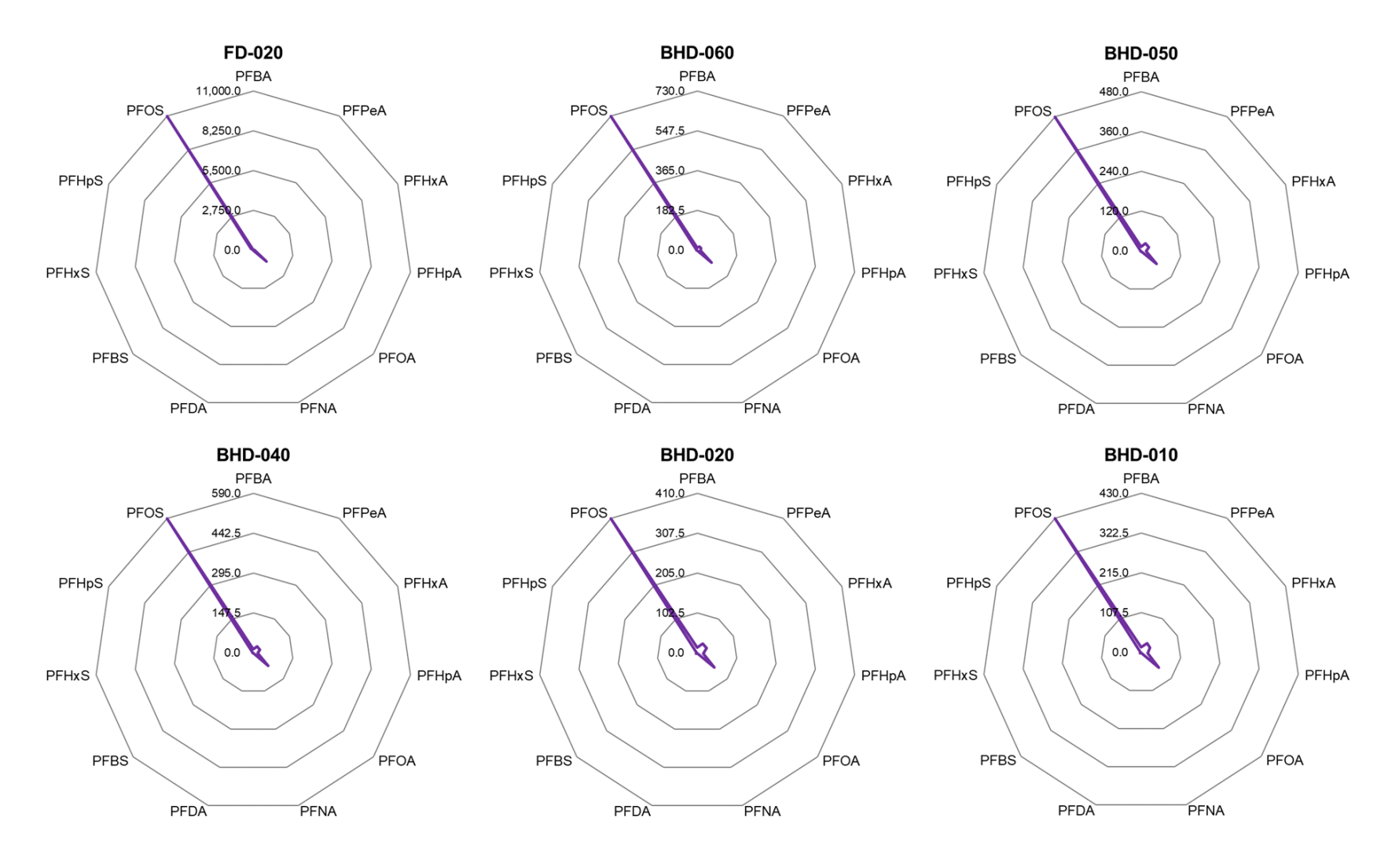


Figure 4.4 Radar plots of select PFAS concentrations (ng/L) in surface water samples influenced by the biosolids-applied field. Sampling locations downstream of the biosolids-applied field are shown in purple. The maximum axis value is the maximum concentration of the most concentrated individual analyte at that sampling location.

PFAS in sediment

The statistics of PFAS concentrations in sediment samples collected in August 2020 are presented in Table 4.5. Eleven PFAS analytes were detected, with PFOS being observed in all of the sediment samples. PFOS was detected at the highest concentration in the sediment samples, followed by PFDA and PFOA, their maximum concentrations were 13,000, 610, and 530 ng/kg, respectively. This differs from the dominant species of PFAS observed in surface water samples, which were PFOS and PFOA. White et al. (2015) examined PFAS concentrations in sediment samples collected from the Upper Cooper River, Lower Cooper River, Ashley River, and Charleston Harbor in South Carolina and found PFOS was the dominant PFAS species, with the maximum concentrations ranging from 3,919 to 7,369 ng/kg. PFDA and PFOA concentrations ranged from 55 – 4,762 ng/kg and 20 – 2,515 ng/kg, respectively. Sources in that area were predominately wastewater treatment plants effluent and urban stormwater and industrial discharges. In the Las Vegas Wash, perfluorodecane sulfonic acid (PFDS) and PFHxA were detected at the highest concentrations in sediments, 88,200 and 18,700 ng/kg, respectively (Bai and Son, 2021).

Table 4.5 Statistics of PFAS (ng/kg) detected in sediment (n = 7) in August 2020

Analyte		PFAS Conce	_ Detection Frequency		
, <u> </u>	Min	Max	Mean	Median	_ 1)
PFBA	ND	ND	ND	ND	0.0%
PFPeA	ND	210	30	ND	14.3%
PFHxA	ND	93	36	ND	42.9%
PFHpA	ND	110	45	46	57.1%
PFOA	ND	530	174	120	57.1%
PFNA	ND	120	26	ND	28.6%
PFDA	ND	610	137	41	85.7%
PFUnA	ND	140	31	ND	28.6%
PFDoA	ND	260	37	ND	14.3%
PFTriA	ND	ND	ND	ND	0.0%
PFTeA	ND	ND	ND	ND	0.0%
PFBS	ND	ND	ND	ND	0.0%
PFPeS	ND	ND	ND	ND	0.0%
PFHxS	ND	76	29	ND	42.9%
PFHpS	ND	ND	ND	ND	0.0%
PFOS	550	13000	3559	1500	100.0%
PFNS	ND	ND	ND	ND	0.0%
PFDS	ND	ND	ND	ND	0.0%
FOSA	ND	240	34	ND	14.3%
NMeFOSAA	ND	ND	ND	ND	0.0%
NEtFOSAA	ND	ND	ND	ND	0.0%
4:2 FTS	ND	ND	ND	ND	0.0%
6:2 FTS	ND	ND	ND	ND	0.0%
8:2 FTS	ND	ND	ND	ND	0.0%
Mean Total PFCA		Mean Total PFSA		Mean Total	PFAS
517 ng/kg		3,588 ng/kg		4,139 ng/kg	

ND: below the method detection limit, PFSA: perfluorosulfonic acids, PFCA: perfluorocarboxylic acids.

The total PFAS concentration, individual PFAS concentration, and relative PFAS composition of sediment samples are shown in Figures 4.5A, 4.5B and 4.5C, respectively. The total PFAS concentration was 2,120 ng/kg at BHD-095, 1,613 ng/kg at BHD-085, 586 ng/kg at BHD 075, 760 ng/kg at BHD-65, 6,181 ng/kg at BHD-045, and 2,493 ng/kg at BHD-025. Unlike the highest total PFAS concentration in the surface water samples (Figure 4.2A), the highest total PFAS concentration (15,220 ng/kg) in the sediment samples was found roughly 2.25 km downstream of the biosolids-applied field at the sampling location BHD-055 (Figure 4.5A).

The discrepancy between the location of the highest total PFAS concentration in surface water vs. the highest total PFAS concentration in sediment could be caused by sediment transport along the Brandymore/Howe Drain. The dominant PFAS species in soil samples from the biosolids-applied field and at sampling locations BHD-055, BHD-045, and BHD-025 were PFOS and PFOA. PFOA was not observed in sediment samples upstream of sampling location BHD-055, excluding sampling location BHD-095 (upstream of the biosolids-applied field), further indicating sediment transport may be occurring (Figure 4.5). PFOS and PFOA were the dominant PFAS species detected in soil samples from the biosolids-applied field and surface water samples and sediment samples collected downstream of the biosolids-applied field, which suggest the biosolids-applied field may be releasing PFAS into the Brandymore/Howe Drain.

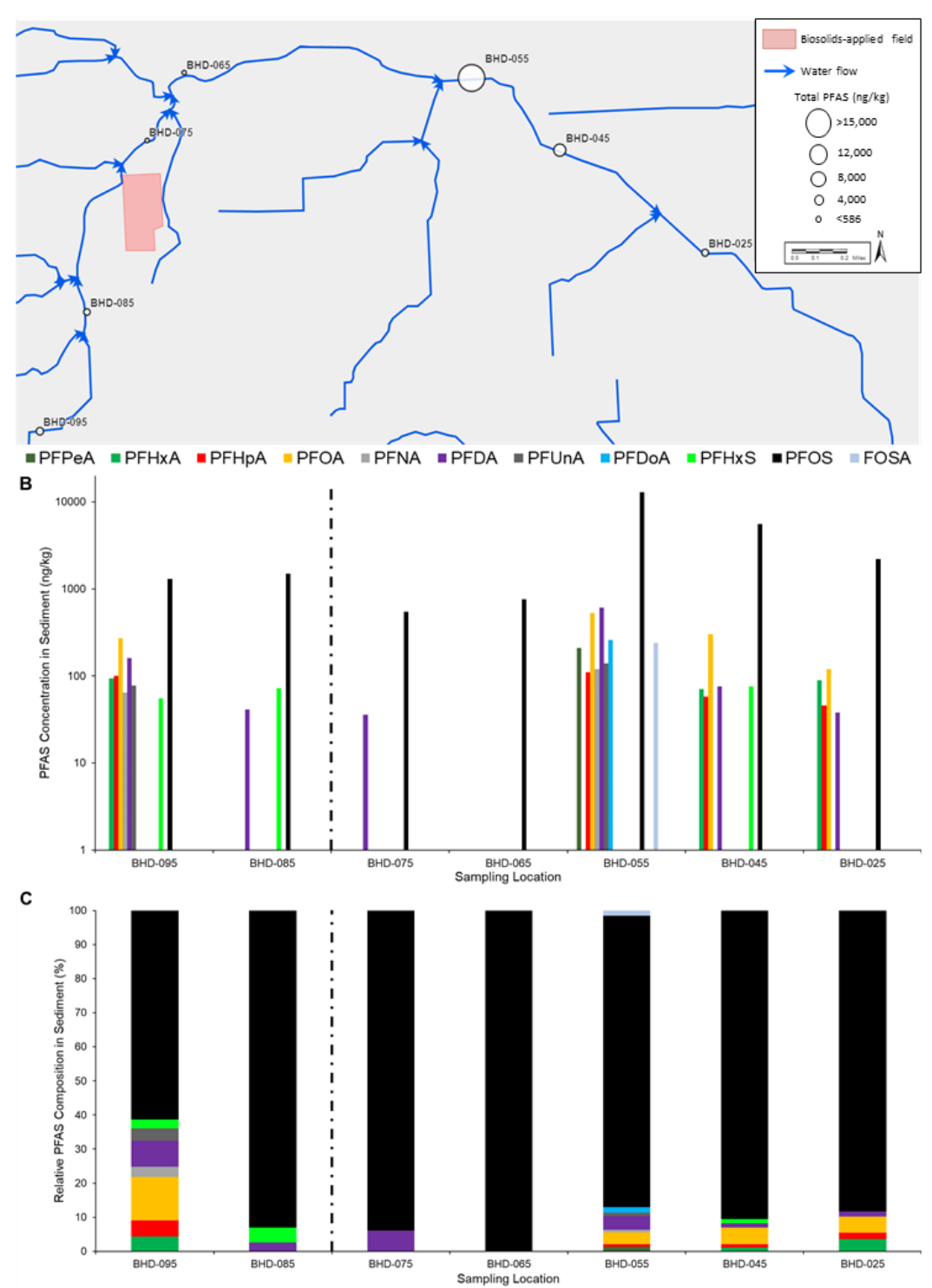


Figure 4.5 PFAS in sediment samples collected in August 2020 (n = 7). (A) Total PFAS concentrations from sediment samples. A field with known historical applications of contaminated biosolids is highlighted in red. Water flow is shown with blue arrows. White circles represent sediment concentrations of total PFAS (ng/kg). (B) Variation of PFAS concentrations and (C) relative composition of PFAS in sediment samples. The dashed line separates samples collected upstream and downstream of the field with known historical applications of contaminated biosolids, with samples upstream appearing to the left of the line.

Paired sediment and surface water

To evaluate the distribution of PFAS in sediments and surface water, three pairs of sediment and surface water samples were collected simultaneously at sampling locations FD-050, BHD-070, and FD-020 (Figure 4.6). PFOS followed by PFOA were the dominant PFAS species detected in these samples. In the sediment samples PFOS concentrations ranged from 3,400 to 60,000 ng/kg, or 81 to 92 % of the total PFAS concentrations, whereas PFOA concentrations ranged from 283 to 2,073 ng/kg, or 3 to 7 % of the total PFAS concentrations. PFOS and PFOA concentrations in the surface water samples ranged from 44 to 3,200 ng/L and 23 to 590 ng/L, respectively, which is equivalent to PFOS and PFOA comprising 33 to 82 % and 11 to 17 %, respectively, of the total PFAS concentration (Figure 4.6).

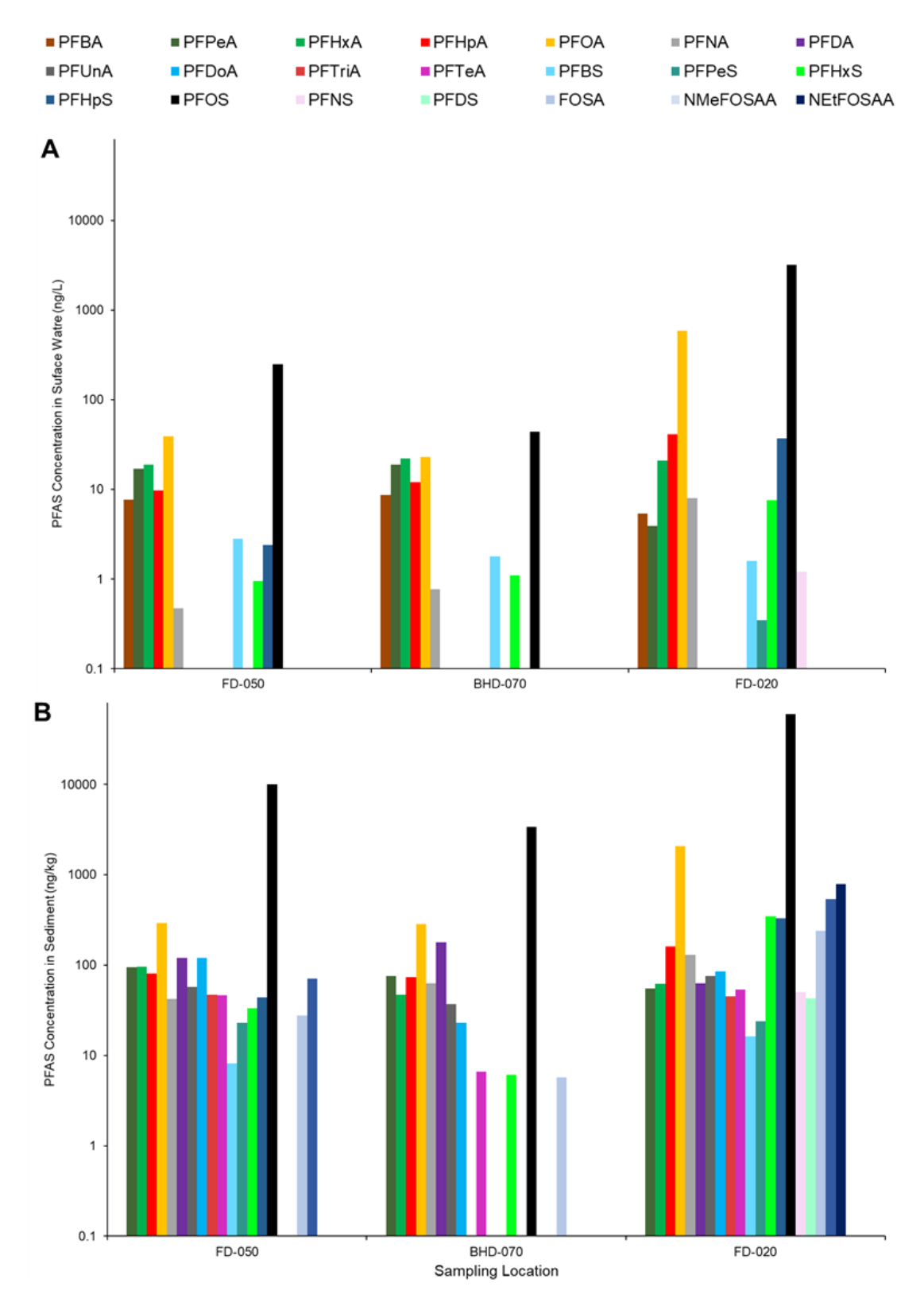


Figure 4.6 Comparison of PFAS concentrations in surface water and sediment samples collected in November 2019 (n = 3). (A) PFAS concentrations in surface water (ng/L). (B) PFAS concentrations in sediment (ng/kg).

Out of the twenty-four analytes examined, twenty analytes were detected in the sediment samples and twelve analytes were detected in the surface water samples. PFDA, perfluoroundecanoic acid (PFUnA), perfluorododecanoic acid (PFDoA), perfluorotridecanoic acid (PFTriA), perfluorotetradecanoic acid (PFTeA), PFDS, FOSA, NMeFOSAA, and NEtFOSAA were detected only in the sediment samples. The presence of the precursors FOSA, NMeFOSAA, and NEtFOSAA in the sediments, but not in the surface waters, could suggest that sorption by sediments prevents transformation of PFAS precursors by preventing hydrolysis reactions. PFBA was detected only in the surface water samples, likely due to its high solubility and weak sorption by sediments (Chen et al., 2016). In the paired surface water and sediment samples, 10 individual long-chain PFAS (i.e., PFOA, PFNA, PFDA, PFUnA, PFDoA, PFTriA, PFTeA, PFOS, PFNS, and PFDS) were found in sediments, while only four individual longchain PFAS (i.e., PFOA, PFNA, PFOS, and PFNS) were found in surface water. These results are consistent with the results reported by several other studies (Bai and Son, 2021; Ahrens, 2011; Zhao et al., 2016). Total PFAS concentrations in the sediment ranged from 4,201 to 65,183 ng/kg and 132 to 3,917 ng/L, respectively. This may have implications for ecotoxicology, where sediment dwelling biota and their predators may be exposed to a greater amount of PFAS, particularly long-chain PFAS (Ahrens et al., 2015).

Temporal changes

Surface water samples were collected at sampling locations FD-010 and FD-020 three times between July to December of 2019, to evaluate temporal changes in PFAS concentrations (Figure 4.7). Total precipitation from the nearest weather station (Port Huron 1.6 W, MI) for 10 days preceding sample collection was 2.82 cm for the July sample collection, 8.94 cm for the

September sample collections, 4.17 cm for the November sample collections, and 0.61 cm for the December sample collections (https://www.cocorahs.org).

Concentrations of PFAS in surface waters at the sampling location FD-010 (located at a tributary to the Brandymore/Howe Drain downstream of the biosolids-applied field) appeared to have little change between July and November (Figure 4.7A). Total PFAS concentrations were 172.1 ng/L in July, 193.1 ng/L in September, and 337.0 ng/L November. Precipitation increased 217% from July to September and decreased 53% from September to November. There appears to be no relation between PFAS concentrations at this sampling location and changes in precipitation preceding collection. This sampling location is not hydrologically connected to the biosolids-applied field, and the source of PFAS in surface waters at this location is unknown.

A discernable trend of decreasing PFAS concentrations in surface water at sampling location FD-020 from September 2019 to December 2019 is shown in Figure 4.7B. Sampling location FD-020 is immediately downstream of the biosolids-applied field, and likely impacted most by PFAS release from the biosolids-applied field (Figures 4.2, 4.3, and 4.4). PFAS concentrations at this location were 11,000 ng/L for PFOS, 1,200 ng/L for PFOA, and 160 ng/L for PFHpS in September, 3,200 ng/L for PFOS, 590 ng/L for PFOA, and 37 ng/L for PFHpS in November, and 62 ng/L for PFOS, 11 ng/L for PFOA, and 0.7 ng/L for PFHpS in December 2019. Concentrations of these PFAS decreased by 51 to 77% from September to November, and ~98% from November to December. Precipitation from September to November decreased by 53% and decreased 85% from November to December. Decreases in the concentrations of PFOS, PFOA, and PFHpS (dominant PFAS species or PFAS species found only in surface waters downstream of the biosolids-applied field) from September to December correlates well with decreases in total precipitation preceding sampling collection. The characteristics of PFAS

release from biosolids-applied fields are not well understood, however, the release of other agricultural pollutants with precipitation, such as nutrients or pesticides, is well documented (Randall and Gross, 2008; Cambardella et al., 1999; Leu et al., 2004; Thorsteinsson et al., 2019).

Bai and Son (2021), Lee et al. (2020), Sun et al. (2016), and Bai et al. (2018), in their examinations of industrial/urban point sources of PFAS, observed decreasing PFAS concentrations due to dilution effects which were caused by increased rainfall, whereas we observed increased PFAS concentrations during similar periods. This may be due to increased surface and subsurface water movement in the biosolids-applied field during times of increased precipitation, leading to an increased release of PFAS or PFAS containing soil particles to surrounding surface waters. This could well explain that at the sampling location FD-020, immediately adjacent to the biosolids-applied field, PFAS concentration appeared positively related the amount of precipitation. At the sampling location FD-010, on a tributary not hydrologically connected to the biosolids-applied field, PFAS concentrations in surface water were much lower and did not have an apparent relation with precipitation. This distinct trend, similar to other agricultural pollutants such as nutrients and pesticides, observed at sampling location FD-020 further suggests PFAS in surface water could be released from land application of PFAS-containing biosolids.

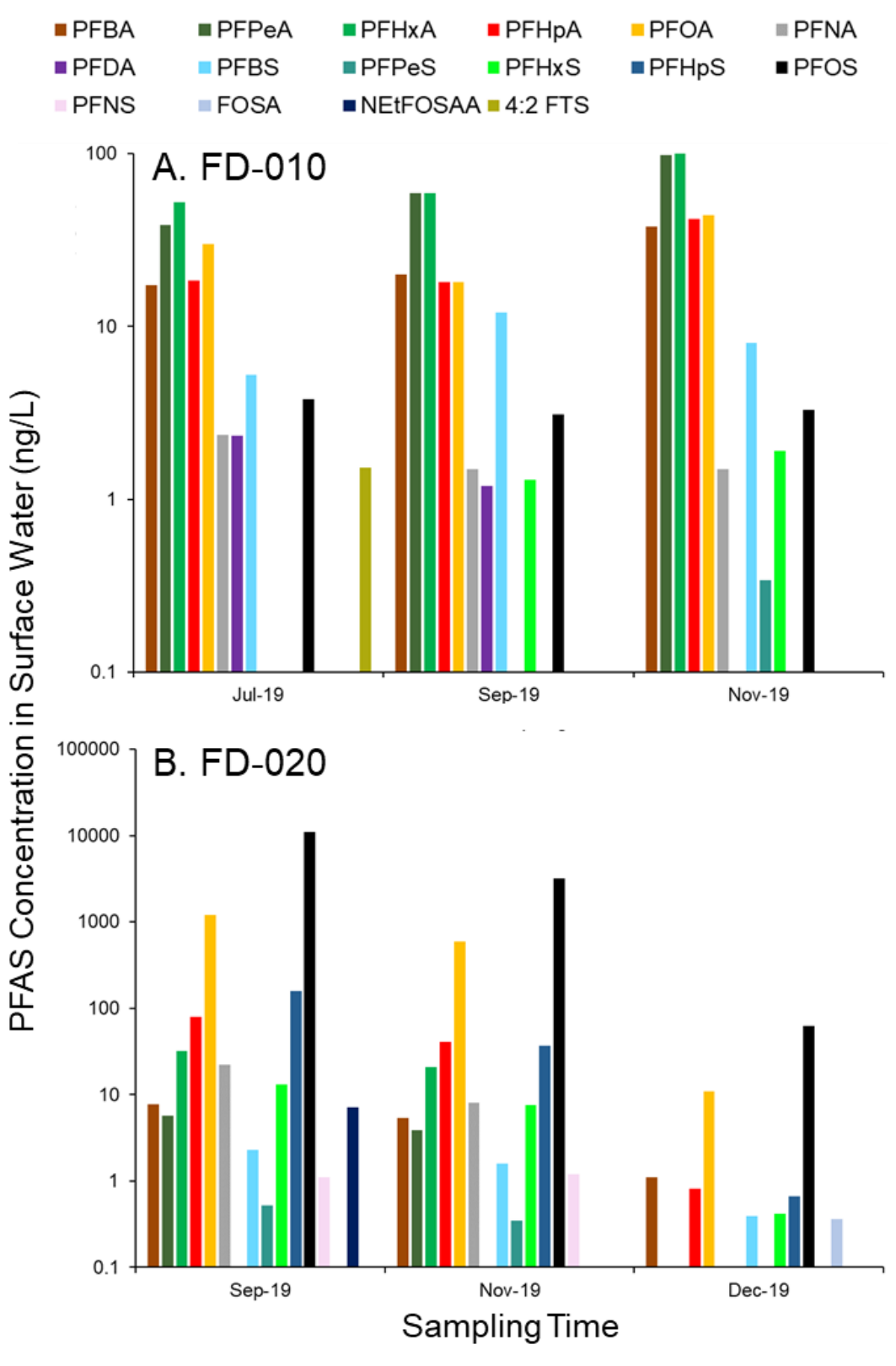


Figure 4.7 Temporal changes of PFAS concentrations in surface water samples (n = 3). (A) Samples collected at FD-010 from July – November 2019. (B) Samples collected at FD-020 from September – December 2019.

CONCLUSION

Although previous research has shown that PFAS present in biosolids can impact soil and groundwater (Pepper et al., 2021; Gottschall et al., 2010), this study reports the wide dissemination of PFAS in surface water and sediments from one known historical application of biosolids to an agricultural field. The results from this study document high concentrations of PFAS found downstream of an agricultural field which received one known application of biosolids in 1983, likely containing high concentrations of PFAS. Total PFAS could be detected at up 12,530 ng/L, immediately downstream of the biosolids-applied field, in surface water. PFOS and PFOA were the dominant PFAS species in the soil, surface water, and sediment samples. The compositional profile of downstream surface water samples was remarkably similar, whereas upstream and unrelated tributary samples appeared to have differing sources. PFAS concentrations in the surface water and sediment samples decreased with increasing distance from the biosolids-applied field. Taken together, these observations suggest that the biosolids-applied field is likely releasing PFAS to the downstream area.

REFERENCES

REFERENCES

- Ahrens, L., 2011. Polyfluoroalkyl compounds in the aquatic environment: a review of their occurrence and fate. J. Environ. Monit. 13, 20–31. https://doi.org/10.1039/C0EM00373E
- Ahrens, L., Norström, K., Viktor, T., Cousins, A.P., Josefsson, S., 2015. Stockholm Arlanda Airport as a source of per- and polyfluoroalkyl substances to water, sediment and fish. Chemosphere 129, 33–38. https://doi.org/10.1016/j.chemosphere.2014.03.136
- Alder, A.C., van der Voet, J., 2015. Occurrence and point source characterization of perfluoroalkyl acids in sewage sludge. Chemosphere 129, 62–73. https://doi.org/10.1016/j.chemosphere.2014.07.045
- Aleksandrov, K., Gehrmann, H.-J., Hauser, M., Mätzing, H., Pigeon, D., Stapf, D., Wexler, M., 2019. Waste incineration of Polytetrafluoroethylene (PTFE) to evaluate potential formation of per- and Poly-Fluorinated Alkyl Substances (PFAS) in flue gas. Chemosphere 226, 898–906. https://doi.org/10.1016/j.chemosphere.2019.03.191
- Armstrong, B., Bohr, J., Schoen, L. Investigation of Per- and Polyfluoroalkyl Substances (PFAS) in Fort Gratiot and Burtchville Townships / St. Clair County and Worth Township / Sanilac County Surface Water Sampling Update November 2019. Surface Water Assessment Section, Water Resources Division, Michigan Department of Environment, Great Lakes, and Energy. Lansing, MI; 2019.
- Bai, X., Lutz, A., Carroll, R., Keteles, K., Dahlin, K., Murphy, M., Nguyen, D., 2018.

 Occurrence, distribution, and seasonality of emerging contaminants in urban watersheds.

 Chemosphere 200, 133–142. https://doi.org/10.1016/j.chemosphere.2018.02.106
- Bai, X., Son, Y., 2021. Perfluoroalkyl substances (PFAS) in surface water and sediments from two urban watersheds in Nevada, USA. Science of The Total Environment 751, 141622. https://doi.org/10.1016/j.scitotenv.2020.141622
- Bossi, R., Strand, J., Sortkjær, O., Larsen, M.M., 2008. Perfluoroalkyl compounds in Danish wastewater treatment plants and aquatic environments. Environment International 34, 443–450. https://doi.org/10.1016/j.envint.2007.10.002
- Brendel, S., Fetter, É., Staude, C., Vierke, L., Biegel-Engler, A., 2018. Short-chain perfluoroalkyl acids: environmental concerns and a regulatory strategy under REACH. Environ Sci Eur 30, 9. https://doi.org/10.1186/s12302-018-0134-4
- Brusseau, M.L., Anderson, R.H., Guo, B., 2020. PFAS concentrations in soils: Background levels versus contaminated sites. Science of The Total Environment 740, 140017. https://doi.org/10.1016/j.scitotenv.2020.140017

- Buck, R.C., Jensen, A.A., 2011. Perfluoroalkyl and polyfluoroalkyl substances in the environment: Terminology, classification, and origins. Integrated Environmental Assessment and Managment 7, 513–541. https://doi.org/10.1002/ieam.258
- Cambardella, C.A., Moorman, T.B., Jaynes, D.B., Hatfield, J.L., Parkin, T.B., Simpkins, W.W., Karlen, D.L., 1999. Water Quality in Walnut Creek Watershed: Nitrate-Nitrogen in Soils, Subsurface Drainage Water, and Shallow Groundwater. J. environ. qual. 28, 25–34. https://doi.org/10.2134/jeq1999.00472425002800010003x
- Chen, H., Zhang, C., Han, J., Yu, Y., Zhang, P., 2012. PFOS and PFOA in influents, effluents, and biosolids of Chinese wastewater treatment plants and effluent-receiving marine environments. Environmental Pollution 170, 26–31. https://doi.org/10.1016/j.envpol.2012.06.016
- Chen, H., Reinhard, M., Nguyen, V.T., Gin, K.Y.-H., 2016. Reversible and irreversible sorption of perfluorinated compounds (PFCs) by sediments of an urban reservoir. Chemosphere 144, 1747–1753. https://doi.org/10.1016/j.chemosphere.2015.10.055
- Dalahmeh, S., Tirgani, S., Komakech, A.J., Niwagaba, C.B., Ahrens, L., 2018. Per- and polyfluoroalkyl substances (PFASs) in water, soil and plants in wetlands and agricultural areas in Kampala, Uganda. Science of The Total Environment 631–632, 660–667. https://doi.org/10.1016/j.scitotenv.2018.03.024
- EGLE, 2021. Michigan PFAS Sites. June 14. Michigan Department of Environment, Great Lakes, and Energy, Lansing, MI; 2021.
- Ellis, D.A., Martin, J.W., De Silva, A.O., Mabury, S.A., Hurley, M.D., Sulbaek Andersen, M.P., Wallington, T.J., 2004. Degradation of Fluorotelomer Alcohols: A Likely Atmospheric Source of Perfluorinated Carboxylic Acids. Environ. Sci. Technol. 38, 3316–3321. https://doi.org/10.1021/es049860w
- Gallen, C., Eaglesham, G., Drage, D., Nguyen, T.H., Mueller, J.F., 2018. A mass estimate of perfluoroalkyl substance (PFAS) release from Australian wastewater treatment plants. Chemosphere 208, 975–983. https://doi.org/10.1016/j.chemosphere.2018.06.024
- Goodrow, S.M., Ruppel, B., Lippincott, R.L., Post, G.B., Procopio, N.A., 2020. Investigation of levels of perfluoroalkyl substances in surface water, sediment and fish tissue in New Jersey, USA. Science of The Total Environment 729, 138839. https://doi.org/10.1016/j.scitotenv.2020.138839
- Gottschall, N., Topp, E., Edwards, M., Russell, P., Payne, M., Kleywegt, S., Curnoe, W., Lapen, D.R., 2010. Polybrominated diphenyl ethers, perfluorinated alkylated substances, and metals in tile drainage and groundwater following applications of municipal biosolids to agricultural fields. Science of The Total Environment 408, 873–883. https://doi.org/10.1016/j.scitotenv.2009.10.063

- Hale, S.E., Arp, H.P.H., Slinde, G.A., Wade, E.J., Bjørseth, K., Breedveld, G.D., Straith, B.F., Moe, K.G., Jartun, M., Høisæter, Å., 2017. Sorbent amendment as a remediation strategy to reduce PFAS mobility and leaching in a contaminated sandy soil from a Norwegian firefighting training facility. Chemosphere 171, 9–18. https://doi.org/10.1016/j.chemosphere.2016.12.057
- Hepburn, E., Madden, C., Szabo, D., Coggan, T.L., Clarke, B., Currell, M., 2019. Contamination of groundwater with per- and polyfluoroalkyl substances (PFAS) from legacy landfills in an urban re-development precinct. Environmental Pollution 248, 101–113. https://doi.org/10.1016/j.envpol.2019.02.018
- Higgins, C.P., Field, J.A., Criddle, C.S., Luthy, R.G., 2005. Quantitative Determination of Perfluorochemicals in Sediments and Domestic Sludge. Environ. Sci. Technol. 39, 3946–3956. https://doi.org/10.1021/es048245p
- Houtz, E.F., Higgins, C.P., Field, J.A., Sedlak, D.L., 2013. Persistence of Perfluoroalkyl Acid Precursors in AFFF-Impacted Groundwater and Soil. Environ. Sci. Technol. 47, 8187–8195. https://doi.org/10.1021/es4018877
- Kim Lazcano, R., Perre, C., Mashtare, M.L., Lee, L.S., 2019. Per- and polyfluoroalkyl substances in commercially available biosolid-based products: The effect of treatment processes. Water Environment Research 91, 1669–1677. https://doi.org/10.1002/wer.1174
- Kwok, K.Y., Yamazaki, E., Yamashita, N., Taniyasu, S., Murphy, M.B., Horii, Y., Petrick, G., Kallerborn, R., Kannan, K., Murano, K., Lam, P.K.S., 2013. Transport of Perfluoroalkyl substances (PFAS) from an arctic glacier to downstream locations: Implications for sources. Science of The Total Environment 447, 46–55. https://doi.org/10.1016/j.scitotenv.2012.10.091
- Lee, Y.-M., Lee, J.-Y., Kim, M.-K., Yang, H., Lee, J.-E., Son, Y., Kho, Y., Choi, K., Zoh, K.-D., 2020. Concentration and distribution of per- and polyfluoroalkyl substances (PFAS) in the Asan Lake area of South Korea. Journal of Hazardous Materials 381, 120909. https://doi.org/10.1016/j.jhazmat.2019.120909
- Leu, C., Singer, H., Stamm, C., Müller, S.R., Schwarzenbach, R.P., 2004. Simultaneous Assessment of Sources, Processes, and Factors Influencing Herbicide Losses to Surface Waters in a Small Agricultural Catchment. Environ. Sci. Technol. 38, 3827–3834. https://doi.org/10.1021/es0499602
- Liou, J.S.-C., Szostek, B., DeRito, C.M., Madsen, E.L., 2010. Investigating the biodegradability of perfluorooctanoic acid. Chemosphere 80, 176–183. https://doi.org/10.1016/j.chemosphere.2010.03.009
- Loganathan, B.G., Sajwan, K.S., Sinclair, E., Senthil Kumar, K., Kannan, K., 2007. Perfluoroalkyl sulfonates and perfluorocarboxylates in two wastewater treatment

- facilities in Kentucky and Georgia. Water Research 41, 4611–4620. https://doi.org/10.1016/j.watres.2007.06.045
- Michigan Department of Environmental Quality Sediment PFAS Sampling Guidance, 06/2019.

 https://www.michigan.gov/documents/pfasresponse/Sediment_PFAS_Sampling_Guidance_e_658388_7.pdf
- Michigan Department of Environmental Quality Soil PFAS Sampling Guidance, 11/2018. https://www.michigan.gov/documents/pfasresponse/Soil_PFAS_Sampling_Guidance_63_9407_7.pdf
- Michigan Department of Environmental Quality Surface Water PFAS Sampling Guidance, 11/2018.

 https://www.michigan.gov/documents/pfasresponse/Surface_Water_PFAS_Sampling_Guidance_639408_7.pdf
- Milinovic, J., Lacorte, S., Vidal, M., Rigol, A., 2015. Sorption behaviour of perfluoroalkyl substances in soils. Science of The Total Environment 511, 63–71. https://doi.org/10.1016/j.scitotenv.2014.12.017
- MPART, 2019. Overview of Michigan's Screening Levels and MCLS for PFAS. Michigan PFAS Action Response Team. Lansing, MI; 2019.
- Murakami, M., Nishikoori, H., Sakai, H., Oguma, K., Takada, H., Takizawa, S., 2013. Formation of perfluorinated surfactants from precursors by indigenous microorganisms in groundwater. Chemosphere 93, 140–145. https://doi.org/10.1016/j.chemosphere.2013.05.010
- Navarro, I., de la Torre, A., Sanz, P., Pro, J., Carbonell, G., Martínez, M. de los Á., 2016. Bioaccumulation of emerging organic compounds (perfluoroalkyl substances and halogenated flame retardants) by earthworm in biosolid amended soils. Environmental Research 149, 32–39. https://doi.org/10.1016/j.envres.2016.05.004
- North East Biosolids and Residuals Association, 2007. A National Biosolids Regulation, Quality, End Use & Disposal Survey Tamworth, NH.
- Pepper, I.L., Brusseau, M.L., Prevatt, F.J., Escobar, B.A., 2021. Incidence of Pfas in soil following long-term application of class B biosolids. Science of The Total Environment 793, 148449. https://doi.org/10.1016/j.scitotenv.2021.148449
- Randall, G.W. and Goss, M.J., 2008. Nitrate losses to surface water through subsurface, tile drainage. In Nitrogen in the Environment (pp. 145-175). Academic Press.
- Sáez, M., de Voogt, P., Parsons, J.R., 2008. Persistence of perfluoroalkylated substances in closed bottle tests with municipal sewage sludge. Environ Sci Pollut Res 15, 472–477. https://doi.org/10.1007/s11356-008-0020-5

- Scher, D.P., Kelly, J.E., Huset, C.A., Barry, K.M., Hoffbeck, R.W., Yingling, V.L., Messing, R.B., 2018. Occurrence of perfluoroalkyl substances (PFAS) in garden produce at homes with a history of PFAS-contaminated drinking water. Chemosphere 196, 548–555. https://doi.org/10.1016/j.chemosphere.2017.12.179
- Schultz, M.M., Higgins, C.P., Huset, C.A., Luthy, R.G., Barofsky, D.F., Field, J.A., 2006. Fluorochemical Mass Flows in a Municipal Wastewater Treatment Facility. Environ. Sci. Technol. 40, 7350–7357. https://doi.org/10.1021/es061025m
- Scott, B.F., Spencer, C., Mabury, S.A., Muir, D.C.G., 2006. Poly and Perfluorinated Carboxylates in North American Precipitation. Environ. Sci. Technol. 40, 7167–7174. https://doi.org/10.1021/es061403n
- Senthil Kumar, K., Zushi, Y., Masunaga, S., Gilligan, M., Pride, C., Sajwan, K.S., 2009. Perfluorinated organic contaminants in sediment and aquatic wildlife, including sharks, from Georgia, USA. Marine Pollution Bulletin 58, 621–629. https://doi.org/10.1016/j.marpolbul.2008.12.006
- Sharp, S., Sardiña, P., Metzeling, L., McKenzie, R., Leahy, P., Menkhorst, P., Hinwood, A., 2021. Per- and Polyfluoroalkyl Substances in Ducks and the Relationship with Concentrations in Water, Sediment, and Soil. Environ Toxicol Chem 40, 846–858. https://doi.org/10.1002/etc.4818
- Shigei, M., Ahrens, L., Hazaymeh, A., Dalahmeh, S.S., 2020. Per- and polyfluoroalkyl substances in water and soil in wastewater-irrigated farmland in Jordan. Science of The Total Environment 716, 137057. https://doi.org/10.1016/j.scitotenv.2020.137057
- Sima, M.W., Jaffé, P.R., 2021. A critical review of modeling Poly- and Perfluoroalkyl Substances (PFAS) in the soil-water environment. Science of The Total Environment 757, 143793. https://doi.org/10.1016/j.scitotenv.2020.143793
- Simcik, M.F., Dorweiler, K.J., 2005. Ratio of Perfluorochemical Concentrations as a Tracer of Atmospheric Deposition to Surface Waters. Environ. Sci. Technol. 39, 8678–8683. https://doi.org/10.1021/es0511218
- Sinclair, E., Kannan, K., 2006. Mass Loading and Fate of Perfluoroalkyl Surfactants in Wastewater Treatment Plants. Environ. Sci. Technol. 40, 1408–1414. https://doi.org/10.1021/es051798v
- Suja, F., Pramanik, B.K., Zain, S., 2009. Contamination, bioaccumulation and toxic effects of perfluorinated chemicals (PFCs) in the water environment: a review paper. Water Science 12. https://doi.org/10.2166/wst.2009.504
- Sun, M., Arevalo, E., Strynar, M., Lindstrom, A., Richardson, M., Kearns, B., Pickett, A., Smith, C., Knappe, D.R.U., 2016. Legacy and Emerging Perfluoroalkyl Substances Are Important Drinking Water Contaminants in the Cape Fear River Watershed of North

- Carolina. Environ. Sci. Technol. Lett. 3, 415–419. https://doi.org/10.1021/acs.estlett.6b00398
- Sunderland, E.M., Hu, X.C., Dassuncao, C., Tokranov, A.K., Wagner, C.C., Allen, J.G., 2019. A review of the pathways of human exposure to poly- and perfluoroalkyl substances (PFASs) and present understanding of health effects. J. Expo. Sci. Environ. Epidemiol. 29 (2), 131–147. https://doi.org/10.1038/s41370-018-0094-1.
- Thorsteinsson, B., Jóhannesson, G.H., Thorlacius, A., Gudmundsson, T., 2019. Precipitation, runoff and nutrient losses from cultivated Histosols in western Iceland. IAS 32, 61–74. https://doi.org/10.16886/IAS.2019.06
- Tuve, R. L.; Jablonski, J. E. Method of extinguishing liquid hydrocarbon fires. U.S. Patent 3,258,423, June 28, 1966.
- Venkatesan, A.K., Halden, R.U., 2013. National inventory of perfluoroalkyl substances in archived U.S. biosolids from the 2001 EPA National Sewage Sludge Survey. Journal of Hazardous Materials 252–253, 413–418. https://doi.org/10.1016/j.jhazmat.2013.03.016
- Wang, N., Liu, J., Buck, R.C., Korzeniowski, S.H., Wolstenholme, B.W., Folsom, P.W., Sulecki, L.M., 2011. 6:2 Fluorotelomer sulfonate aerobic biotransformation in activated sludge of waste water treatment plants. Chemosphere 82, 853–858. https://doi.org/10.1016/j.chemosphere.2010.11.003
- Washington, J.W., Yoo, H., Ellington, J.J., Jenkins, T.M., Libelo, E.L., 2010. Concentrations, Distribution, and Persistence of Perfluoroalkylates in Sludge-Applied Soils near Decatur, Alabama, USA. Environ. Sci. Technol. 44, 8390–8396. https://doi.org/10.1021/es1003846
- White, N.D., Balthis, L., Kannan, K., De Silva, A.O., Wu, Q., French, K.M., Daugomah, J., Spencer, C., Fair, P.A., 2015. Elevated levels of perfluoroalkyl substances in estuarine sediments of Charleston, SC. Science of The Total Environment 521–522, 79–89. https://doi.org/10.1016/j.scitotenv.2015.03.078
- Zhao, P., Xia, X., Dong, J., Xia, N., Jiang, X., Li, Y., Zhu, Y., 2016. Short- and long-chain perfluoroalkyl substances in the water, suspended particulate matter, and surface sediment of a turbid river. Science of The Total Environment 568, 57–65. https://doi.org/10.1016/j.scitotenv.2016.05.221

CHAPTER V. FUTURE RESEARCH

This research highlighted that (1) uptake and accumulation of cephalexin, a contaminant of emerging concern (CEC), from water varied among lettuce, celery, and radish, cephalexin accumulation ranked in the order of lettuce roots > celery roots > radish roots. No cephalexin could be found in the shoots of these three vegetables. This varied pattern of uptake and accumulation could be explained by in vitro measurements of cephalexin sorption by and affinity to vegetable tissues and cephalexin reaction with vegetable enzyme extracts. (2) Plant Casparian strip reduced root to shoot translocation of PFAS (molecular weight between 260 and 620 g/mol). The shoot accumulation of PFAS molecular weight >450 g/mol appeared to be more related to the sorption of these compounds to root surfaces and root tissues than the barrier presented by the Casparian strip. No impact on the translocation of carbamazepine, a small sized (~250 g/mol), neutrally charged, and intermediately hydrophobic pharmaceutical, was observed. (3) The historical application of PFAS containing biosolids to agricultural land can release PFAS to downstream surface water and sediments. An agricultural field in Fort Gratiot, Michigan, received one known application of PFAS containing biosolids in 1983, appeared to still serve as a significant source to disseminate PFAS to the downstream area.

According to the present research, the following research avenues are suggested as future research.

IN VITRO SCREENING OF CHEMICALS OF EMERGING CONCERN FOR ASSESSING PLANT UPTAKE AND ACCUMULATION

In vivo studies on the uptake and accumulation of CECs are time-consuming and difficult to conduct. *In vitro* experiments examining CECs and their interaction with plant root tissues, their transformation with plant enzyme extracts, and their uptake across plant membranes may be beneficial in developing quick and easy evaluation on their potential for accumulation in plants.

USE OF SALK_043282 ARABIDOPSIS THALIANA MUTANT TO FURTHER EXAMINE THE IMPACT OF THE CASPARIAN STRIP

The *A. thaliana* mutant described in Chapter 3 could be used with a more diverse set of CECs to fully elucidate the interplay between the Casparian strip and the symplastic/apoplastic pathways. The PFAS used in the Chapter 3 had little variation in physiochemical properties excluding molecular size. The insights gained on the role of the Casparian strip as a barrier in the root-to-shoot translocation may be used to develop mitigation strategies for plant uptake of CECs.

GENETIC SCREENING OF CROP VARIETIES FOR VARIATIONS IN THE CASPARIAN STRIP

Mutant *Arabidopsis thaliana*, with an incompletely formed Casparian strip, demonstrated increased translocation of PFAS in comparison to wild type. There may be natural variation in the formation of the Casparian strip among crop varieties; certain varieties might demonstrate increased or decreased Casparian strip formation. If this can be determined through visualization of propidium iodide staining or lignin autofluorescence, the information could be used to select crop varieties with decreased root to shoot translocation.

EXAMINATION OF ADDITIONAL IMPACTS FROM PFAS IN SURFACE WATER AND SEDIMENTS

Much is yet to be learned regarding the chronic exposure of plants, fish, animals, and humans to low levels of PFAS. Furthermore, little is known about the role of PFAS precursors in the dissemination of PFAS in surface water, and their sorption and transformation in watersheds. Additional research is needed to screen other types of PFAS using non-target mass spectroscopy

analysis. These unknown PFAS could pose an additional, but unnoticed, threats to water and sediment quality